Geothermal energy at Hoogeveen

Feasibility study

Client	Gemeente Hoogeveen
	HOOGEVEEN
	T 0528 - 291 687
	E w.hermans@hoogeveen.nl
	Contact person: Wilbert Hermans
Consultants	IF Technology
	6800 AP ARNHEM
	T 026 - 35 35 555
	E info@iftechnology.nl
	Contact person: Mark Gankema
	DNV KEMA
	6800 ET ARNHEM
	T 026 – 356 9111
	E contact@kema.com
	Contact person : Jules Smeets
Authors	K. van der Hoorn
	B. Rombaut
	C. Maaijwee
	M. Gankema
	J. Smeets
Verified by	A. Lokhorst (geology)
	P. Betts (petrophysics)
	G. Diephuis (geology, geophysics)
	G. Nitters (hydraulic fracturing)
	N. Buik (reservoir engineering)
	B. de Zwart (power plant and business case)
	H. Cornelissen WEP (well engineering)
	R. van Kessel DNV KEMA (power plant)

KEMA

if

Contents

1   Executive summary

The municipality of Hoogeveen has the intention to achieve a share of 8% renewable energy in 2015 and has a roadmap for further reduction of carbon dioxide. A detailed feasibility study was carried out to assess the potential of geothermal energy as an alternative and renewable energy source.

Based on current information and insights, a deep geothermal project at Hoogeveen seems technically feasible. The project contains considerable risks, in the sense that this projects harbours a great deal of novel subsurface techniques, to be applied at depths not reached before in The Netherlands. However, the techniques have been applied separately in the oil and gas industry.

The capacity of the geothermal installation can supply enough electricity for 100% of the households of the municipality of Hoogeveen and heat for 30% of the households. Further the project will reduce the CO_2 emission significantly.

A geological study has been executed to identify a suitable reservoir and to estimate rock properties of the target formation. Several hydraulic fracturing scenarios have been modelled with purpose to obtain an insight into possible improvements of reservoir characteristics for heat and fluid transport. Taking these modelling results into consideration, a productive -high flow rate- reservoir seems feasible.

The most likely reservoir system is based on shear -water- fracturing. The realisation of such a system calls for an investment of approximately 105 million euro. Annual revenues are about 15 million euro, including CO_2 credits and SDE subsidy. This amount also includes the delivery of 10 MW_{th} of residual heat.

Risk coverage for major risks is necessary in order to finance and realise a deep geothermal project. The next project phase aims to assess possible subsurface scenarios and to quantify the flow rate risk. The quantitative risk analysis is required to enable risk coverage by an insurance or a combination with a governmental guarantee fund.

Geology

A previous national study indicates potential for deep geothermal energy in the Carboniferous Zeeland Formation. This formation was deposited during the Early Carboniferous. Its main lithology is comprises different types of limestones and dolomites. After a lithostratigraphic review of four deep wells in the Netherlands it is concluded that this formation may exhibit favourable reservoir potential below Hoogeveen. Previous studies have concluded that Hoogeveen is located in a basin between adjacent carbonate platforms.

Depth and thickness of objective

Based on a national study and analysis of four deep wells, the depth of the Zeeland Formation below Hoogeveen is estimated to be between 6,500 and 7,000 m below NAP. Seismic data interpretation results in a approximate depth estimate of 6,800 m.

The local thickness of the reservoir -based on the four deep wells- is estimated to be between 200 and 800 m. The thickness estimation based on seismic data interpretation is 400 m, with an uncertainty of 200 m.

Both the local depth of the Zeeland Formation, as well as its thickness are subject to very considerable uncertainty. It is noted that the deepest well in onshore The Netherlands has reached a depth of approximately 6 km below NAP - in this well the Zeeland Formation was not reached - and that a geothermal well near Hoogeveen will have to reach at least a depth of 6,500 m.

Temperature

Estimation of the temperature at 7,000 m depth is initially based on two gradients. The average Dutch gradient is based on a large number of wells, which are however not deeper than around 3,000 m. This gradient amounts to 30 ºC/km, which is considered a conservative estimate for larger depths.

In four deep wells an increased gradient has been found below depths of 3,000 m. This increase may be contributed to insulating clay layers in the sequence on top of the Zeeland Formation. The increased gradient has been determined to be 44 ºC/km.

In addition, a 1D temperature model is constructed based on conductivities and heatflow, that can predict temperatures beyond drilled depths. Based on these gradients and the model, the temperature at a depth of 7,000 m is estimated to be approximately 260±20 ºC.

Rock properties

Core and log measurements of the Zeeland Formation have been used to determine a porosity-permeability relationship for the Zeeland Formation. The average primary porosity and permeability over the Carboniferous reservoir section are very low for each of the three deep wells LTG-01, UHM-02 and WSK-01, in the order of 1% porosity and 0.1 mD permeability.

Fault zones

High quality seismic data is required to map fault zones at great depths. This kind of data is not available at the project location, since the available seismic has been acquired for much shallower –gas- objectives. This inhibits further interpretation of fault zone characteristics such as dimensions and displacement at the target depth. The only available information comes from regional studies on the occurrence of shallower fault zones.

Based on shallow data the orientation of the deeper fault structures is believed to be WNW-ESE to NW-SE. This direction is almost similar to the direction of the maximum horizontal stress. Therefore we assume to be in a normal stress regime.

Open faults are most likely located on the intersections of the main fault direction (WNW-ESE) with the Riedel faults (N-S).

Hydraulic fracturing

Hydraulic fracturing is a method to create paths through which the fluid can flow. The fracture also creates a large surface-area for heat exchange between the cold injection fluid and host rock.

In a conventional oil and gas industry fracturing job a tensile fracture is created, and the fracture is filled with proppants to achieve a high permeability in the fracture and to prevent the fracture from closing when the injection pressure decreases. This study has focussed on tensile -propped- fracturing as a most conservative fall back scenario.

Another technique –shear or water fracturing– relies on shear displacement along the fracture which should prevent the fracture from closing due to fracture wall roughness. This technique has not been modelled in this study.

Fracture and reservoir modelling

Application of a conventional tensile -propped- hydraulic fracturing treatment has been modelled in this study. Data from well LTG-01 have been used for the simulations. Logs are constructed of the four major rock parameters. These are Young's modulus, Poisson's ratio, the minimum horizontal stress and the host rock matrix permeability. Together with the treatment design these parameters are the most important input parameters for the model software.

The modelling exercise resulted in eight fracture scenarios, each with its own dimensions and fracture permeability. Calculations have been performed on each scenario in order to assess achievable flow rates.

The impact of the number of fractures on the temperature decline in the production well was also modelled. The main result is that there exists a scenario that shows a good overall performance in terms of temperature drop with optimum number and dimensions of fractures. This scenario involves a fracture system with approximately 20 fractures enabling a sufficiently high flow rate of 110 kg/s combined with an acceptable projected temperature drop.

Extrapolating simulation results to other locations comes with a high uncertainty due to variations in lithology and rock properties. However, the sensitivity analysis shows that the model is most sensitive to changes in Young's modulus and the minimum horizontal stress. Based on a range of literature values for limestone, we do not expect a large difference in Young's modulus. However, as the lithology of the Zeeland Formation below Hoogeveen might have a higher content of clay, the value of Young's modulus might be lower.

The value of the minimum horizontal stress in the Zeeland Formation will very likely increase from LTG-01 towards Hoogeveen because the depth increases. However, if we assume that the ratio of the three principal stresses does not change, this will not have an impact on the fracture design.

Hydraulic fracturing with proppant is the most expensive option, however it provides the highest certainty to creating a producible reservoir. Cores and borehole images need to be analyzed in detail in order to assess the potential of shear -water- fractures, and a modelling study has to be performed. Tensile -propped- fracturing will serve as a backup scenario in case of failure of the shear -water- fracturing.

Power plant

A study executed by KEMA analyses the technical and economical feasibility of the surface part of the geothermal project. The power plant is a significant part of the investment; it represents one third of the initial investment costs and the greater part of the operational costs.

The binary cycle, consisting of a single organic Rankine cycle, is the best option for Hoogeveen. This type of power plant has a good efficiency at the expected temperature, a high availability and can be considered as proven technology.

For the cooling an induced draft wet cooling tower is selected. This type of cooling represents a balance between (1) the parasitic electrical load for the fans, (2) the height and visibility of the tower, and (3) the amount of water usage.

A net power production of about 14.1 MW_e is possible. This would meet more than the electricity demand of all households in the municipality of Hoogeveen. Without reducing the electrical capacity, also approx. 10 MW_{th} of residual heat for domestic heating can be supplied. It is also possible to supply more heat, in that case the electrical capacity will decline.

Business case

In this business case scenarios for (1) different fracture reservoirs and (2) percentage of residual heat delivered have been analyzed.

The base case scenario is based on a water fractured reservoir system without residual heat delivery. The Internal Rate of Return (IRR) for the base case is nearly 7% and the simple payout time (SPOT) is 13 years. The cost price of electricity is about 0,09 €/kWh.

The business case becomes better with increasing residual heat delivery. In case all residual heat (10 MW_{th}) is delivered, the IRR will be nearly 9% and the SPOT will be 9 years. In order to further improve the business case, more heat needs to be delivered. In case 30 MW_{th} is delivered –while reducing the electrical capacity with approx. 2 MW_e– the IRR increases to about 13%.

In a worst case scenario the water fractured reservoir will not generate enough flow rate and a propped fractured reservoir has to be implemented. The investment for a propped fractures reservoir is higher, the cost price will be about 0,11 €/kWh. The IRR for the worst case is nearly 6% and the SPOT is 17 years.

All technologies to be applied are separately considered as proven technology. However, the project is novel both in concept as well as in the drilling of a deep, horizontal section.

As a consequence, intrinsic uncertainties are large with their effects on economic parameters.

A sensitivity analysis on the base case including residual heat delivery, demonstrates that the drilling cost is the most important parameter. An increase of 50% of the drilling cost will result in an IRR of 7%, which is still a reasonable positive project return. From this analysis can be concluded that the base case IRR should be reported as 9 % ± 2% (2 standard deviations, 95% confidence interval).

In the base case scenario the CO_2 reduction is over 77.000 ton per year. The CO_2 reduction increases with residual heat delivery up to over 100.000 ton per year.
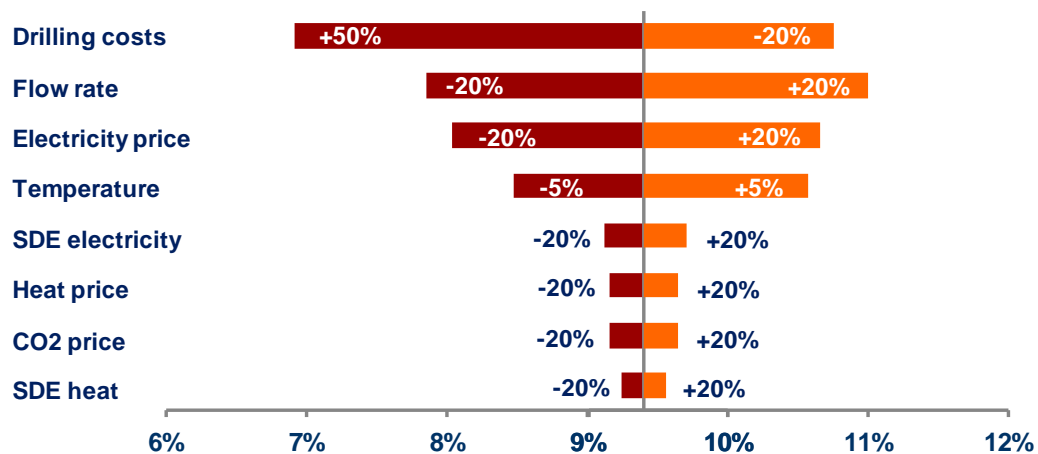
Figure 1.1   Tornado diagram with influence of main parameters on the IRR.

Plan for public acceptance

A plan to obtain support and acceptance from main stakeholders and public groups has been drafted. Three main categories of stakeholders have been identified: inhabitants, governmental bodies and environmental interest groups.

A number of communication events are proposed, ranging from 1-to-1 meetings, presentation meetings and (simple) mass media deliverables such as a website and press releases. For each event one or more stakeholder groups are being targeted.

The main messages to be delivered fall into two categories: emphasizing the advantages of a geothermal project and addressing the main issues, taking possible concerns seriously.

Conclusions and Recommendations

A number of recommendations result from this study which can be executed in one of the following phases.

New seismic lines need to be acquired in order to enable interpretation of the Zeeland Formation. This is a costly operation and is recommended to be executed in the phase 5 -exploration- (see table 1).

For this project, a suitable fracturing fluid needs to be found or developed. Further, the cheaper sand proppant will experience some crushing after the fracture closes thereby reducing newly gained fracture permeability. Both the fracturing fluids and effect of crushing will be partly studied in phase 3 -flow rate risk- and in phase 6 -preparation-.

The potential of shear -water- fracs is very high. A shear -water- frac treatment is cheaper as it uses less expensive fracturing fluids and low to zero proppant masses. An inventory of requirements, advantages, limitations and risks needs to be set up. Shear fracturing will be a substantial part of the next phase.

The rock properties of UHM-02 and other wells need to be determined from the logs of the well. They need to be compared to LTG-01 to see to what extent the properties of the Zeeland Formation vary spatially. Laboratory measurements need to be performed on the available cores in order to form a database of mechanical rock properties of the Zeeland Formation. Also, the effects of shear fracturing on Zeeland Formation cores can be simulated in the lab.

Although natural fractures have been observed in all investigated cores of the Zeeland Formation, it is unlikely that they will contribute significantly to flow since most of them are cemented. A more or less open natural fracture network is therefore likely absent at the locations of the cores. Also, the orientation and dimensions of the hydraulically generated fractures might not be affected if the natural fractures are not abundantly present. This is a common assumption on which the used industry model software is based. However, well log and core analysis should be performed on LTG-01 and UHM-02 to quantify the characteristics of the natural fractures and to assess whether this assumption holds. The characteristics and orientation of a natural fracture network at Hoogeveen are uncertain.

Proposed Project phases

Table 1.2   Project phases

Phase	Description
1	Feasibility – First assessment
2	Feasibility – Potential
3	Feasibility – Flow rate risk
4	Feasibility – Other risks
	- Pre FID -
5	Exploration
6	Realization preparation
	- Final Investment Decision (FID) -
7	Realization

For the total project six phases have been defined to realize a geothermal installation. This study concerns phase 2, the next steps in the action plan are on phase 3 - flow rate risk.

Next phase – Flow rate risk

Please find below an overview of the next phase of activities.

In the decision tree, the various options (shear/water, tensile/propped) are explored for the creation of the subsurface heat exchanger. The decision tree is converted into a statistical model and the models of the various options are integrated. With a Monte Carlo function, the distribution of the output will be determined in terms of flow rate and productivity.

Laboratory core analysis -special core analysis- will be carried out to gain a better understanding of the mechanical characteristics of the Zeeland Formation. Core analysis will also provide information on natural fracture properties. The information will be translated to the properties of the formation below Hoogeveen.

Laboratory tests can also provide insights into the mechanisms behind shear fracturing and the effects of this method on Zeeland Formation cores.

On the basis of boreholes in the vicinity of Hoogeveen as well as regional data, the direction and magnitude of the stress field will be determined. Slip and dilation tendencies are determined on the basis of stress magnitude and stress directions, which indicate to what extent the fractures are 'open' or not.

A model is established to determine the output (flow rate, productivity) of a water / shear fracture system. Important factors are the shear stress, the quantity of injected water and the fracture surface properties of the rock. Also a model is established to determine the output of a tensile/propped fracturing system. Important factors here are Young's modulus, Poisson ratio, the stress situation and permeability.
For all input parameters of the above two models statistical distributions are determined. Already available data, the basic data or literature data will be applied. In extreme cases, conservative assumptions are made.

2 Introduction

Goal

The town of Hoogeveen is home to 55.000 inhabitants. The municipal counsel of Hoogeveen has a target to reduce CO2 emissions and to convert the energy supply to 8% renewable energy in 2015. Because of their interest in cost-efficient and clean energy, the municipality has asked IF Technology to carry out a feasibility study.

This feasibility study is carried out to assess the potential of deep geothermal energy for electricity production for the households of the city of Hoogeveen.

Deep geothermal energy

Conventional geothermal energy is a source of clean energy in the Netherlands with several commercial projects being realized.

Deep geothermal energy is a novel technique that has only been applied on a small scale in the world. However, the concept shows great potential due to the high temperatures from which electricity can be produced. For more information on deep geothermal energy you are referred to the website http://en.wikipedia.org/wiki/Geothermal_energy.

For electricity or steam production a suitable geological reservoir is required. The reservoir has to meet certain requirements such as depth, temperature, thickness, brittleness, secondary porosity etc. Studies on the potential of the deeper geological formations in the Netherlands have already been performed (IFWEP, 2011).

One of the results of the above study is that the potentially most suitable reservoir for deep geothermal energy is the Zeeland Formation. These Early Carboniferous deposits consist of limestones and dolomites. They are probably present at large depths in most of the Netherlands and therefore have a high temperature. Although the primary porosity at these depths is likely to be very low, the brittleness of the carbonates makes them suitable for reservoir stimulation.

Because of its suitable reservoir properties, the focus in this study is on the limestones and dolomites of the Early Carboniferous. Because of its low primary porosity and permeability, a conventional geothermal system is not applicable. The primary drilling target is therefore a fault zone because of its increased permeability. This study pays attention to the location and potential of fault zones in the vicinity of Hoogeveen.

If fault zones are not an option, a subsurface heat exchanger can be created by reservoir stimulation. This comprises a network of fractures from injection to production well. The effects of hydraulic fracturing of the limestone are studied.
Formations above and below the Zeeland Formation are not suitable for either a conventional or unconventional geothermal system as they consist mainly of claystones with intercalating thin sands.

Outline of the report

The layout of this report is shortly described. The geology below Hoogeveen is described in chapter 3. A most suitable formation for application of deep geothermal energy is chosen based on lithology, depth, thickness and temperature. Estimates of the depth and thickness of the target formation are made based on regional data as well as on interpretation of seismic data.

Core and log measurements are evaluated in the next chapter to find a relationship between the porosity and permeability of the target formation. Chapter 5 illustrates the potential of fault zones and describes if these kind of structures can be found below Hoogeveen and if so, what are their characteristics. In chapter 6, a modeling study is performed to study the effects of a hydraulic fracturing treatment on the target formation. An ideal fracture design is the result of this study.

In chapter 7, the fluid and heat flow properties of the designed fractures are put into a reservoir model and their effects are evaluated. Chapter 8 gives a preliminary well design based on the geological data. Chapters 9 and 10 focus on the power plant and financial aspect of a deep geothermal project, applied to the location of Hoogeveen. Chapter 11 presents a plan for public acceptance of realizing this geothermal project. The last chapter contains conclusions and recommendations from the results of this study..

3 Geology

3.1 Structural setting

Below a short summary is given of the structural and depositional history from the Carboniferous to present. An overview of the tectonic phases and their related plate-tectonic events is given in figure 3.4.

3.1.1 Carboniferous

A horst-and-graben topography dominated the Southern North Sea region from the Middle Devonian. This topography was triggered by back-arc rifting (Geluk et al., 2007). Differential subsidence of the horst-and-graben topography during the Dinantian strongly influenced facies distribution. The topography effectively stopped the clastics from the Mid North Sea High coming in to the carbonate realm in the northern and southern Netherlands. Widespread carbonate deposition took place in the Netherlands.

The depositional model by Geluk et al (2007) and Kombrink (2008) includes a series of fault bounded carbonate platforms and basins (see Figure 3.1).

Figure 3.1   Map of Early Carboniferous structural elements. Location of Hoogeveen (black circle) in the basin. From Geluk et al., 2007.

An older publication by Ziegler (1990) shows a different view on the structural environment during the Early Carboniferous (figure 3.2). Ziegler postulates the presence of a coherent carbonate platform stretching from England to Poland in the Early Carboniferous with a SE-NW graben structure crossing the Netherlands. This is significantly different from the theory of isolated platforms with interspersed basins from Geluk et al (2007) and Kombrink (2008).
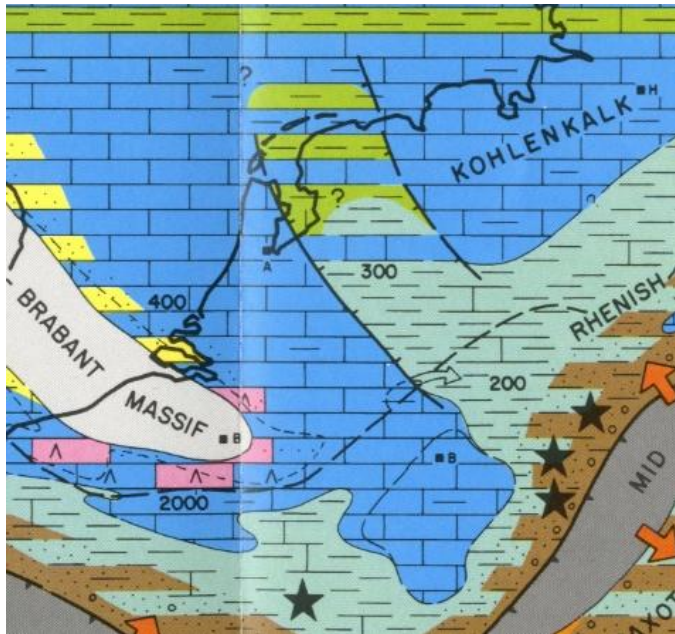
Figure 3.2   Facies map of the Netherlands and surroundings in the Dinantien (Ziegler, 1990).

Both figures show that during the beginning of the Carboniferous Hoogeveen was situated in a basin. Figure 3.1 indicates the presence of the Texel-IJsselmeer High. This high is a prominent structural element that has had a lot of influence on the local depositional history. This high is believed to have been present since Paleozoic times and is part of a number of similar NW-SE trending structural highs that dominated the Netherlands area. Paproth et al (1986) argues that the long-lasting effects of NW-SE trending structures in the Netherlands are inherited from Precambrian basement. Ziegler (1990) does not show the presence of this high, but nonetheless Hoogeveen can be found in the graben structure.

It is believed that during the Dinantian the highs -whether isolated of widespread- formed shallow platform areas where thick carbonates were deposited. In the basins a succession of dominantly dark siliceous limestones was deposited (Kombrink. 2008). Sea level lowering during and at the end of the Visean -end of Dinantian- resulted in karstification of these platforms due to exposure.

During the Late Carboniferous Hoogeveen was in a shallow basin part of the Eems Deep (figure 3.3). Namurian transgression caused the carbonate platforms to gradually become flooded allowing deposition of marine influenced delta and pro-delta sediments covering the platforms and filling the basins. Fluvial influence increased during the Westphalian A and Westphalian B and swampy areas between rivers produced peat on a large scale.

These peat/coal sequences, the Maurits Formation, form the major source rock for the Dutch natural gas reservoirs.
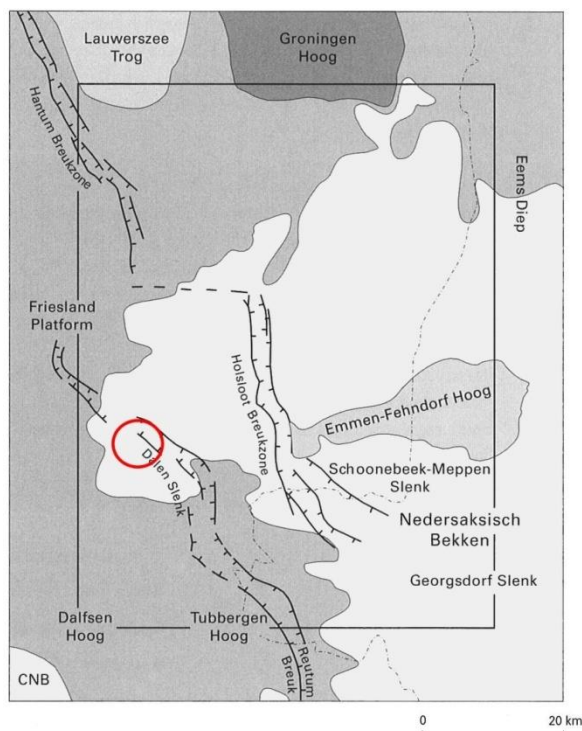
Figure 3.3   Map of regional structural elements. Location of Hoogeveen (red circle) in the basin is also given. From TNO-NITG, 2000.

From the Westphalian C sedimentation increasingly concentrated east of Hoogeveen. Compressional forces reactivated a number of NW-SE directed fault zones. Deposits from the Westphalian D and Stephanian are absent at Hoogeveen largely due to erosion during the Early Permian.

3.1.2   Permian

The erosional event at the Early Permian marks the transition to the Kimmerian tectonic phases that accompanied the breakup of the supercontinent Pangea and the opening of the Atlantic Ocean which took place during the Late Triassic to Early Cretaceous. Wrench- and tear movements in the Early Permian caused strong subsidence in the Eems deep whilst uplifting occurred on the Friesland platform and Groningen Hoog (figure 3.3). At the end of the Early Permian tensional forces with an EW direction led to formation of deep faults in combination with volcanism east of Hoogeveen.

A large basin, stretching from the UK to Poland was formed in the Late Permian. The Rotliegend Group was deposited in this basin. Hoogeveen was situated on the edge of this basin, where desert-like conditions dominated. Due to fast subsidence of the basin and periodic influxes of seawater in the Late Permian, thick Zechstein salt and carbonate sequences were deposited.

3.1.3 Triassic

During the Early Triassic a vast, flat floodplain developed in the area of Hoogeveen. Under the influence of steady subsidence a N-S trending graben structure formed with a lacustine to playa depositional environment. Clastics originated from the Varistic mountains situated to the south. Late in the Early Triassic the Hardegsen phase caused erosion of around 100 m in the Eems Deep. Hardegsen phase comprised around three short lived extension tectonic pulses alternated by longer periods of gradual subsidence. Hardegsen phase also caused initial movement of the Zechstein salt in this area.

The disintegration of Pangea accompanied an increase in tectonic instability from the Middle Triassic to the Early Cretaceous. The Kimmerian phases dominated much of the Northwest European structural evolution and are ascribed to the major hiatuses in the stratigraphic sequence.

3.1.4 Jurassic

Differential subsidence continued during the Late Jurassic and Early Cretaceous to form the Nedersaksen Basin. Hoogeveen is on the North-western edge of the structural element. Stagnation in the marine basin resulted in deposition of sediments rich in organic material i.e. the Posidonia Shale Formation.

The orientation of the fault structures (E-W) changed with respect to the Late Triassic. The Late Kimmerian Phase, characterised by ENE-WSW directed tension, led to the formation of the Lower Saxony Basin. Subsidence continued through the Late Jurassic.

3.1.5 Cretaceous

The Cretaceous is characterised by gradual sea level rise which reached its highpoint in the Late Cretaceous. The Cretaceous transgression was probably related to the increase in ocean spreading causing increase in volume of the mid-oceanic ridges.

Inversion tectonics of the Subhercynian pulse led to uplift of the Lower Saxon Basin and subsidence of the former highs as Europe and Africa collided. At the end of the Cretaceous regional basis subsidence again commenced allowing deposition of the upper Chalk Group.

3.1.6 Cenozoic

Sedimentation during the Tertiary was heavily influenced by fluctuations in the sea level and a couple of tectonic pulses and is largely influenced by the formation of the North Sea basin. To this day the basin continues to determine sedimentation. Ongoing subsidence and sea level rise has led to de deposition of approximately 3000m of sediment in the centre of the basin. However, around Hoogeveen subsidence has been much more moderate.

Throughout the Tertiary a number of tectonic phases related to the Alpine orogeny have also caused a number of intermittent erosional events leading to hiatuses in the Upper North Sea Supergroup. Tertiary fault movements concentrated in the Late Kimmerian faults zones such as the Hantum faultzone, the Dalen Graben en de Holsloot faultzone (see figure 3.3).
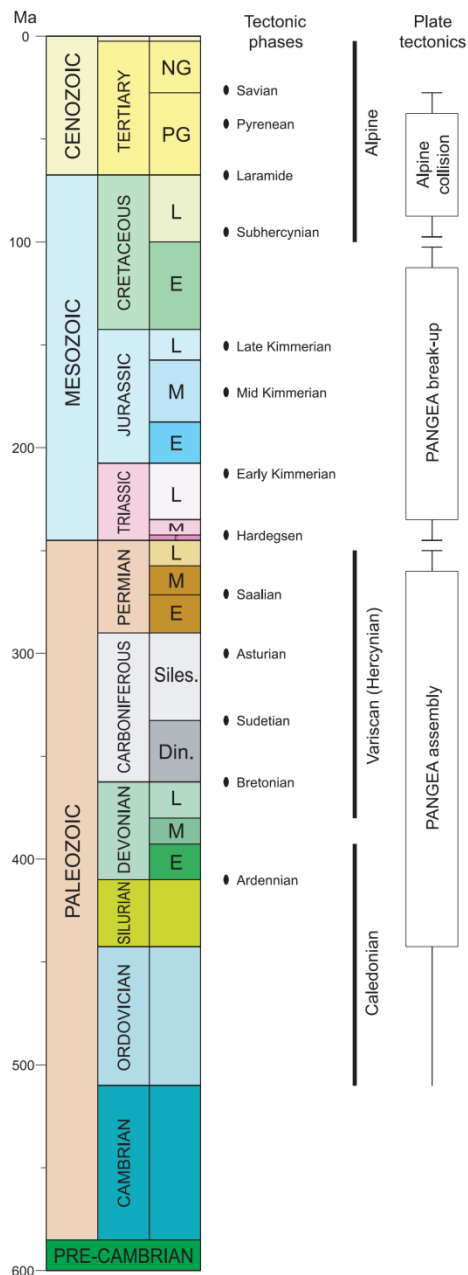

Figure 3.4   Geologic time scale with tectonic phases in the Netherlands and their relation to plate-tectonic events (from De Jager, 2007)

3.2   Stratigraphy and lithology

As mentioned in the introduction, the focus of this study is on the limestones and dolo-mites of the Early Carboniferous. This chapter describes the available data on those deposits from wells, seismic data and literature.

3.2.1   Stratigraphy

The Early Carboniferous in the Netherlands is represented officially by two groups. According to the Southern Permian Base Atlas (Doornenbal & Stevenson, 2010) and Geluk et al (2007) these are: the Carboniferous Limestone Group and the Farne Group. These groups have been subdivided into formations and members, which will be addressed shortly. Another common name for the Carboniferous Limestone Group is the Kolenkalk Group. This name occurs in German and Dutch literature, but is not included in the no-menclature. For this study, this name is rejected. The Kulm facies is originally from Germany. These deposits are possibly equivalent to the Early Carboniferous deposits found in the Netherlands. A description of the three groups is given below.

-   The Farne Group is deposited in a paralic -at or near sea level- to shallow-marine environment. The deposits comprise of claystones and sandstones. Minor coal seams and a variable amount of limestone and dolomite beds are also encountered. The group is divided into three formations, but none of them have been distinguished in Dutch onshore wells. Overall, the group is characterized by an increased clastic input compared to the Carboniferous Limestone Group.

-   The Carboniferous Limestone Group contains light-grey, brown and black carbonates. Variable intercalations of claystones and siltstones are also found. It is likely that structural highs and fault zones formed shallow platforms during the Early Carbonifer-ous. These were bordered by fault-bounded basins (Geluk et al, 2007). The group is represented by the Zeeland Formation that is subdivided into three members: the Go-eree, Schouwen and Beveland Member. The Beveland Member is characterized by a high content of dolomite and dolomitic limestone.

-   The starved-basin or Kulm facies encountered is characterized by thin-bedded, partly silicified limestone and dolomite. In Münsterland-1 these consists of different kinds of *Schiefers* (or shales) and *Kieselkalk* or (quartz-rich limestone). Geluk et al (2007) notes it is likely that this facies also occurs in the Netherlands in the basins between the carbonate platforms.

3.2.2   Wells

In order to produce at high temperatures, depths of over 5,000 m have to be reached. Data from the deeper subsurface beyond 4,000 m depth, are scarce. Early Carboniferous deposits are found in a small number of wells in the Netherlands. In the very south of the country, the formation occurs relatively close to the surface, less than 1,000 m depth. It is therefore penetrated in approximately ten wells, specifically drilled for mining purposes. Towards the north the depth of the formation quickly increases.

The number of deep onshore wells in the Netherlands is very limited. Early Carboniferous deposits are found in only three deep wells; just 30 km into Germany a fourth well also reached this formation.

The three deep wells in the north and east of the Netherlands penetrating the Early Carboniferous are LTG-01, UHM-02 and WSK-01. The German well Münsterland-1 also penetrates the Early Carboniferous and is therefore also included in the analysis. The Early Carboniferous is found at great depths in all four wells. It is therefore expected that these deposits occur at great depth below Hoogeveen. Figure 3.5 shows the locations of the four deep wells mentioned above, the location of Hoogeveen and two more wells in the southern parts of the Netherlands. Including in the figure are depth contours lines. This interpretation of the depth of the top of the Early Carboniferous deposits is based on the structures from figure 3.1 and regional seismic research (Geluk et al., 2007).
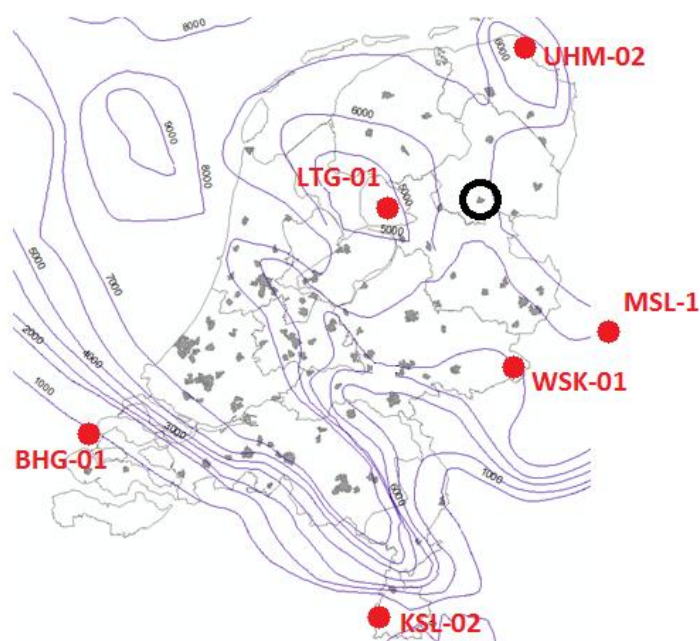
Figure 3.5   Depth map including the location of Hoogeveen (black circle), the four
        wells that penetrate the   Early Carboniferous deposits closest to
        Hoogeveen, and two southern wells (adapted from Geluk et al, 2007).

The shallower wells penetrating the Early Carboniferous deposits - in the provinces of Limburg (KSL-02) and offshore of Zeeland(BHG-01) - are not analyzed in this study. The reason for this is that they are far from the project location and reached the objective at much shallower depths. Future studies could include analysis of the Early Carboniferous deposits from these wells as well.

3.2.3 Lithology

In the lithology description different types of limestone are being distinguished. The limestone classification used in this study is adopted from Wright (1992), who revised the most widely used classification scheme of Dunham (1962). Figure 3.6 shows the different types of limestone.

Predominantly limestones of depositional type have been found in the four deep wells. If a limestone is classified as the depositional type, for example a calci-mudstone, it does not exclude the presence of bioclasts. Appendix 1.1 describes the terms that are used for limestones and other sediments that are encountered in the next paragraphs. Appendix 1.2 shows the different environments of deposition for carbonates as they are encountered in the Carboniferous Limestone Group.

DEPOSITIONAL				BIOLOGICAL			DIAGENETIC			
Matrix-supported (clay & silt grade)		Grain-supported		In situ organisms			Non-obliterative			Obliter- -ative
<10% grains	>10% grains	with matrix	no matrix	Encrusting binding organisms	Organisms acted to baffle	Rigid organisms dominant	Main component is cement	Many grain contacts as microstylol- -ites	Most grain contacts are microstylol- -ites	Crystals >10μm
Calci- -mudstone	Wackestone	Packstone	Grainstone	Boundstone	Bafflestone	Framestone	Cementstone	Condensed grainstone	Fitted grainstone	Sparstone
	Floatstone	Rudstone								Crystals <10um
	Grains >2mm									Microspar- -stone

Figure 3.6   The revised classification of limestones (Wright, 1992)

Not included in the classification are secondary processes affecting the limestones. The two most significant secondary processes are karstification and dolomitization. Indications of dissolved limestones have been found in some of the deep wells, mostly in the top of the formation. In addition, vuggy (secondary) porosity, caused by leeching, has been found in the deep wells. Dolomites have also been found in most of the deep wells. Appendix 1.3 describes these two processes in more detail. This study only briefly addresses this subject. Analysis of mud losses and the difference in rock properties between dolomite and limestone can be part of future studies.

In most wells, fossil finds have been reported. Fossils can be correlated to their depositional environment. A brief description is given in appendix 1.4 of the type of encountered fossils.

The lithostratigraphy is described for each of the deep wells and subdivided into sections. The lithostratigraphic descriptions can be found in appendix 2.1. A visualization of the lithostratigraphy of each well can be found in appendix 2.2.

3.3 Seismic interpretation

This chapter describes the process of interpreting 3D seismic data in the vicinity of Hoogeveen to locate the Zeeland Formation and to determine its depth and thickness.

3.3.1 Available data and method

For the seismic interpretation data were used from the following sources:
- Filtered and scaled 3D migration data, time volume
  o L3NAM1989G (Hoogeveen Zuid)
  o L3NAM1989H (Hoogeveen Midden)
  o L3NAM1989I (Hoogeveen Noord)
  o L3NAM1993B (Hijken)
- Filtered and scaled 2D data, time volume
  o L2DGP1986A, lines 8606B and 8606C
- Nearby wells
  o DWL-02
  o ELV-101
  o GRL-01
  o GSB-01
  o HBG-02-S1
  o HGW-01
  o LTG-01
  o WYK-21

The seismic interpretation was performed with the program OpendTect, version 4.2.0c .

Seismic surveys

A merged dataset has been made from four 3D surveys: Hijken, Hoogeveen Noord, Hoogeveen Midden and Hoogeveen Zuid, all publicly available 3D datasets. The proce-dure of merging was to first extend or cut all the surveys to 1251 samples. The second step was to adjust the gain of all surveys to match the Hoogeveen Midden survey. Finally, the surveys were cut according to the area of interest and then combined (see table 3.1).

Table 3.1   Overview of the 3D survey merge.

Survey	Original crossline range	New crossline range	Gain factor
L3NAM1993B	6,150 – 7,360	6,161 – 7,360	2.16
L3NAM1989I	5,770 - 6,370	5,860 – 6,160	$1.20*10^{-5}$
L3NAM1989H	5,500 – 5,940	5,580 - 5,859	1.00
L3NAM1989G	5,213 – 5,680	5,213 – 5,579	2.09

The seismic dataset is a post-stack time migrated volume recorded and stored according to the SEG polarity convention, i.e. negative numbers represent an increase in acoustic impedance. Conforming to the European display variant, negative numbers, representing hard kicks, are displayed as white. All figures in this report are displayed according to this European variant. Below the main characteristics of the merged dataset are given.

- Inline* range: 7,065 - 8,595
- Crossline* range: 5,213 - 7,360
- Z range: 0-5,000 ms with a sampling rate of 4 ms
- Bin size: 25m x 25m

Figure 3.7 shows the positions of and the area covered by the original four surveys. Also shown are the surface locations of the wells used in the seismic interpretation.
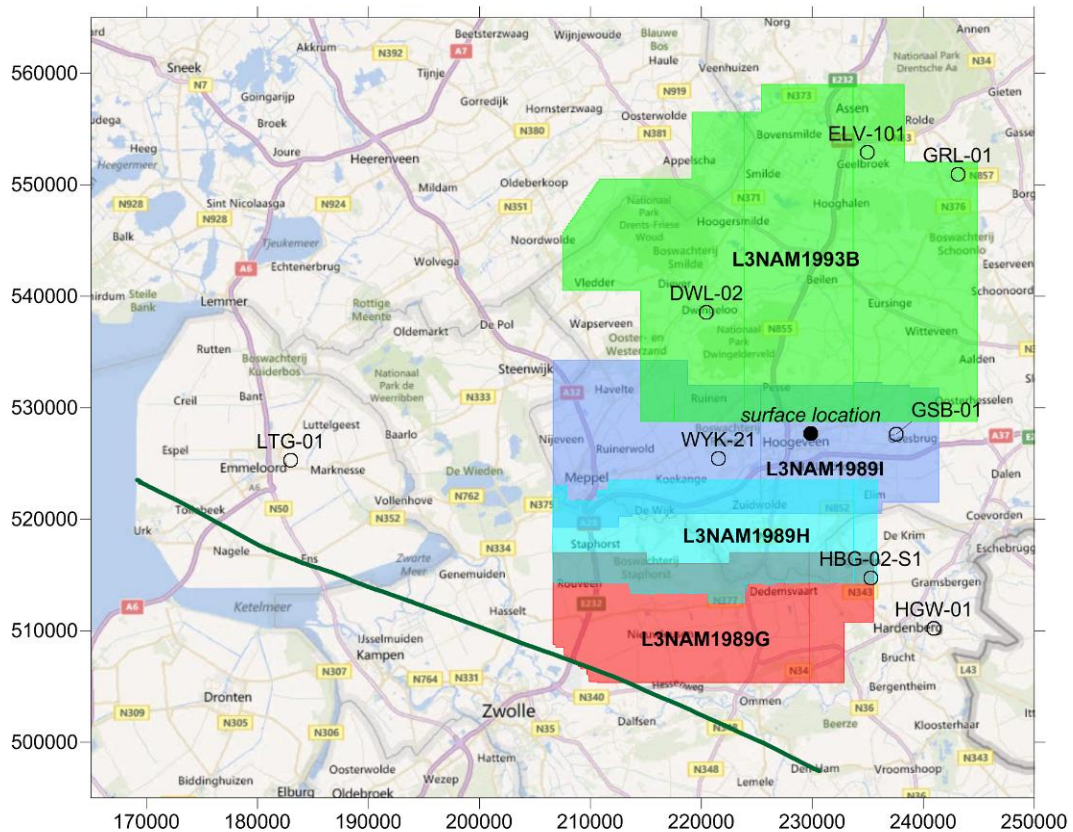

Figure 3.7   Map of the area showing the original four surveys used in the merge. Shown are Hijken (green), Hoogeveen Noord (purple), Hoogeveen Midden (blue) and Hoogeveen Zuid (red). All wells used during the seismic analysis are shown as open circles. The surface location is marked by the closed circle. The green line indicates the position of the 2D lines 8606B and 8606C.

Boreholes

A total of 7 wells have been used during the interpretation. Deviation- and lithology data as well as completion logs were obtained directly from publically available data. In order to perform depth to time conversion, different methods were applied to different wells in accordance with data availability (see table 3.2).

Well specific depth to time conversion tables are available from the public domain (www.nlog.nl) for the wells GRL-01, GSB-01, HBG-02-S1, HGW-01 and WYK-21. It is known however that these tables may not represent an optimum T-Z relation for well to seismic matching purposes. For the wells DWL-02 and ELV-101 a new depth to time conversion model was made. This was done with the use of the regional velocity model VELMOD-1 (TNO-NITG 2002).

Table 3.2   Overview of the wells used during the seismic interpretation.

Borehole	x-coordinate (RD)	y-coordinate (RD)	Spud year	Deepest formation	VSP*/CS**	Time-depth model
DWL-02	220,465	538,568	1954	DCCB	-	VELMOD-1
ELV-101	234,956	552,881	1971	DCHL	CS	VELMOD-1
GRL-01	243,130	550,934	1980	DCCU	CS	nlog
GSB-01	237,559	527,629	1992	DCCU	VSP	nlog
HBG-02-S1	235,288	514,731	1967	DCCR	-	nlog
HGW-01	240,959	510,211	1987	DCCU	CS	nlog
LTG-01	183,004	525,283	2004	OB	VSP	nlog
WYK-21	221,563	525,439	1981	DCCU	CS	nlog

*Vertical Seismic Profile
** Checkshot data

3.3.2 Horizons

Ten seismic markers (i.e. horizons) were identified and mapped based on their geological relevance and seismic character. These comprise Base North Sea Super Group (BNS), Base Chalk Group (BCK), Base Rijnland Group (BKN), Base Niedersaksen Group (BSK), Base Altena (BAT), Base Lower Germanic Trias Group (BRB), Top Z2 Basal Anhydrite Member (TZEZ2A), Base Zechstein Group (BZE) and Base Upper Rotliegend Group (BRO). The identification of reflections associated to each marker was based on experience and on their positions in time at well locations. Synthetic seismograms have not been created due to the limited time available. Consequently proper well to seismic matches have not been carried out.

The top and base of the Zeeland Formation could not be unambiguously identified in the seismic. Consequently they were derived on the basis of the base of the Zechstein Group combined with long distance well stratigraphic data and correlation along 2D seismic lines.

Figure 3.8 displays the results of the mapping in the 3D model for the Top Z2 Basal An-hydrite Member. The main characteristics of all the mapped horizons are given in table 3.3.
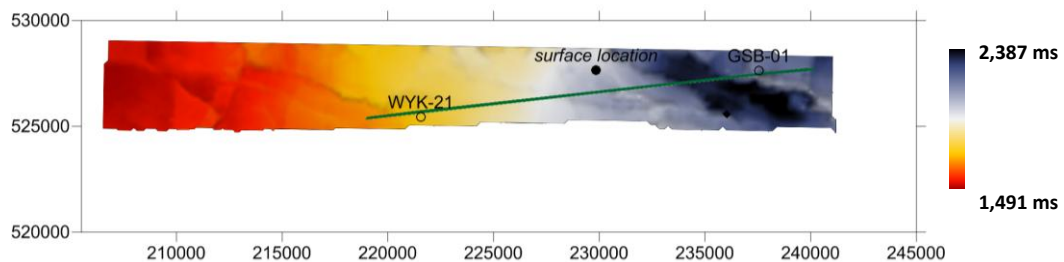
Figure 3.8   Two way traveltime map of the Top Z2 Basal Anhydrite Member. The target surface location and the surface locations of the wells WYK-21 and GSB-01 are also shown. The green line represents the random line presented in figure 3.9.

Table 3.3   Characteristics of the interpreted horizons.

Horizon	Seismic Character	Correlation	Mappability
Base North Sea Supergroup	Hardkick; unconformable on underlying Lower Chalk Gr.	Weak	Poor
Base Chalk Group	Softkick	Average	Average
Base Rijnland Group	Hardkick; unconformable on underlying Nierdersaksen Gr. and Altena Gr.	Good	Good
Base Niedersaksen Group	Hardkick	Average	Average
Base Altena	Hardkick	Good	Good
Base Lower Germanic Trias Group	Softkick	Poor	Poor
Top Z2 Basal Anhydrite Member	Hardkick	Good	Very good
Base Zechstein Group	Softkick	Poor	Poor
Base Upper Rotliegend Group	Hardkick; Hercynian unconformity	Poor	Poor / Very Poor
Top Zeeland Formation	Hardkick	Very poor	Very poor
Base Zeeland Formation	Softkick	Very poor	Very poor

3.3.3   Faults

The seismic shows that the area of investigation is considerably faulted. Major faults have been mapped which were found to be most dominant for this area. Figure 3.9 displays a random line crossing the approximate target location and the wells WYK-21 and GSB-01, facing south (see map figure 3.8). Most obvious is the main fault which displaces Tertiary to possibly the Carboniferous deposits. Variations in sediment thickness seem to indicate fault activity since late Triassic and inversion tectonics during Jurassic and Cretaceous times. Please note that the Base Upper Rotliegend Group has not been interpreted on this line. This is due to the fact that the Slochteren Formation along this section is very thin which makes it difficult to differentiate between Base Zechstein Group and Base Upper Rotliegend Group.
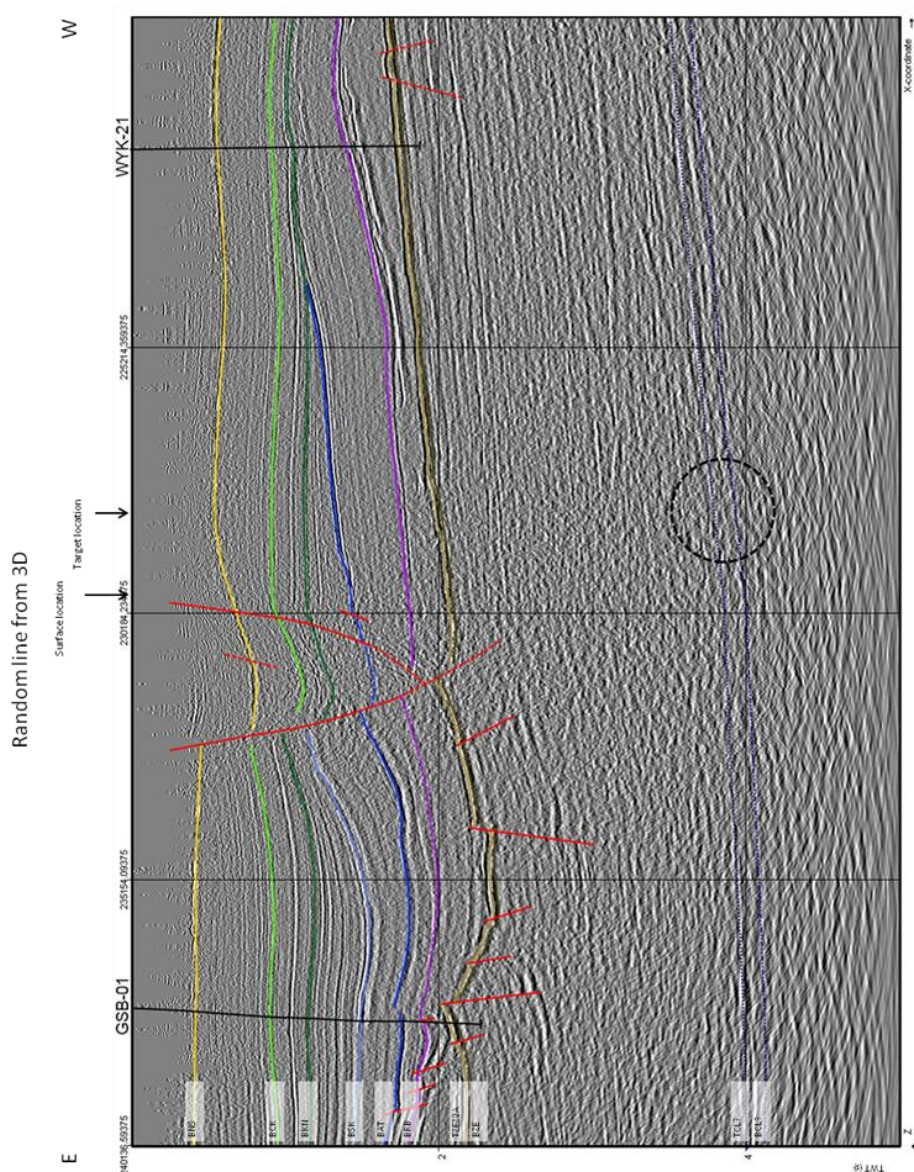
Figure 3.9   Interpretation of a random line through the wells GSB-01 and WYK-21 and the
target location at depth (black circle). Interpretations shown: Base North Sea Su-
per Group (yellow), Base Chalk Group (light green), Base Rijnland Group (dark
green), Base Niedersaksen Group (light blue), Base Altena Group (dark blue),
Base Lower Germanic Trias Group (purple), Top Z2 Basal Anhydrite Member
(light brown), Base Zechstein Group (dark brown). Tentative interpretations of the
Top and Base Zeeland Formation are also given (dotted purple). Faults are
displayed in red. Base Upper Rotliegend Group (BRO) could not be made out on
this section (see text above).

A similar analysis has been applied to the data (see figure 3.10). Here, similarity represents the degree of analogy between neighbouring traces. Generally, similarity is low along faults. Figure 3.10 shows similarity projected on Top Z2 Basal Anhydrite Member. A clear distintion can be observed between the East and the West. In the West, overall similarity is quite high and individual fault traces can be distinguished. Towards the East, similarity is overall much lower and individual faults are hard to make out. The similarity analysis also illustrates the overall NW-SE trend of the major faults.
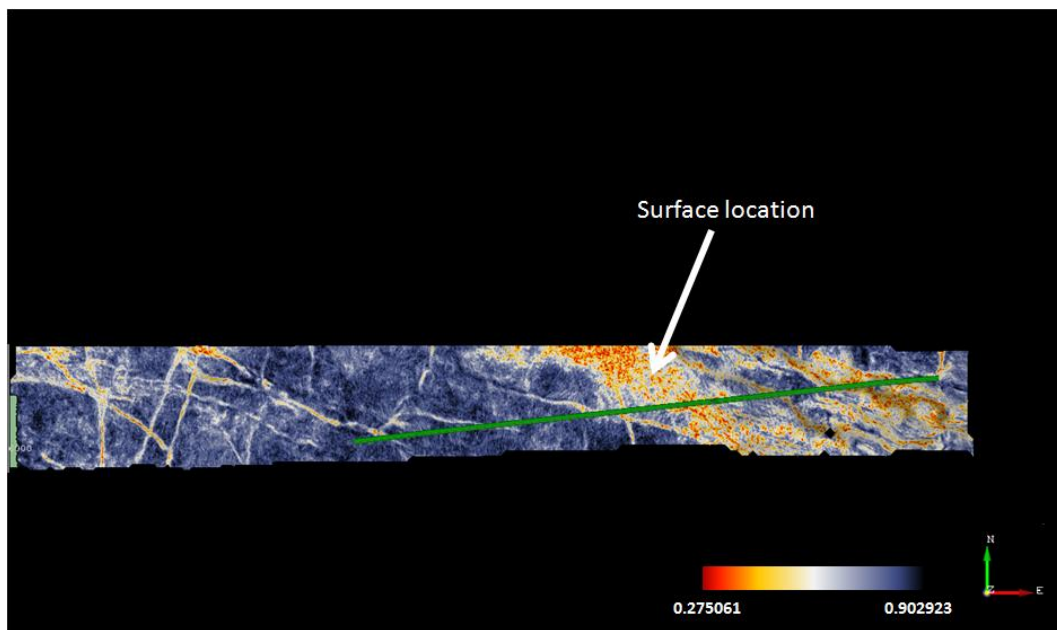
Figure 3.10   Seismic similarity as projected on Top Z2 Basal Anhydrite Member. Blue colours indicate high similarity and coincide with good lateral reflector continuity. Red colours indicate low similarity and are related to fault structures. The green line indicates the position of the random line presented in figure 3.9.

3.3.4   Time-depth model

Due to time constraints, a local velocity model could not be derived. Instead, a regional velocity model has been applied. This layer cake based model which utilizes linear instantaneous velocity approximations (TNO-NITG 2002). A linear velocity model is suitable when sediments are mainly affected by compaction under the load of overburden.

Era	Period	Lithostratigraphy (S → N)	Sublayers	Main layers	Lithology
CENOZOIC	Neogene	Upper North Sea Group – NU	a	1	Clays, silts, fine- to coarse-grained sands and sandstones
	Paleogene	Middle North Sea Group – NM Lower North Sea Group – NL	b		
MESOZOIC	Cretaceous	Chalk Group – CK		2	Mainly limestones (chalk), also marls and claystones
		Rijnland Group – KN — Holland Formation – KNGL	a	3	Argillaceous and marly deposits, sandstone beds
		Rijnland Group – KN — Vlieland subgroup – KNN	b		
		Schieland Group SL — Schieland, Scruff and Niedersachsen groups SL, SG, SK		4	Claystones, sandstones, limestones, evaporites and coal seams
	Jurassic	Altena Group – AT		5	Argillaceous deposits with calcareous intercalations and clastic sediments
	Triassic	Upper Germanic Trias Group – RN	a	6	Silty claystones, evaporites, carbonates, sandstones and siltstones
		Lower Germanic Trias Group – RB	b		
PALEOZOIC	Permian	Zechstein Group – ZE		7	Evaporites and carbonates
		Upper Rotliegend Group – RO		8	Coarse and fine-grained clastic sediments
		Lower Rotliegend Group – RV			
	Carboniferous	Limburg Group – DC		9	Fine-grained siliciclastic sediments and coal seams
		Carboniferous Limestone Group – CL			

Figure 3.11   Graphical representation of the used velocity model compared to the lihological column (from TNO, 2007).

The model applied here comprises 10 individual layers (see figure 3.9; the tenth layer comprises the Zeeland Formation). The linear increase in velocity in the upper eight layers is described according to:

$$V_z = V_0 + k \cdot z$$

Where V_z is the instantaneous velocity at depth z and V_0 and k are the intercept and slope of the relation. Table 3.4 presents the variables belonging to the upper eight groups. The thickness of the Zechstein Group is determined by:

$$d = (V_h \cdot \Delta t) + c$$

Where d is thickness (m), V_h is interval velocity of halite (4,402 m/s), Δt is time interval zechstein (s) and c is a constant (25.7).

For the Limburg Group an interval velocity of 4,200 m/s is adopted from Kombrink et al. (2010). This interval velocity is derived from the sonic log from the well Tjuchem-02 (TJM-02) and is supported by checkshot measurements taken from the same well. Please note that the entire Limburg Group at TJM-02 is situated much shallower than likely is the case at Hoogeveen which may result in an underestimation of velocity. However, this currently is the best available estimation based on direct measurements. A velocity model for the Limburg Group with a linear depth dependency has been presented in VELMOD-2 (Dalfsen et al., 2007; TNO-NITG 2007). This model results in higher velocities at Hoogeveen, but is based on data derived almost exlusively from the upper formations of the Limburg Group. Checkshot measurements from TJM-02 suggest that the lower Limburg Group formations such as the Epen Formation are characterised by relatively low velocities. Also, considering the depth of the Limburg Group at Hoogeveen, an extrapolation of the data is needed (Dalfsen et al., 2007). At great depths, an extrapolation of a velocity model with a linear depth dependency quickly leads to an overestimation of velocity because the rate of compaction slows exponentially. With regards to the above, the VELMOD-2 velocity model is regarded as the maximum estimation whilst the interval velocity of 4200 m/s is regarded as close to a minimum estimation. Since the interval velocity was derived based on well data covering the entire Limburg Group, it is deemed the best approximation.

Based on literature an interval velocity of 6,000 m/s is assumed for the Carboniferous Limburg Group (Smith et al., 1998). This velocity is consistent with typical tight limestone seismic velocities. Maximum and minimum velocities are therefore assumed to be 6,500 m/s and 5,500 m/s respectively.

Table 3.4   Regional velocity model based on the instantaneous velocity model (TNO-NITG 2002, TNO-NITG 2007) < geef in deze table de afkortingen aan die je in de volgende table gebruikt>

Group	V_0 [m/s]	k [1/s]
North Sea Supergroup	1,696	0.49
Chalk Group	2,092	1.08
Rijnland Group	2,020	0.63
Nedersaksen Group	2,285	0.57
Altena Group	2,093	0.48
Upper- and Lower Germanic Trias Group*	3,200	0.37
Upper Rotliegend Group	2,979	0.35
Limburg Group**	3,400	0.27

*V_0 and k values based on VELMOD-2

**maximum velocity model; V_0 and k values based on VELMOD-2

3.3.5   Time-depth model quality control

The horizons created in the seismic time volume have been converted with respect to depth at the target location (at depth) by applying the velocity model described above. In order to assess the quality of the seismic interpretation and validity of the velocity model, a quality control has been performed.

For the quality control, the true vertical depth of the base of each group, as recorded in the wells, is compared to the true vertical depth at the well which follows from the seismic interpretation after application of the velocity model. Since none of the wells in the imme-diate surroundings penetrate the Zeeland Formation, the time-depth model for could not checked for the deepest markers. The error related to the parameter true vertical depth in the well is assumed negligible, because it represents direct observations from the well. The results indicate an error range between -2 % and +5% for all horizons. Tables 3.5 and 3.6 shows the results for the wells GSB-01 and WYK-21 respectively. Evident from tables 3.5 and 3.6 is the observation that the error is quite low and the error does not appear to increase considerably with depth. Please note that the errors presented here are the result of inaccuracies in the time-depth model presented in the previous section as well as inaccuracies in the time-depth models used to present the well tracks in a time domain (see table 3.2).

Table 3.5   Quality control of the velocity model as derived for the well GSB-01.

Marker	Seismic TWT	Seismic depth TVDss	Well depth TVDss	Error	Error
	[s]	[m]	[m]	[m]	[%]
BNS	0.39	-347	-330	17.25	5.2
BCK	0.898	-1,068	-1,039	29.16	2.8
BRN	1.151	-1,423	-1,448	-25.94	-1.8
BSK	1.47	-1,939	-1,863	76.46	4.1
BAT	1.752	-2,381	-2,356	24.49	1.0
BRB	1.956	-2,804	-2,803	1.03	0.0
BZE	2.075	-3,092	-3,091	0.27	0.0

Table 3.6   Quality control of the velocity model as derived for the well WYK-21.

Marker	Seismic TWT	Seismic depth TVDss	Well depth TVDss	Error	Error
	[s]	[m]	[m]	[m]	[%]
BNS	0.545	-494	-484	10.44	2.2
BCK	0.911	-1,026	-1,043	-17.02	-1.6
BRN	1.091	-1,273	-1,269	3.61	0.3
BRB	1.438	-1,930	-1,876	53.85	2.9
BZE	1.765	-2,675	-2,612	62.71	2.4

Random line combination

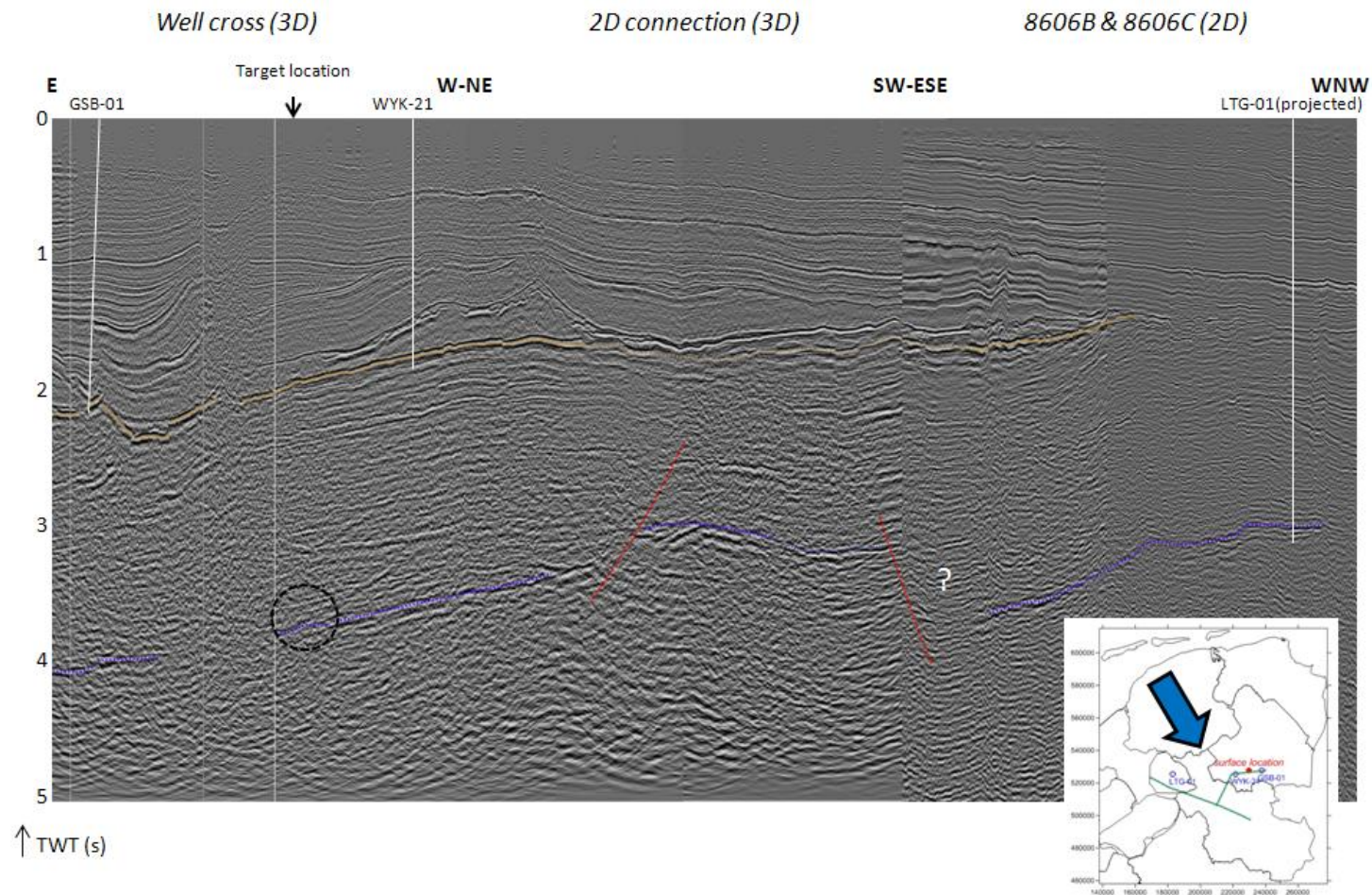Well cross (3D)   2D connection (3D)   8606B & 8606C (2D)

Figure 3.12   (previous page) Top Zeeland Formation correlation. Shown are the ran-
dom line trough GSB-01 and WYK-21 (see figure 3.9 also), a random line
from the 3D connecting to the 2D line 8606B and the 2D lines 8606B and
8606C. The position of the well LTG-01 as projected on 8606C is also
shown. Interpreted horizons are Top Z2 Basal Anhydrite Member (brown)
and Top Zeeland Formation (purple). Faults are displayed in red. The
inlay shows the position of the lines and the viewing direction.

Table 3.7

Marker	Seismic TWT	Seismic depth TVDss (constant interval velocity)	Seismic depth TVDss (VELMOD-2)
	[s]	[m]	[m]
Base Upper Rotliegend Group	2.026	-3,061	-3,061
Top Carboniferous Limestone	3.810	-6,807	-7,339
Base Carboniferous Limestone	3.940	-7,197	-7,729

3.3.6   Uncertainties and recommendations

The two velocity models derived for the Limburg Group result in an 8% difference in
depth of the Top Carboniferous Limestone. When also accounting for the uncertainty with
respect to the consistency of the mapping, a total uncertainty of 10% is assumed to be
applicable to the reservoir depth estimation of the top of the Carboniferous Limestone.
The same uncertainty has been attributed to the estimation of the base of the Carbonifer-
ous Limestone. Note that determining the velocity of the Limburg Group and the Zeeland
Formation on the basis of the available data is extremely difficult and comes with consid-
erable uncertainty. Improving the certainty with respect to the local Limburg Group veloci-
ty should be one of the first steps in improving the model presented here. Also, the above
concerns an exploratory mapping exercise as becomes evident from the mapping extent
in figure 3.8. Mapping a larger area might reveal some significant geological features.
The uncertainty of the thickness of the Carboniferous Limestone is about 200 m. This is
based on the range in ΔTWT of the Carboniferous Limestone in the immediate surround-
ings of the target location and the range of interval velocities of the Carboniferous Lime-
stone.

Several factors make interpretation of the Carboniferous Limestone difficult in the
Hoogeveen area. Besides the high burial depth, the strongly deformed overburden com-
plicates interpretation as intrinsically weak reflections are often hard to distinguish from
multiples generated by Zechstein and younger strata. Also, Westfalian coal packages
locally can impair on the primary signal to noise ratio, which hinders detailed mapping.
Some improvement may possibly be achieved by removing short-period peg-leg multi-
ples. However, the adverse acquisition parameters for deep objectives such as the Car-
boniferous limestones, make it extremely unlikely that major improvement can be made in
the imaging of deep structures. Full pre-stack reprocessing does not seem to offer suffi-
cient scope in view of the adverse acquisition parameters. It is noted that the seismic
data volume has been post-stack time migrated, not deemed appropriate for deep and
complicated structures.

3.4 Geological interpretation

3.4.1 Interpretation per well

Lithology and stratigraphy information were obtained from lithologs and composite well logs. This paragraph gives an interpretation of the depositional environment for each of the four wells.

From the fossil finds in appendix 1.4 it can be concluded that most fossils indicate marine environments. Based on the fossils that were found, no further distinction can be made as far as waterdepth is concerned. Only peloids and ooids indicate upper ramp (platform) environment as can be seen from figure 3.13. Corals indicate a close-to-platform environment. When present, only these fossils will be named in this paragraph.
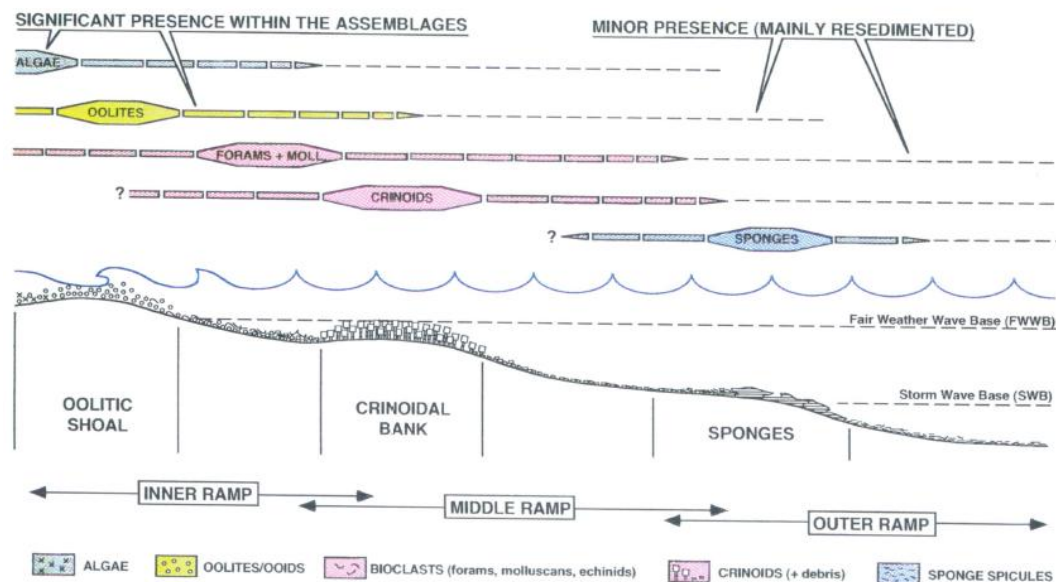
Figure 3.13   Carbonate ramp model (Elf Aquitaine, 1986).

Münsterland-1
The Lower Carboniferous in Münsterland-1 is a relatively thin sequence compared to the three deep Dutch wells. It consists mostly of deposits of the *Kulm* facies: *Tonsteins* (claystone) and intercalations of limestone and claystone. Only in the bottom part dolomitic limestone is abundant. The presence of calcimudstones and claystones indicates a low-energy environment.

LTG-01
LTG-01 is characterized by soft white calcimudstones in the upper 100. The next 100 m is harder and darker. The middle section (300 m) shows a slight increase in grainstones but calcimudstones remain abundant. Coral fossils in the middle section indicate a reef environment. Next 200 m calcimudstones are still abundant, but accompanied by packstones/grainstones and dolomite traces. Lowest 80 m is characterized by an increase in dolomite. These deposits also characterize a platform environment.

The entire Early Carboniferous sequence in well LTG-01 is interpreted as Farne Group by TNO. However, the lithology comprises of only limestones with occasionally a slightly dolomitic or clayey input. This does not correspond with the lithology of the Farne Group in literature. Also, because in literature LTG-01 is situated on a high, the clastic input is suspected to be minor. For these reasons, it is suggested to classify this sequence as Zeeland Formation. The bottom 80 m of LTG-01 is characterized by a strong increase in dolomite that therefore could be classified as Beveland Member.

UHM-02
The top 100 m of the UHM-02 well contains white cementstone with intercalations of calcimudstone or wackestone or packstone. Ooids indicate a shallow tropical sea environment. The middle section of 350 m is characterized by packstones and grainstones, indicating a shallower marine setting. Colours range from white to dark grey. Coral found in samples indicate a reef environment. The bottom 220 m (classified as Beveland Member) consists of dolomitic packstone and grainstone. Again reef fossils have been found.

WSK-01
The limestones in WSK-01 could be present in the form of calcimudstones and packstones and grainstones. This leaves open a lot of potential depositional environments.

The Early Carboniferous in WSK-01 is defined as Zeeland Formation by TNO and as Kulm facies by the RGD in 1988. The Kulm facies in WSK-01 is described as comprising clayey and silty deposits that dominate the carbonate content (RGD, ibidem). The RGD believes these sediments have been deposited in relatively shallow waters, but others (quote from RGD report, 1988) believe the sediments are deep-marine deposits.

The WSK-01 lithostratigraphic column shows little resemblance with the Zeeland Formation in the northern wells LTG-01 and UHM-02; it is more similar to the deposits in Münsterland-1. Whether these basin deposits should belong to the Zeeland Formation or the Kulm facies is unknown at this point.

3.4.2 Reconstruction of paleo-environment at Hoogeveen

With the exception of WSK-01, the bottom deposits of the Lower Carboniferous sequence in every well comprise of dolomitic limestone. In WSK-01 the description of lithology does not mention any dolomite. Based on palynologic research, the bottom section of WSK-01 is correlated to the *Ostracodenkalk* in Germany and the *Hastiere Formatie* in Belgium – both represent the base of the Tournaisian. The bottom section in Münsterland-1 is also interpreted as limestone from the Tournaisian *(*Wolburg, 1963). Either the very coarse lithology description does not mention any dolomite, or it is simply not present. The rest of the lithology of WSK-01 and Münsterland-01 leans towards a basin-type sequence with a higher clay content in Münsterland-1 and slightly higher clay content in WSK-01 compared to the northern wells.

In UHM-02 and LTG-01 the dolomitic limestone is considerably thicker. Dolomites occur only in the bottom sections. This indicates a correlation with age or specific mineral presence in the bottom sections.

The northern wells LTG-01 and UHM-02 have in common that the build-up of the column is very similar. There is a sequence of dolomitic limestones on the bottom, followed by a middle section that has an increased content of grainstone, followed by a top section that has an increased mud content (in the form of mudstone, wackestone and packstone).

The differences between the two northern wells are the grain content in the limestone and the fossil appearances. LTG-01 appears to have an overall higher mud content than UHM-02 that might indicate an overall lower-energy depositional environment. Grainstones usually indicate a high-energy depositional environment but they can also form by diagenetic processes, i.e. desiccation on exposure. The presence of ooids and peloids in UHM-02 indicates a depositional environment on the platform (the upper ramp), whereas the lack of these fossils – and the presence of crinoids and coral instead – in LTG-01 indicates an environment on the middle ramp. This is visualized in appendix 1.2.

These arguments support the theory of carbonate platforms as they are believed to be present in the LTG-01 and UHM-02 areas. Whether these platforms are situated on Early Carboniferous structural highs -the Texel-IJsselmeer High and Groningen High- as believed by Geluk et al (2007), or as a widespread platform stretching from the Netherlands to England (Ziegler, 1990), is still uncertain.

Based on the data from LTG-01 -which was not present at the time of Ziegler's publication- the location of the western border of the graben structure intersecting the Netherlands is false. However, it is not possible to decide if Ziegler's interpretation is not right at all. The western border of the graben could be situated more to the east. There is simply not enough well data to confirm or reject the interpretations from either Geluk et al (2007) or Ziegler (1990).

When including the eastern wells WSK-01 and Münsterland-1, there is a large difference in lithology between these and the northern wells. This is corroborated by the maps, published by Ziegler in 1990, which show a basin-like facies near WSK-01 entering the Netherlands from Germany, probably the Kulm facies (figure 3.2). Geluk et al (2007) assumes the Early Carboniferous deposits in WSK-01 not to belong to the Kulm facies. More detailed studying of the WSK-01 core -and comparing to Münsterland-1- is required to decide which of the authors is correct.

Whereas Ziegler believes in the presence of a coherent carbonate platform stretching from England to Poland in the Early Carboniferous, Geluk et al (2007) and Kombrink (2008) believe in the presence of isolated carbonate platforms with basin-type limestones and possibly shales in the interlying basins. In either of the two interpretations, Hoogeveen is expected to be located in the basin. However, as opposed to the carbonate platforms -which are proven to be present by LTG-01 and UHM-02-, there is no well data in the vicinity of Hoogeveen supporting these theories. Only new 3D seismic data can possibly provide better insights in the depth -and therefore depositional environment- of the Carboniferous Limestone Group below Hoogeveen.

In the remainder of this study, the deposits of the Carboniferous Limestone Group below Hoogeveen will be referred to as Zeeland Formation. Though the deposits could theoretically be part of the Kulm facies -if this would stretch far enough to the north, the official nomenclature of the Netherlands refers to all deposits of the Early Carboniferous that are not part of the Farne Group to be the Zeeland Formation.

3.4.3 Depth and thickness

Depth and thickness based on regional data
The depth of the base of the Limburg Group is documented by Geluk et al (2007). This depth coincides with the top of the Zeeland Formation. The map with the contour lines is shown in figure 3.5. Hoogeveen is believed to be situated in a basin. This is confirmed by the contour map by Geluk as well as by the map from Ziegler. The depth of the top of the Zeeland Formation is assumed to be between 6,500 and 7,000 m below mean sea level (figure 3.5).

The thickness of the Zeeland Formation is estimated to be between 200 and 800 m. These are the lower and upper boundaries of the thicknesses found in the deep wells. Wells LTG-01 and UHM-02 are drilled into a platform, whereas the facies of the Carboniferous Limestone Group in WSK-01 is uncertain. Based on regional maps Hoogeveen is situated in the basin. However, there is no evidence of an increase or decrease in thickness when moving from the carbonate platforms into the basin.

Depth and thickness based on seismic data
The top and base of the Zeeland Formation could not be unambiguously identified in the seismic. Especially in the Hoogeveen area, the seismic quality at the two way traveltimes involved is too low. However, with the help of several high offset 2D seismic lines and a correlation with the well LTG-01, a tentative interpretation has been composed (see figure 3.12). In table 3.7, the results for the target location are presented for the constant interval velocity model and VELMOD-2.

Using the constant interval velocity model for the Limburg Group, a depth of -6,807 m TVD has been derived for the top of the Zeeland Formation. This implies a Limburg Group thickness of 3,746 m. This is considerably more than found at any of the Dutch wells that fully penetrate the Limburg Group. An explanation may be that the seismic suggests most of these wells are located in carbonate platforms whilst the target location is not (Kombrink, 2008). Figure 3.12 also shows considerable differences in depth. The true vertical thickness derived for Hoogeveen amounts to 400 m, which is considerably less than the corresponding value at LTG-01 of 767 m and UHM-02 of 662 m but more than the value at WSK-01 of 186 m.

3.5 Temperature-depth relation

3.5.1 Geothermal gradient

The geothermal gradient has been determined from bottomhole temperature measurements from logs.

These have been performed in the deep wells LTG-01, WSK-01, UHM-02 and Münster-land-1. Furthermore data from relatively shallow wells -up to 2,000 m depth- has been checked to see if they fit the average geothermal gradient of the Netherlands. These wells are situated within a 30 km radius of Hoogeveen.

Figure 3.14 shows the relation between the temperature and depth. Bottomhole temperatures are corrected with the Horner method. Due to the drilling, the mud temperature is lower than the original formation temperature at the moment of logging. Multiple logging runs exhibit higher bottomhole temperatures, which can be used to apply so-called Horner corrections in order to estimate the true formation temperature.

The dotted dark line shows the average temperature gradient of the Netherlands of around 30 °C per km depth. The shallow wells -up to 2,000 m- wells will be scattered around the average geothermal gradient.

The deeper temperature measurements indicate a sharp increase in the temperature gradient around 2,700 m depth. For UHM-02 this increase could be caused by the possible presence of a volcanic intrusion. Another explanation, also for LTG-01, could be found in the presence of insulating shale and/or coal layers on top of the Zeeland Formation. This causes the heat to accumulate in the deeper areas.

We assume the depth of the onset of the increased gradient to be controlled by lithology - the insulating coal and organic layers. In figure 3.14 the averaged depth of this onset is around 2,700 m. This cannot be applied to Hoogeveen because the lithology below Hoogeveen needs to be taken into account. Table 3.8 shows the lithology below Hoogeveen and the depth of the insulating clay layers (the Caumer and Geul Subgroups). The onset of the increased gradient is therefore believed to be at a depth of 3,400 m below Hoogeveen. The slope of the increased gradient below Hoogeveen is assumed to be equal to the one found in figure 3.14.

For an estimation of the temperature in the Zeeland Formation below Hoogeveen, we propose two scenarios:
- For the full depth range: the average geothermal gradient in the Netherlands can be used: 30 °C/km.
- For a depth range of 0 to 3,400 m the normal gradient and deeper: an increased geothermal gradient of 44 °C/km

As mentioned in the previous paragraph, the depth of the top of the Zeeland Formation is estimated between 6,500 and 7,000 m. Assuming an average surface temperature of 10 °C and the average geothermal gradient of the Netherlands, the temperature at 7,000 m below Hoogeveen is estimated at 220 °C. Assuming the increased gradient, the temperature at 7,000 m below Hoogeveen is estimated to be 270 °C.

In order to assess the most plausible assumption for the estimation of temperatures at 7,000 m below Hoogeveen, a 1D temperature model has been constructed. This temperature model is presented below.
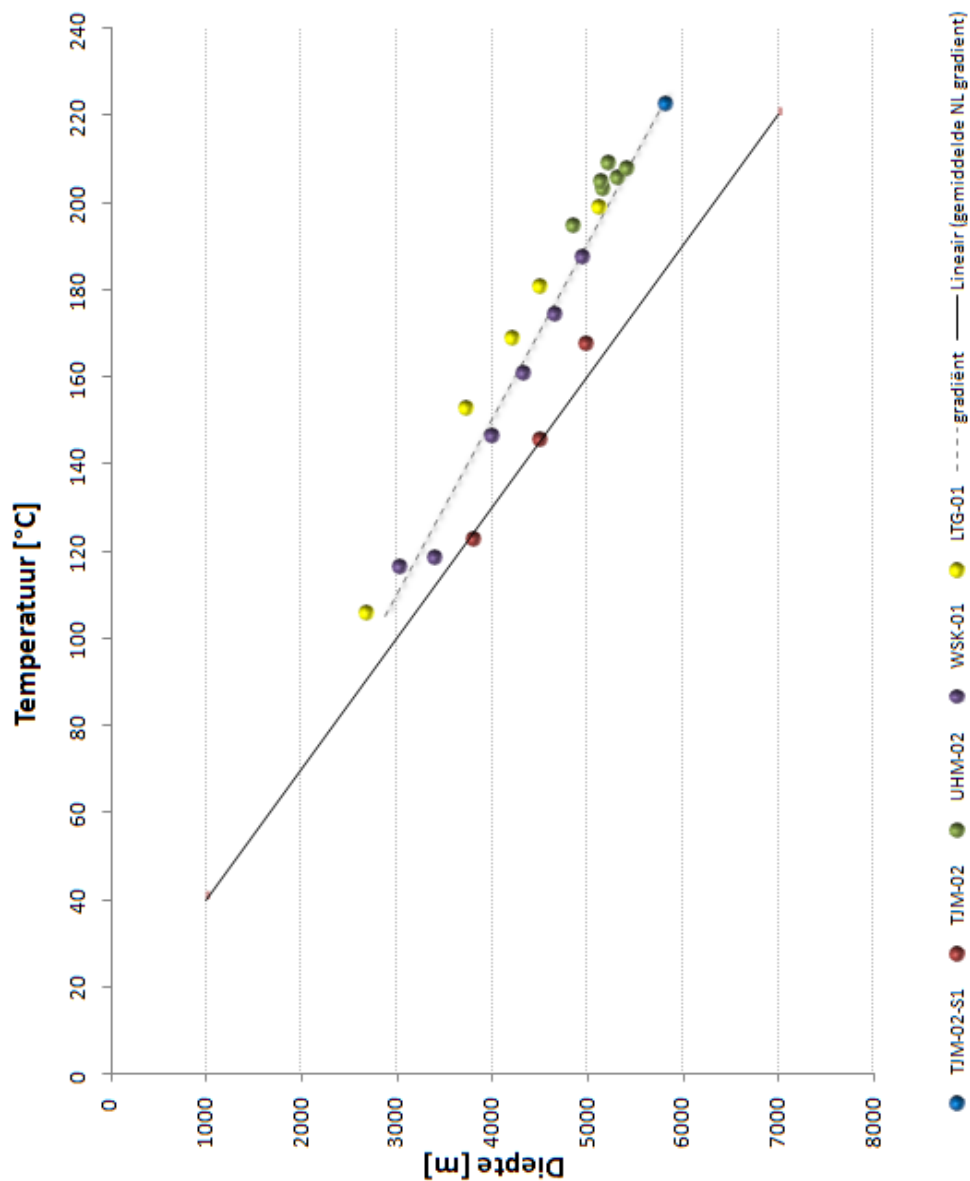
Figure 3.14   Corrected temperature measurements versus depth for the deep wells.

3.5.2   1D temperature model

The 1D temperature model is based on a fixed vertical heat flow and varying thermal conductivities due to changes in lithology. It is being applied to predict temperatures at 7 km depth below Hoogeveen. Based on a crustal thickness of about 30 km (Ziegler & Dezes, 2005), an average vertical heat flow of 70 mW/m^2 is assumed in the upper 7,000 m (Cloetingh et al., 2010).

The lithostratigraphy at Hoogeveen is estimated from TNO depth maps down to the Upper Rotliegend Group. The thicknesses of the Carboniferous lithologic units are estimated from literature (Geluk et al., 2007), deep wells and seismic data. A total of thirteen lithologic units have been discerned in Hoogeveen's subsurface. A thermal conductivity has been estimated for each of these units. The range of thermal conductivities has initially been derived from literature. Subsequently, bottom hole temperatures from a large amount of wells were used for fine-tuning. and determining the most likely thermal conductivity.

Table 3.8 presents the lithologic units below Hoogeveen with their depth, thickness, thermal conductivity and temperature. Figure 3.15 presents the temperature evolution in the subsurface of Hoogeveen. The model predicts a temperature of about 257°C at 7 km depth. Based on a comparison of the model results with bottom hole temperatures, the uncertainty of the model is ± 10°C at these depths.

The low thermal conductivities of the Caumer- (coal bearing) and especially Geul Subgroup (organic rich) have an insulating effect. The most important conclusion from table 3.8 and figure 3.15 is that there in an increase in geothermal gradient below these units. The insulating effect of coal and organic rich clays is also described by Cercone et al. (1996) in the Appalachian Basin.

Table 3.8   Base depth, thickness, thermal conductivity and temperature at base depth for each lithologic unit below Hoogeveen.

Lithologic Unit	TVD (m)	Thickness (m)	Thermal conductivity (W/mK)	Temp (°C)
North Sea Supergroup	505	505	2.2 ± 0.1	26 ± 1
Upper Cretaceous Supergroup	1,040	535	2.1 ± 0.1	44 ± 2
Lower Cretaceous Supergroup	1,329	289	2.1 ± 0.2	54 ± 3
Jurassic Supergroup	1,419	90	2.2 ± 0.4	57 ± 3
Altena Group	1,626	207	1.9 ± 0.1	65 ± 4
Upper Germanic Trias Group	2,046	420	2.4 ± 0.4	77 ± 5
Lower Germanic Trias Group	2,414	368	2.2 ± 0.4	89 ± 6
Zechstein	3,061	647	3.2 ± 0.8	103 ± 9
Rotliegend	3,071	10	2.8 ± 0.6	104 ± 9
Hunzel & Dinkel Subgroup	3,400	329	2.8 ± 0.2	112 ± 10
Caumer Subgroup (coal rich)	4,900	1,500	2.0 ± 0.1	165 ± 12
Geul Subgroup (organic rich)	6,800	1,900	1.6 ± 0.1	250 ± 17
Carb. Limestone Group	7,000	200	2.2 ± 0.2	256 ± 18
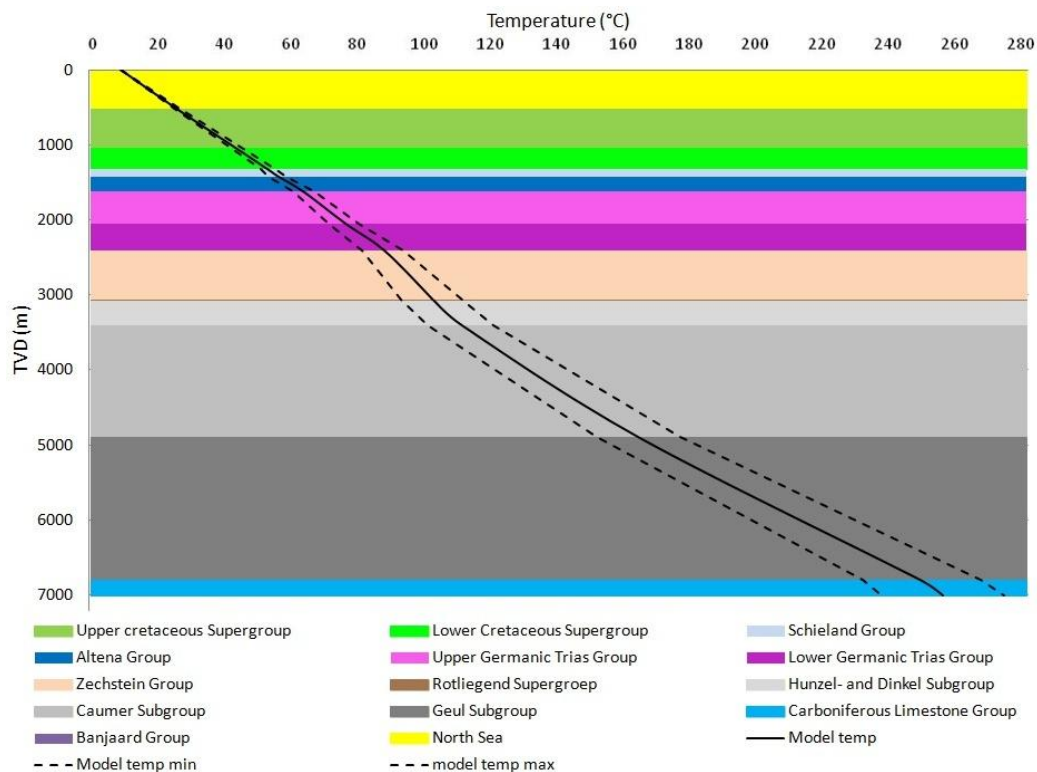
Fig 3.15   Temperature profile in the subsurface of Hoogeveen applying a 1D temperature model.

3.6   Summary

The Zeeland Formation is the target of the geothermal exploration below Hoogeveen. This formation consists mainly of limestones and possibly shales and dolomites. The spatial distribution of the formation depends of the location of paleohighs and basins. The extent of these structural elements is estimated from regional maps. Hoogeveen is believed to be in a basin but this assumption is only based on literature and regional studies. The lithology of the Zeeland Formation is strongly dependent on the position relative to highs and basins. Because of uncertainty in its position, the local lithology is somewhat subject to uncertainty.

Based on regional studies the depth of the top of the formation is estimated to be between 6,500 and 7,000 m. Interpretation of seismic data yields a more accurate depth determination of approximately 6,800 m. At these depths temperatures are sufficient for geothermal activities. Temperature data from deep wells show an increase in geothermal gradient below insulating clay layers on top of the Zeeland Formation. A 1D temperature model shows the same effect. The temperature at 7,000 m is therefore estimated to be approximately 260 ±20 ºC. Based on literature data the thickness of the formation is estimated to be between 200 and 800 m. Seismic interpretations have resulted in a thickness estimate of approximately 400 m - with an uncertainty of 200 m.

4 Rock properties

4.1 Geomechanics

In chapter 3 the lithology of the limestone of the Zeeland Formation has already been discussed. For modelling studies it is also important to understand the behaviour of the material under stress conditions. In fracture modelling the mechanical properties of the rock influence the dimensions of the created fracture. Additionally, the magnitude and orientation of the principal stresses determine the orientation of the fracture.

The mechanical properties of a rock are dependent on the characteristics of the constituting minerals, their fluid fill and the presence of fractures. The most important rock properties in this aspect are Young's modulus and Poisson's ratio.

Young's modulus describes the stiffness of a rock in simple uniaxial compression. In other words, it is a measure of the rock's ability to compress under a certain stress. From the shear and compressional wave velocity and the bulk density of the overlying rock, Young's modulus can be calculated:

$$E = \frac{\rho V_s^2 (3V_p^2 - 4V_s^2)}{(V_p^2 - V_s^2)}$$

where E = Young's modulus (GPa), ρ = bulk density (kg/m³) V_p = the compressional wave velocity (m/s) and V_s = the shear wave velocity (m/s).

Poisson's ratio is the ratio of lateral expansion to axial shortening, instigated by a certain stress. From the shear and compressional sonic wave velocity logs a Poisson's ratio log can be constructed using the following formula (Zoback, 2008 and others):

$$v = \frac{V_p^2 - 2V_s^2}{2(V_p^2 - V_s^2)}$$

where v = the dimensionless Poisson's ratio. These two parameters are required in order to perform fracture modelling. Typical values of E and v are found in literature for different materials with varying porosities (Mavko et al, 1998)

According to Lama and Vutukuri (1978) the Young's modulus of a limestone is highly dependent on its porosity. High porosity limestones (>16%) have Young's moduli of 30 MPa. Low porosity limestone (<8%) have Young's moduli around 80 MPa.

The average Poisson's ratio for a limestone is around 0.25, virtually independent of porosity (Lama and Vutukuri, 1978).

Elastic moduli such as Young's modulus and Poisson's ratio are temperature dependent. Lion et al (2005) have performed experiments on a Bourgogne limestone with a porosity of 20%, Young's modulus of 25 MPa and Poisson's ratio of 0.26. They found that the change in E and v is insignificant as the rock is heated up to 150ºC. Only when the temperature is increased to 250ºC, E drops to 23.7 MPa and v to 0.24. These changes are still very small. Therefore it is assumed that the effect of temperature on Young's modulus and Poisson's ratio is insignificant.

This gives an idea of typical values of E and v. However, values can be more or less directly obtained from laboratory tests on core samples under specified circumstances. There are no publicly available core data of any of the four deep wells. Performing laboratory tests is beyond the scope of this study. Therefore, the well logs of the three deepest wells in the Netherlands, LTG-01, UHM-02 and WSK-01 are evaluated to estimate the rock properties. Poisson's ratio and Young's modulus can be obtained from logged P and S-wave velocities in combination with interpreted porosity. For LTG-01 and UHM-02 logs are publicly available that enable the establishment of the elastic moduli. This process will be described in chapter 6.

Well WSK-01 is rather old and consequently lacks the S-wave velocity log. Therefore, logs of the elastic moduli could not be constructed for this well.

Other rock properties such as porosity and permeability have not been studied from literature. The range of values that can be encountered is very large and depends on depth, pressure, temperature, fluid fill and mineral composition. The adequate method involves determining these parameters from the available data, as described next.

4.2   Petrophysical analysis

Carbonates, which are more soluble in water than sandstones, have usually grown in place, and then evolved via cementation compaction, dolomitization and dissolution (Jerry Lucia, 2004). An important factor in petrophysical analysis for carbonates is pore size distribution, while for sandstone this is clay effects. Most important properties which should be determined for carbonates are porosity and permeability. Clay volume is less important.

4.2.1   Data

A petrophysical analysis has been performed on five wells to determine the properties of the Carboniferous Limestones. The surface locations are shown in figure 3.5 (Münsterland-1 is not included in this analysis). An overview of the available logs and core measurements are given in table 4.1.

if

The three deep wells, LTG-01, UHM-02 and WSK-01, have been drilled to determine whether the Carboniferous Limestones are gas or oil bearing. They were all found to be dry. These particular wells have been chosen as they are the sole ones containing Carboniferous Limestone core measurements. The WSK-01 core measurements do not include permeability measurements.

Table 4.1　　　Available log measurements

Well	Drilling year	Gamma ray	Sonic	Shear Sonic	Density	Neutron porosity	Resistivity
LTG-01	2004	yes	yes	yes	yes	yes	yes
UHM-02	2002	yes	yes	yes	yes	yes	yes
BHG-01	1978	yes	yes	-	yes	yes	yes
KSL-02	1981	yes	yes	-	yes	yes	yes
WSK-01	1978	Yes	yes	-	yes	yes	yes

4.2.2　Core measurements

From four wells, 123 Lower Carboniferous Limestone Group core measurements are available. For the KSL-02 well, an additional 20 core measurements are included from the Bosscheveld Formation (Banjaard Group). The WSK-01 well did not contain permeability measurements. Table 4.2 gives an overview of the available core data which includes the range and average of the raw porosity and permeability measurements.

Table 4.2　　　Available core data

Well	Formation	Measured depth [m]	# measurements	Porosity [%]			Permeability [mD]		
				Min	Ave	Max	Min	Ave	Max
LTG-01	Zeeland Formation	4,378-4,473	4	1.0	1.3	1.6	0.2	4.6	9.6
UHM-02	Zeeland Formation	4,751-4,758	21	0.9	1.2	1.9	0	0.1	0.7
BHG-01	Zeeland Formation	2,160-2,390	88	0.4	1.9	5.7	0.5	1.3	1.9
KSL-02	Zeeland & Bosscheveld Formation	320-500	30	0.3	3.4	28.1	0.7	2.1	21.2

Porosity

Porosity measurements have been carried out under atmospheric pressure. To determine the porosity at depth, a correction factor needs to be applied. This factor is determined by the pressure within the reservoir. A correction factor of 0.90 has been applied. This correction factor is slightly lower than the usual applied correction factor (0.95) due to the overpressures measured in LTG-01.

The distribution of the corrected core porosity of the Carboniferous Limestone Group versus depth is given in figure 4.1 for each well. Anomalously high porosity values of 20-30% in the KSL-01 well have been ignored, and were probably caused by karstification.

The graph in figure 4.1 shows that the porosity range decreases with depth, which can be primarily explained by compaction. The lack of core measurements in the deep wells may also contribute to the limited range in porosity. A remark that should be made is that these measurements have been carried out on the matrix. The actual porosity will be slightly higher due to the natural fracture system and vugs that have been observed in the cores (see section 5.4).
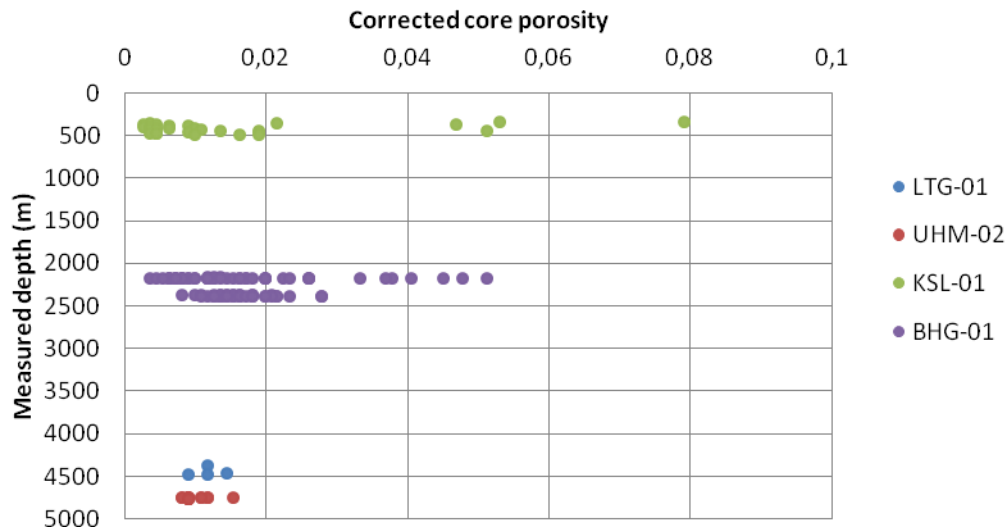
Figure 4.1   Corrected core porosity of the Carboniferous Limestone Group in the wells LTG-01, KSL-02, UHM-02, BHG-01

Permeability
The measurements of permeability have been performed under atmospheric pressure and using air instead of water. The air permeability differs from the permeability of water. Furthermore, the permeability generally decreases by increasing pressure from overburden rock. Therefore, the data need to be corrected. The measurements of the permeability have been corrected using the Juhasz compaction correction (Juhasz 1986). As all permeability measurements are less than 160 mD, the following relation yields for all measurements:

K_{air} < 160 mD:
$K_{brine} = A\, K_{air}^{B}\,(PHIE/PHIT)^{C}$
With: $A = 4.14\,\sigma^{-0.390}$, $B = 0.80\,\sigma^{0.058}$ and $C = 2.04\,\sigma^{0.058}$

Where K_{air} is the air-permeability, K_{brine} the water-permeability, PHIE the effective porosity, PHIT the total porosity and σ the effective in-situ uniaxial stress in the reservoir in psi. The uniaxial stress has been determined based on the RFT measurements and the overburden pressure. Table 4.3 represents the calculated effective in-situ uniaxial stress that has been applied for each well.

Table 4.3   Uniaxial stress

Well	Depth (TVD)	Effective uniaxial stress σ (MPa)
LTG-01	4,558	42.4
UHM-02	5,154	47.9
BHG-01	2,608	29.5
KSL-02	419	3.9

The distribution of the corrected core permeabilities are given in figure 4.2 for each well
The permeability range is clearly higher for both deep wells than for the two shallower
wells. The highest permeability values of the deep wells can be attributed to micro-
fracture permeability. This is supported by the natural fracture system in the cores.
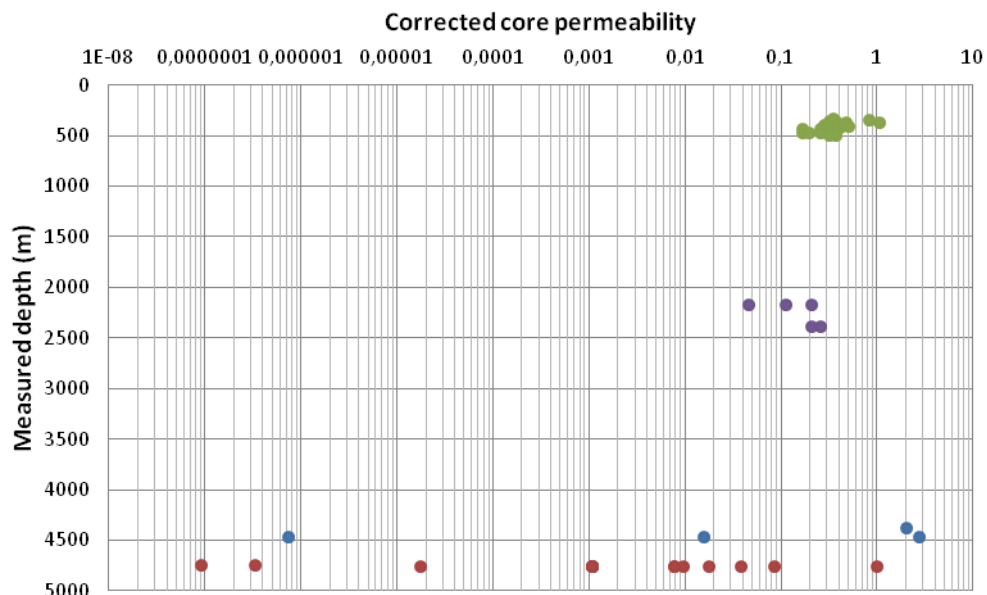
Figure 4.2   Corrected permeability of the Carboniferous Limestone Group in the wells LTG-
01, KSL-02, UHM-02, BHG-01

4.2.3   Porosity – permeability relationship

The porosity and permeability measured in the core analyses can be used to determine
direct relationships between the two. The graph in figure 4.3 shows the corrected core
porosity versus corrected permeability measurements of the Carboniferous Limestone
Group. Based on the distribution of porosity versus permeability, there is no clear rela-
tionship between permeability and porosity below 4,000 m. This can be mainly attributed
to the presence of the natural fracture systems, which affect the permeability measure-
ments and not the porosity measurements. In order to avoid a practically straight vertical
line for the poro-perm relation, separate relations have been derived for the two deep
wells and the two shallower ones with RMA[1]-regression. Corrected permeabilities lower
than the error range of 0.001 have not been taken into account.

---

[1] *RMA*: Reduced Major Axis.

The intersection of the two relations lies at a porosity of 0.0134 and a permeability of 0.319 mD. The resulting combined relationship is considered to represent the optimal relation between the porosity and permeability for this limited dataset:

LTG-01 & UHM-02

$$K = 10^{-7.70703 + 539.391 * \emptyset}$$ (1)

KSL-02 & BHG-01

$$K = 10^{-0.607489 + 8.37216 * \emptyset}$$ (2)

where K is the permeability in mD and $\emptyset$ the porosity in fraction. The correlation coefficients (R^2) of these relations are 0.048002 (1) and 0.121608 (2).
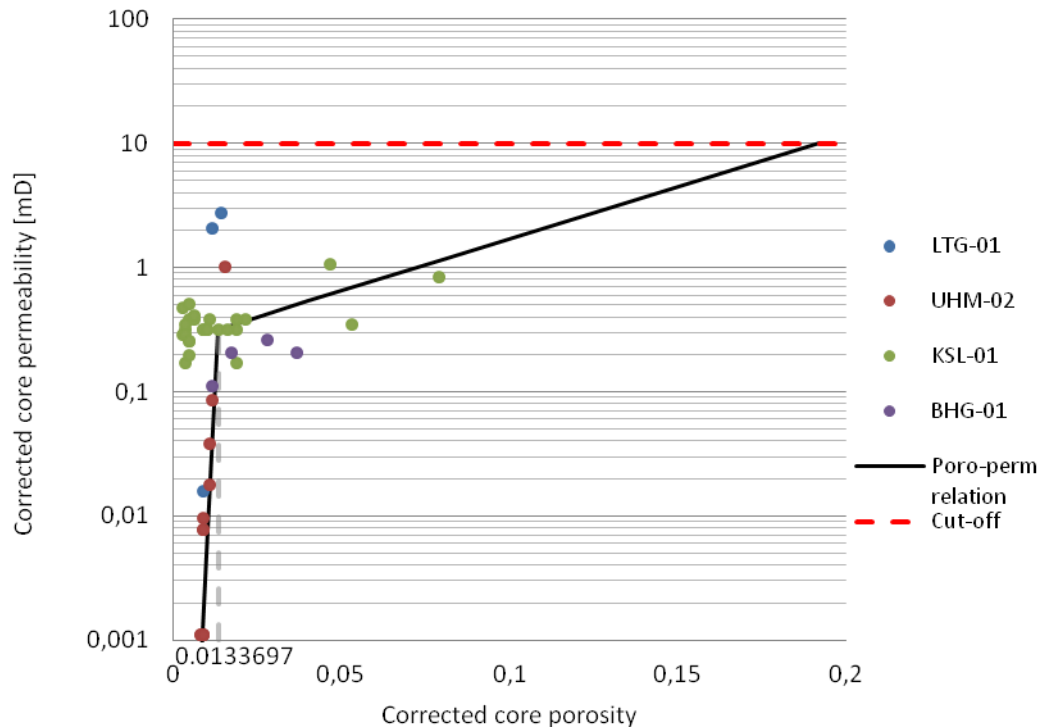
Figure 4.3   Corrected core porosity versus permeability of the wells LTG-01, KSL-02, UHM-02, BHG-01

4.2.4   Results

Well log measurements have been used to determine the porosity of the Carboniferous Limestone Group. The evaluation was made using the Interactive Petrophysics software following a standard industry deterministic approach. Shale volume was calculated from a combination of the gamma ray and neutron/density logs. Thereafter, porosity was calculated from the density/neutron log combination in the dolomitic sections and the density log in the pure limestone layers. Log plots from LTG-01, UHM-02 and WSK-01 are presented in Appendix 3.

The resulting porosities have been compared to the porosity of the core measurements. Figure 4.4 gives the correlation between the calculated and the measured porosity of the Carboniferous Limestone Group for the LTG-01 and UHM-02 well. This plot shows that there is some discrepancy between the calculated porosity and corrected measured porosity.

The discrepancy can be explained by the uncertainty in both the core and the log measurements at such low porosities. Also the problem of depth matching the core with the log data is another contributing factor.

Core porosity vs log porosity
Multi well Interval plot

20 points plotted out of 11260

Well	Depths
● (1) Luttelgeest-1	4300 M - 5176.57 M
● (4) Uithuizermeede	4600 M - 5439.16 M
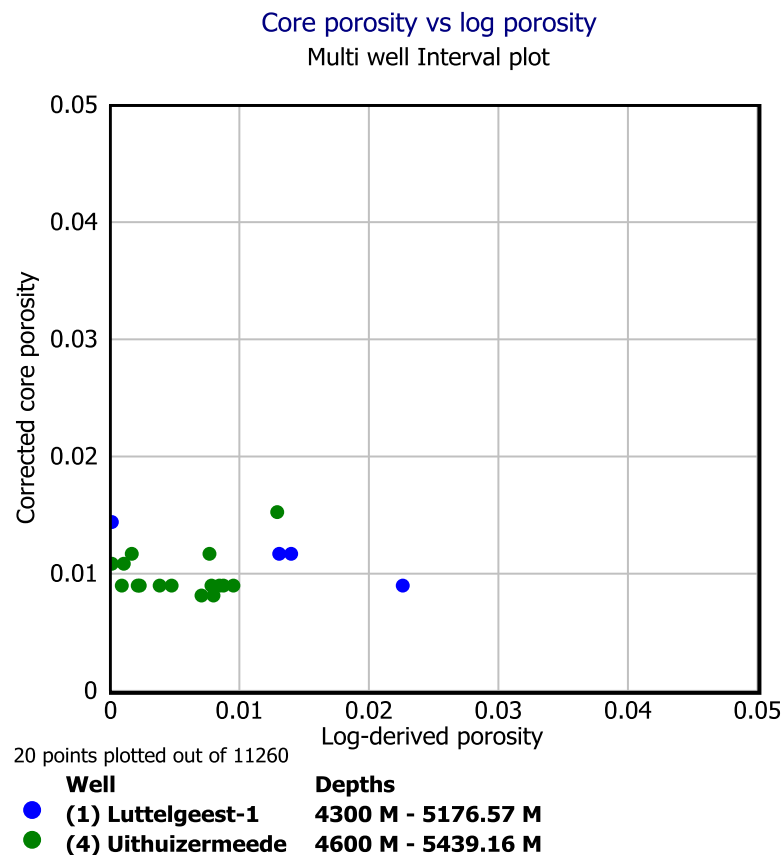
Figure 4.4   Corrected core porosity versus log-derived porosity of the Carboniferous Limestone Group.

The porosity log has been used to calculate a permeability log for three deep wells based on the porosity-permeability relationship. The transmissivity is determined by multiplying the mean permeability with the netto reservoir thickness. The arithmetic mean of the permeability has been calculated to determine average permeability.
The average porosities and permeabilities are not at all sufficient for a conventional geothermal doublet system.

if

Table 4.4   Deterministic results of the petrophysical evaluation of the wells

	TVDSS Base [m]	Net thickness [m MD]	Average porosity [%]	Average permeability [mD]	Transmissivity [Dm]	Measured TDS [mg/l]
Carboniferous Limestone Group.						
LTG-01	5,123	763	0.80	0.094	0.071	/
UHM-02	4,906	660	0.50	0.037	0.024	185
WSK-01	4,455	174	1.6	0.239	0.042	/

4.2.5 Water quality

The TDS has been determined in the UHM-02 well from a formation fluid sample. A TDS value of 185 mg/l has been measured at a depth of 5,154.5 m MD and a temperature of 205°C. The TDS is especially important to determine the construction materials of a geo-thermal system. This value can change with respect to the project location but there is no reason to assume an increase with depth.

4.2.6 Uncertainties

For clastic reservoirs it is common to perform an uncertainty analysis on each of the res-ervoir properties. In this case, it was decided to not execute the uncertainty analysis as the porosities and permeabilities of the limestone dominated reservoir are far too low to allow sufficient water throughput for conventional geothermic purposes.

4.3 Conclusions

The aim of this extended petrophysical study was to estimate the potential flow rate of the reservoir without stimulation. The reservoir is characterized by a large depth, some natu-ral fracture systems, and low porosity and permeability. The core measurements however exhibit a large uncertainty because of the presence of secondary permeability and by the small dataset.

Core permeability measurements rarely exceed 1 mD. The average permeability of all measurements is below 0.1 mD. This is roughly 1000 times below what is needed for a conventional geothermal system. Therefore it is concluded that reservoir stimulation is needed.

A literature indication of the elastic rock properties of limestone is also given. These will be compared to in-situ log measurements which are analysed in chapter 6.

5 Fault systems

5.1 Fault interpretation

In the structural deformation history of the NE Netherlands, the Lauwerszee Trough plays a dominant role. From the Hantum fault zone and West Groningen fault zone, NW-SE tectonics can be traced down to the Holsloot fault zone and Coevorden fault zone (see figure 5.1). From the orientation of regional fracture patterns, Frikken (1999) suggests an extensional wrench tectonic regime that may have been active from Carboniferous times to the present. This is supported by core data and borehole image logs (Frikken, 1999). More specifically, a further analysis of the local antithetic and synthetic fault orientations indicates dextral wrenching. Predominantly, N-S striking extensional antithetic Riedel shear systems show a large number of open fractures, which are responsible for improved permeability in the overall tight Zechstein Carbonate gas reservoirs (Frikken, 1999).

Hoogeveen is located along the Coevorden fault zone. The similarity analysis performed on interpretation of the top of the Z2 Anhydrite Member shows the dominant fault trends (figure 5.2). The fault patterns found at Hoogeveen appear to support the findings from Frikken (1999). Open fractures are more likely found in the N-S Riedel shear systems and near fault intersections. Please note that the area interpreted here is quite small. A different picture may arise when a larger area is interpreted.
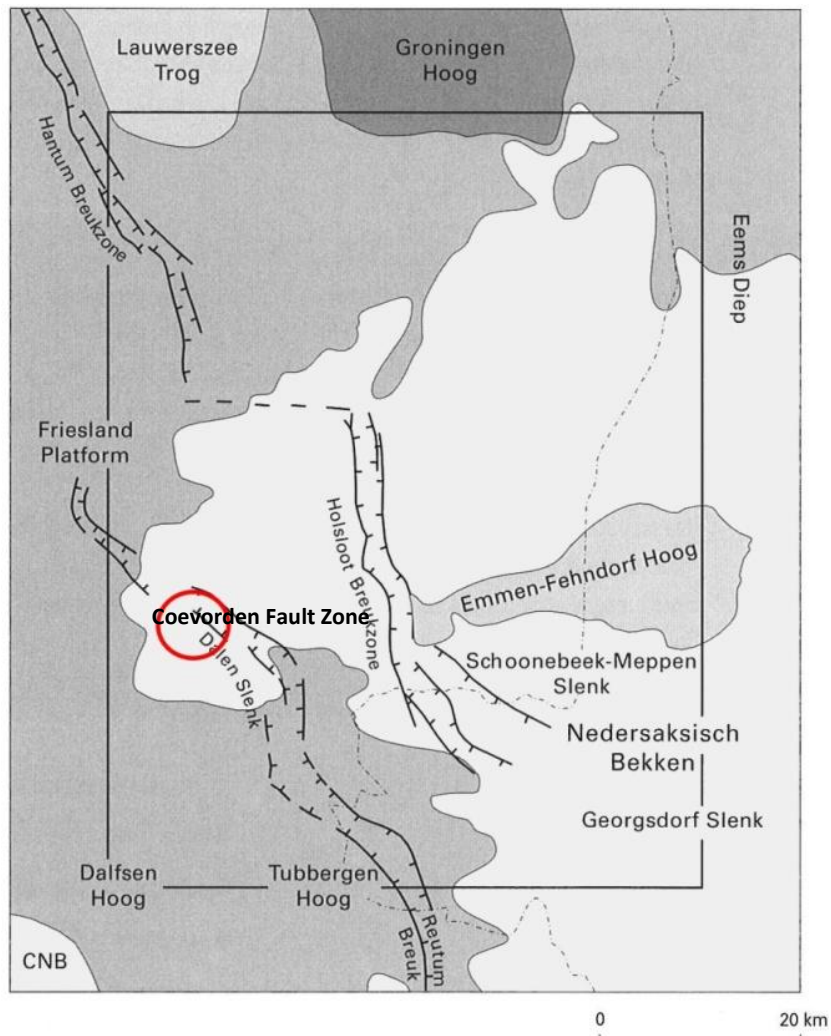
Figure 5.1   Map of regional structural elements. Also shown is the position of Hoogeveen (red circle) with respect to the Coevorden fault zone (adopted from TNO-NITG, 2000).
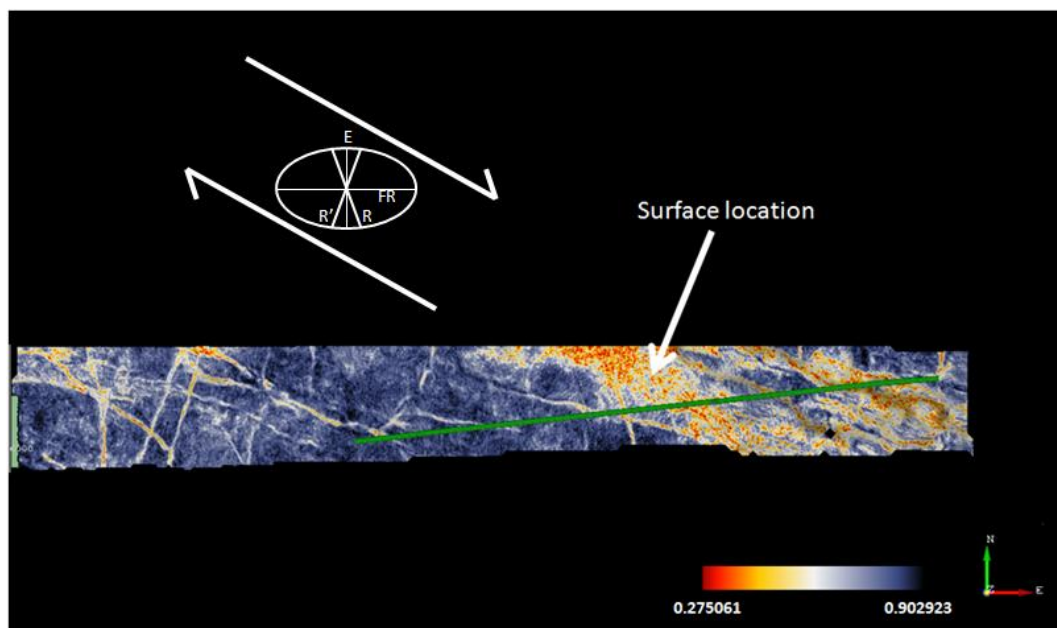
Figure 5.2   Faults in the lower Zechstein as indicated through a similarity analysis on Top Z2 Basal Anhydrite Member. Also shown is the suggested strain ellipsoid with deformation features belonging to dextral wrenching; reverse fault (compression, FR), synthetic Riedel shear fault (R), antithetic riedel shear fault (R') and normal fault (E).

The exact position of faults in the Early Carboniferous deposits is highly uncertain. Information on faults usually comes from seismic images. The quality of the seismic available for Hoogeveen is not high enough at the depth of the Zeeland Formation. This is illustrated in figure 5.3. Faults are easily recognizable down to a depth of 2,000 to 2,500 m. Any deeper image is blurry.

It is reasonable to assume that some of the larger faults continue down into deeper formations. Which of the faults behave like this is uncertain. Possibly new seismic data will provide better insights into the location of fault zones at depths of 5,000 m and more.

The dominant orientation of the faults in figure 5.2 is WNW-ESE. Assuming that there are faults present in the Zeeland Formation below Hoogeveen, their orientation will very likely resemble the orientation at shallower depths. Again, high quality new seismic images are required to support this theory.
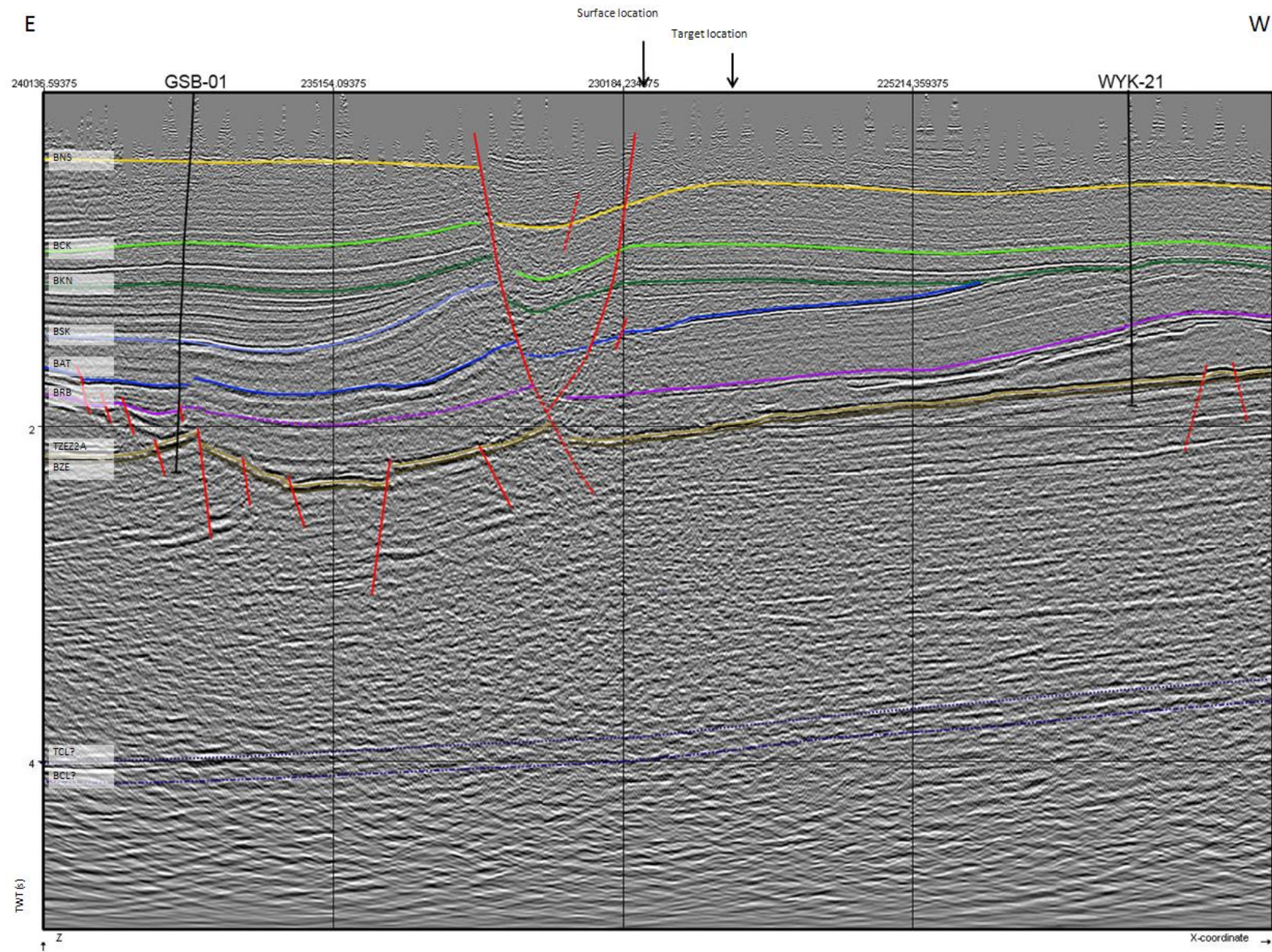
Figure 5.3   Image of a random line through the target location and the wells GSB-01 and WYK-21 showing the local major fault structures (in red). Horizons shown are: Base North Sea Super Group (yellow), Base Chalk Group (light green), Base Rijnland Group (dark green), Base Niedersaksen Group (light blue), Base Altena Group (dark blue), Base Lower Germanic Trias Group (purple), Top Z2 Basal Anhydrite Member (light brown), Base Zechstein Group (dark brown). Tentative interpretations of the Top and Base Zeeland Formation are also given (dotted purple). Black arrow indicates the surface location.

5.2   Stress regime

The nature of the present-day stress regime plays a role in:
- The potential of existing faults for geothermal exploration (paragraph 5.3)
- The orientation of hydraulically created fractures (chapter 6)

Figure 5.4 shows the maximum horizontal stress (Sh_{max}) directions in the Netherlands and surroundings. The general orientation of the present-day maximum horizontal stress is NW-SE to NNW-SSE. If the present-day maximum horizontal stress orientation is similar to the orientation of a pre-existing fault, the faulting environment is most likely normal (Zoback, 2008). This is the case because the faults at Hoogeveen also have a NW-SE to WNW-ESE orientation. Therefore, we assume a normal stress regime to be present at Hoogeveen. In addition, active tectonics and fault-guided subsidence in the central and southern Netherlands also point to a normal stress regime.

The orientation of the minimum horizontal stress is always perpendicular to that of the maximum horizontal stress. Therefore we assume this direction to be NE-SW to NNE-SSW.
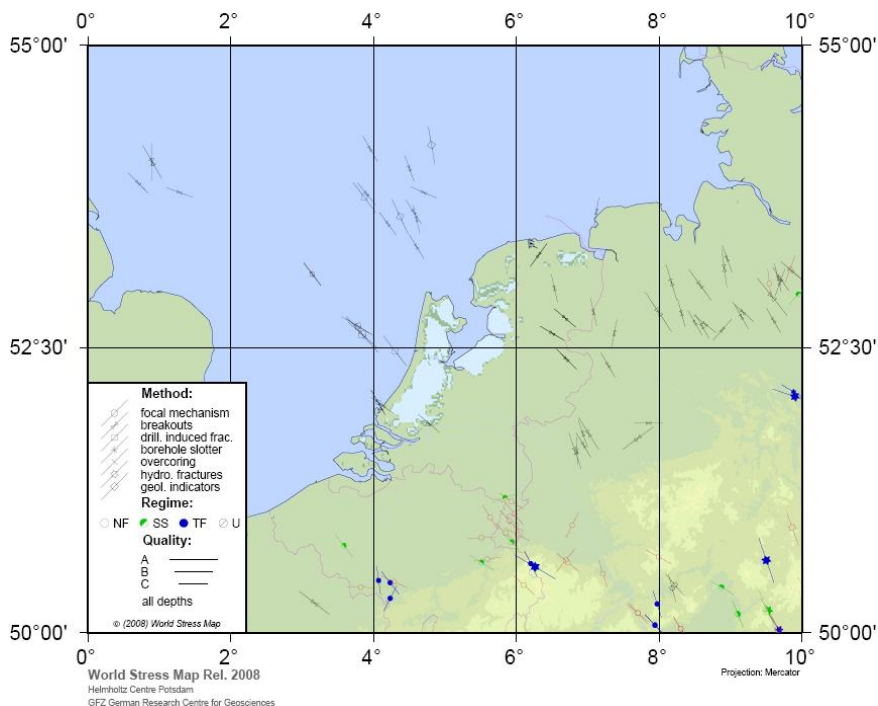
Figure 5.4   Maximum horizontal stress measurements in the Netherlands and surrounding areas, from the World Stress Map (Heidbach et al (2008).

To precisely determine the present-day stress regime and for further calculations, the magnitudes of the three principal stresses are required. The three principal stresses are:
-    The vertical (or overburden) stress (S_v)
-    The minimum horizontal stress (Sh_{min})
-    The maximum horizontal stress (Sh_{max})

The vertical stress magnitude in the Zeeland Formation is obtained from the thickness and average density of the overlying rocks. This can be calculated for any location in the Netherlands.

The magnitude of the minimum and maximum horizontal stress cannot be directly calculated for the location of Hoogeveen. Stress magnitudes can be obtained from borehole data from LTG-01 or UHM-02 and stress orientations can be obtained from borehole breakouts but these have to be extrapolated to the location of Hoogeveen. Moreover, this detailed borehole analysis is beyond the scope of this study. Estimates of the two horizontal stresses can be made, but these come with a high degree of uncertainty, especially for Sh_{max}.

5.3   Slip and dilation tendency

Faults showing a tendency to open and/or shear are preferred targets because of an expected increase in fracture permeability. Whether this is the case depends on the geometry of the faults and the recent stress field. Preferred exploration targets are zones where the fault orientation changes.

Slip is likely to occur when the shear stress τ equals or exceeds the normal stress acting across the fault plane σn. The ratio of these stresses is therefore taken as a measure for the tendency of a fault to slip:

$$Ts = \frac{\tau}{\sigma n}$$

The range of Ts lies between 0 and 1. The slip tendency (Ts) can be related to the frictional resistance μ of the rock to slip. When it exceeds μ, slip can occur. For normal faulting regimes Ts >0.85 implies the fault is ideally oriented for slip (Moeck et al, 2009). A large slip tendency indicates zones with increased fracture density and enhanced fracture permeability are likely to be present.

The dilation tendency (Td) describes the potential of the aperture of the fractures to further open. A larger aperture means a larger ability to transmit fluids. The dilation tendency can be calculated with the stress tensor (Morris, 1996):

$$Td = \frac{(\sigma 1 - \sigma n)}{(\sigma 1 - \sigma 3)}$$

The range of Td lies between 0 and 1. A high dilation tendency of 1 indicates the fault has the highest possibly aperture.

For the calculation of the shear and normal stresses, characteristics of the fault under investigation are required. The dip and strike need to be known, as well as the maximum horizontal stress. Because the characteristics of fault in the Zeeland Formation are highly uncertain, these calculations are not performed at this stage. Also, the magnitude of Sh_{max} is uncertain. Obtaining these parameters requires high quality seismic data and borehole data analysis of LTG-01 and UHM-02. This is beyond the scope of this study.

5.4   Natural fracture network

The presence of a natural fracture network has a large influence on fluid flow within the reservoir. If the primary permeability of the reservoir is low, a connected network of fractures from injection to production well increases fluid flow. This could be an outcome for the tight Zeeland Formation.

Cores of LTG-01, UHM-02 and WSK-01 have been studied. Fractures are abundant throughout every core. Fractures appear to be closed -or filled with mineral precipitation.

It is however necessary to distinguish between drilling induced fractures and naturally occurring fractures and to look at these fractures in more detail. When a fracture is filled with a mineral deposit -in limestone mostly calcite- it can be assumed it is a natural fracture. These kind of fractures were found in many cores from each of the deep wells.

Analysis of borehole images, borehole breakouts and fluid loss data is required to quantify the fracture density, dimensions and orientation. These parameters are needed to get an insight in the present natural fracture network model and consequently to enable the building of a digital model. Such a model could quantify the effect of natural fractures on fluid flow and provide insight in whether or not such a system could be feasible.

When a natural fracture network does not facilitate high enough flow rates, reservoir stimulation is an option. When hydraulically fracturing a reservoir, the orientation and dimensions of naturally occurring fractures plays a major role. They can affect the designed fracture orientation and dimensions. To account for these effects, the fracture network properties are required as described in the previous paragraph.

Currently, there is a lot of debate about the simulation of hydraulically fracturing a naturally fractured reservoir. Mostly the methods of simulation are under discussion. Worldwide, significant amount of research is focused on this subject. Industry software is available but comes from the oil and gas industry, such as MShale. Though geothermal experts are sometimes sceptical about the use of this software, the experience of the oil and gas industry is high. The software from this industry has been applied in many fracturing treatments around the world and has been proven to be reliable. The software is capable of modelling hydraulic fracture initiation and propagation in a discrete fracture network. Modelling naturally fractured reservoirs and the application of this software can be the subject of a following study.

5.5   Summary

The presence of fault zones in the Zeeland Formation is uncertain due to the absence of reliable seismic data. Faults can only be followed down to the Zechstein Group. The main fault that marks the Coevorden fault zone could possibly continue down to the Early Carboniferous deposits but this can only be checked with new seismic images.

The orientation of the faults in the vicinity of Hoogeveen is WNW-ESE. This is quite similar to the orientation of the maximum horizontal stress. Therefore we can assume to be in a normal stress regime. This has implications for the dimensions of the fractures that are designed in the next chapter.

The calculation of the slip and dilation tendency was not possible because characteristics of individual faults could not be obtained from the available data at larger depths. This is only possible if better quality seismic data becomes available.

Natural fractures are observed in many core samples and slabs of the Zeeland Formation. They can cause secondary permeability in the reservoir that has a beneficial effect on the flow rate and area of influence.

However, the fractures can also affect orientation and dimensions of the pre-designed created fractures. This can be negative. Literature research and analysis of borehole data is required to further study the effects of natural fractures on geothermal fracturing activities.

6 Hydraulic fracturing

6.1 Introduction

From the petrophysical analysis it was concluded that the primary porosity and permeability of the Zeeland Formation are very low. They appear to be too low for efficient energy production from a conventional hydrothermal system. To enhance production, stimulation techniques can be applied to a reservoir.

The most used technique in the oil and gas industry to improve productivity of hydrocarbons is hydraulic fracturing. Fluid is injected into the reservoir at a rate higher than the rate at which the reservoir matrix can accept the fluid. The pressure build-up will cause the reservoir rock to break. The fracture that is created is usually filled with sand or a ceramic material known as proppant. The fracture then serves as a path through which the flow will be much faster than through the rock matrix.

In the hydrocarbon industry hydraulic fracturing enhances oil and gas production. In the geothermal industry the same technique is applied. However, in the hydrocarbon industry it is a matter of producing the energy that is contained in the oil and gas. In the geothermal industry, the energy is essentially in the hot rock. It has to be transferred to the water first that then has to be produced. So there are other processes involved and moreover, flow properties of water are different from those of oil and gas.

In low-permeability reservoirs, waterfracs are another way of creating fracture permeability. Without or with very low proppant concentration, waterfracs rely on misalignment of the fracture faces. For this to occur, a shear stress component has to be present in the Zeeland Formation. Both methods will be explained in more detail in this chapter.

The project location is assumed to be in a normal stress regime (as seen in chapter 5). The global shape of the fracture is therefore known beforehand. In a normal stress regime, the fracture is vertical and would normally propagate in the direction of the maximum horizontal stress. This, however, can be influenced by the presence of a natural fracture network. Depending on the vertical stress profile, the length of the fracture is often larger than the height. The minimum horizontal stress acts perpendicular to the propagation direction.

As shown in figure 6.1, the concept is to first drill to a considerable depth after which a lateral section is drilled into the reservoir. The first well is being stimulated to create fracture wings to either side of the wellbore. The dimensions and orientation of the created fractures will be monitored with seismic stations.

After multiple fractures are created, two more wells are drilled to penetrate the tips of the created fracture wings. Now, a subsurface heat exchanger is deployed. The results of this chapter will be whether such a system can potentially facilitate high enough flow rates and production temperatures. The well design is explained in more detail in chapter 8.
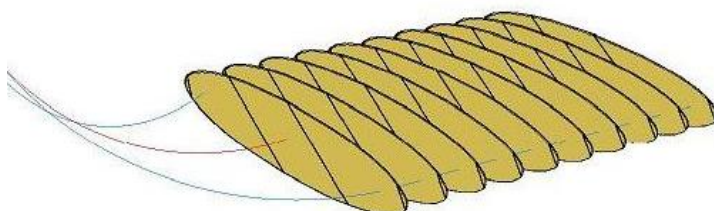

Figure 6.1   Multiple fractures perpendicular to the horizontal well trajectory.

It should be emphasized that the primary target in the Zeeland Formation are fault zones or naturally fractured networks. If these are found at depth and have a high permeability, they will be exploited for geothermal purposes. The secondary target will be waterfracs of shear fractures.

Only if the first two options do not show any potential or turn out to be inapplicable, hydraulic fracturing as described in this chapter will be applied. The costs of this method are considerably higher than the first two options. However, this method also has the highest degree of certainty. It is therefore necessary to have this method investigated as a back-up scenario.

6.2   Modelling methods

6.2.1   Data assimilation

Data of the Zeeland Formation is not available for the location of Hoogeveen. The closest well penetrating the formation is LTG-01, approximately 50 km to the east. In chapter 3 it was described that Hoogeveen is expected to be located in a basin between adjacent carbonate platforms. Because there is still a possibility that Hoogeveen is located on or near a platforms, we wanted to simulate both structural environments.

The only deep well in the Netherlands that -probably- penetrates basin deposits of the Zeeland Formation, is WSK-01. As mentioned in paragraph 4.1, this well is old and lacks a shear velocity log, making it impossible to construct reliable logs of the elastic moduli. We concluded that it is not possible to simulate the effect of a hydraulic fracturing treatment in basin-like deposits. Only well LTG-01 was simulated. In the remainder of this chapter, data and characteristics of well WSK-01 will still be mentioned to give insight into the rock properties of the -supposed- basin-type deposits.

Well LTG-01 was simulated using an advanced fracture simulation software package called MFrac. The software requires a large dataset of input parameters to accurately simulate a well. For LTG-01, this dataset can be assembled from the available logs.

We are simulating LTG-01 to give an impression of the effects of a fracturing treatment in platforms carbonates. To assess what the effects of this treatment are on the Zeeland

Formation below Hoogeveen -likely basin carbonates-, an impression of the relative effects of the input parameters on the output is required. Therefore a sensitivity analysis is performed.

Well UHM-02 also has all the required logs to perform a fracture design study. In this study, the well was not simulated because we tried to distinguish between basin and reef-like limestone. The limestone in wells UHM-02 and LTG-01 is believed to be quite similar. However, for future studies it will be advised to compare the rock properties and resulting fracture design of LTG-01 to that of UHM-02.

The software models fluid and heat flow, proppant transport and fracture geometry development. The software assumes the properties of the formation to be constant in the horizontal plane. The MFrac software package cannot include a shear stress component. Therefore, in this stage of this study, it is not possible to model hydraulic fracturing effect with waterfracs. The focus of this modeling study will be on hydraulic gel-proppant stimulation.

The reservoir section of LTG-01 is characterized by a low porosity and permeability. For the reservoir section: ϕ_{avg} = 0.3% and k_{avg} = 0.025 mD.

Logs of Poisson's ratio and Young's modulus were constructed based on the formulas provided in chapter 4.1.

Eaton's formula (Zoback, 2008) uses Poisson's ratio, the overburden pressure and the pore pressure to calculate the minimum horizontal stress:

$$Sh_{min} = \frac{v}{1-v}(S_v - P_p) + P_p$$

where S_v = the overburden stress (MPa) and P_p = the pore pressure (MPa). The overburden pressure is based on the average density for the overlying rocks of 2670 m³/kg. The pore pressure is assumed to be hydrostatic. We assume no tectonic stress component to be present.

When comparing the rock properties of LTG-01 and WSK-01, a major difference between the two is the porosity and permeability. These are an order of magnitude larger in WSK-01. For the reservoir section: ϕ_{avg} = 2% and k_{avg} = 0.27 mD.

6.2.2 Fracture design

The MFrac software simulates fracture initiation and propagation in the host rock. The result is a fracture design. The fracture design consists of dimensions of the fracture: length, width and height. These depend on the rock properties input and volume and viscosity of the fracturing fluid. Also the fracture permeability is calculated. This is based on the concentration and type of proppant that is injected with the fracturing fluid. After assessing the sensitivity of the four main input parameters on LTG-01, an ideal fracture was designed. The fracture should be designed to establish a high enough flow rate, that does not result in a thermal breakthrough. The temperature around the production well will decrease as a result of injecting cold water in the injection well. This temperature drop needs to remain within a few degrees after 30 years of production.

Before simulating a fracture in MFrac, analytical flow calculations indicate that a fracture of approximately 150 m high, 700 m long and 5 mm wide results in sufficient flow rates. These calculations are based on Darcy's Law. Achieving these dimensions is the aim of the fracture design.

First, a perforation interval is selected based on the stress profile. This is where the fracturing fluid flows from the well into the formation and initiates the fracture. To contain the fracture within a certain depth, an interval with relatively low stress compared to adjacent beds is selected.

The rock properties are constant throughout the design phase. The only way to influence the fracture dimensions and permeability is to vary the treatment schedule. Parameters of the treatment schedule that are varied are:
- The volume of fracturing fluid that is pumped into the well and formation
- The velocity at which the fracturing fluid and proppant are pumped into the wellbore
- The type -viscosity and temperature tolerance- of fracturing fluid
- The particle size of the proppant
- The proppant concentration

A treatment schedule usually begins with injecting a pad volume. This volume does not yet contain any proppant. It is merely meant to initiate the fracture that can be extended and propped in the next stage. After the pad volume, a mixture of fracturing fluid and proppant is injected. The fracturing fluid is meant to further open and extend the fracture and to transport the proppant. The proppant is meant to keep the fracture open and to create permeability in the fracture.

6.2.3 Sensitivity analysis

A sensitivity analysis was conducted to assess the (relative) effect of a change in input parameter on the output. Figure 6.2 shows the effect of an increase in four major input parameters on the fracture dimensions and net pressure. The net pressure is the difference between the pressure in the rock and the pressure required for the rock to break (the pressure in the fracture). The fluid leakoff rate is the amount of injected fluid that leaks off from the fracture to the formation. It is a function of the reservoir permeability.

Variable	Effect of an Increase in Selected Variable			
	Height	Length	Width	Net Pressure
Fracture Toughness, K_{1c}	Decrease	Decrease	Increase	Increase
Young's Modulus, E	Increase	Increase	Decrease	Increase
In-Situ Stress, σ	Decrease	Decrease	Decrease	Decrease
Fluid Leakoff Rate, q_L	Decrease	Decrease	Decrease	Decrease

Figure 6.2   Qualitative effect of increase in rock properties on the fracture dimensions and net pressure.

In the sensitivity analysis four parameters are being assessed on their (relative) effect on the model output. These parameters are:
- Young's modulus (E)
- Poisson's ratio (v)
- Minimum horizontal stress (Sh_{min})
- Host rock permeability (k)

The most important output parameters are the fracture dimensions
- Propped length (L)
- Propped width (w)
- Propped height (h)
- Fracture permeability ($k_{fracture}$).

The unpropped dimensions are considerably larger, because initially not the entire fracture is filled with proppant. The part of the fracture that is not propped during the injection process will close when the pressure drops.

The model is first run with a base scenario. In this scenario, every input parameter has its original, log-derived, value. LTG-01 is used because this well has the most complete log record as mentioned above. A variation from the base scenario is successively applied to each of the four input parameters, while keeping the other parameters constant. A minus and plus 20% variation is applied to each of the four parameter's logs.

The variation of minus and plus 20% is validated by comparing the log-derived values of LTG-01 to common literature values of the rock properties for limestone. An indication of literature values is given in figure 6.3.
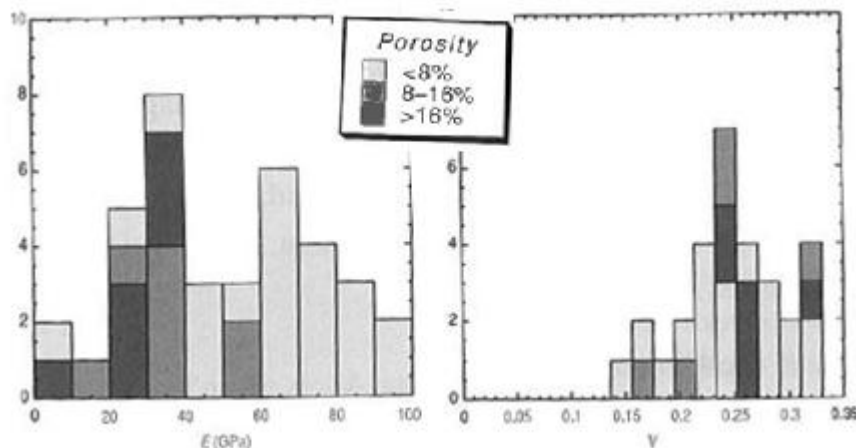
Figure 6.3   Typical values of static measurements of Young's modulus and Poisson's ratio for a limestone (adapted from Zoback, 2008).

The average log value of Poisson's ratio is 0.32. This is a reasonable high value compared to literature findings. This can be explained by the large depth at which the formation is found. High confining pressures cause the rock to be hard and compact.

The average log value of Young's modulus is 68 GPa. Compared to literature values this value is quite average.

The average log value of Sh_{min} is 82 MPa. Literature data of minimum horizontal stresses in a limestone are not useful in this situation because it all depends on the stress regime and depth. However, when looking at Eaton's equation, large variations are not expected. The value of Poisson's ratio does not vary greatly. Also the values for pore pressure and vertical stress are determined under feasible assumptions. Therefore a 20% variation in Sh_{min} is assumed to be very reasonable.

The 20% variation in the host rock permeability is not very realistic. Values are expected to very maybe a couple orders of magnitudes. However, because the average permeability is only 0.025 mD, even with a high variation the value is still very small. Larger values are even beneficial for the project because there is more water to be extracted from the host rock.

6.3 Modelling results

6.3.1 Simulation LTG-01

A stress profile is constructed for this well that is presented in figure 6.4.
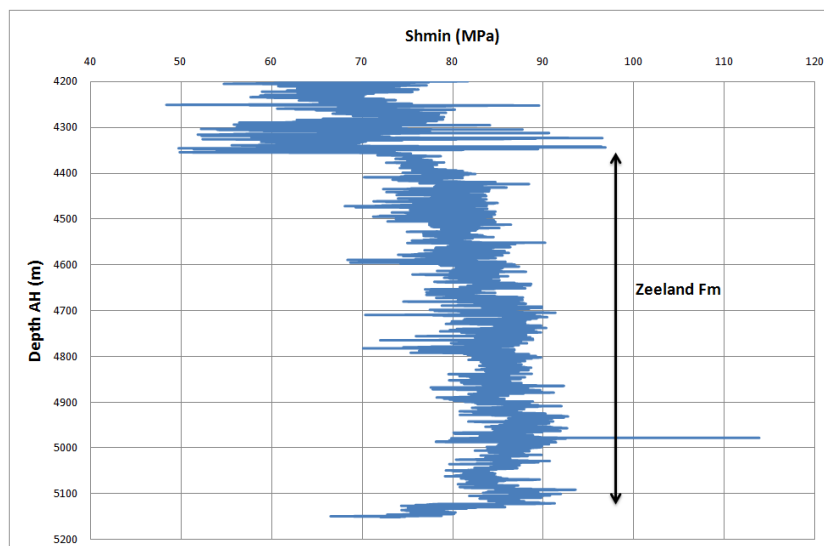
Figure 6.4   Minimum horizontal stress profile of LTG-01.

The perforation interval is at a depth of 4,740 m in a low stress zone in the middle of the formation. As a consequence, the fracture is contained within an interval of approximately 200 m. Because the log is subject to a degree of uncertainty, it is very important to conduct a mini-frac test in the future well to have full understanding of the stresses in the formation. Such mini-frac tests are common practice before the actual fracturing treatment is started.

Placing the perforations lower or higher results in uncontrolled fracture propagation into shallower or deeper formations. This will cause the amount of fracturing fluid to be spread out over a larger volume. As a result the fracture will not be adequately propped. It is hard to design a treatment schedule and keep in control of costs if it is unsure what the approximate dimensions of the created fracture will be.

Moreover, the formations above and below the limestone consist of claystone. This would impose dealing with a different geochemical environment. Though geochemical calculations are not included in this study, it is definitely something that has to be taken into account in future studies.

The viscosity of the fracturing fluid is an important parameter in the treatment schedule. Therefore, two fracture scenarios are designed in which the viscosity is different.
1) Decreasing viscosity fracturing fluid
2) Constant viscosity fracturing fluid

In each scenario the model is run four times, each time with increasing proppant mass. In total, eight simulations are carried out.

Scenario 1: decreasing viscosity fracturing fluid
In the first scenario a fracture is created with 1200 m³ of a conventional fracturing fluid. The viscosity of this fluid decreases with time. Because it does so, proppant is released from the suspension after a while and starts to settle. The goal is to have a good propped fracture so that the created fracture dimensions are present after closure.

A solution to counteract early settling can be to inject large volumes of proppant. The total proppant mass is varied from 1,500 to 3,000 tons kg. These are large amounts compared to conventional oil and gas fracturing treatments. It is however expected that the amount of proppant that can be injected is constraint by costs rather than by its volume.

The proppant is a conventional natural sand and is relatively cheap. Results of scenario 1 are shown in table 6.1. Visualization of the fracture design is presented in figure 6.5.

Table 6.1   Scenario 1 results fracture simulation of LTG-01

Ton prop (kg)	l (m)	w (mm)	h (m)	k (mD)
1,500	769	3.5	107	69,404
2,000	853	3.8	129	69,628
2,500	750	5.2	143	69,123
3,000	552	8.1	77	68,836
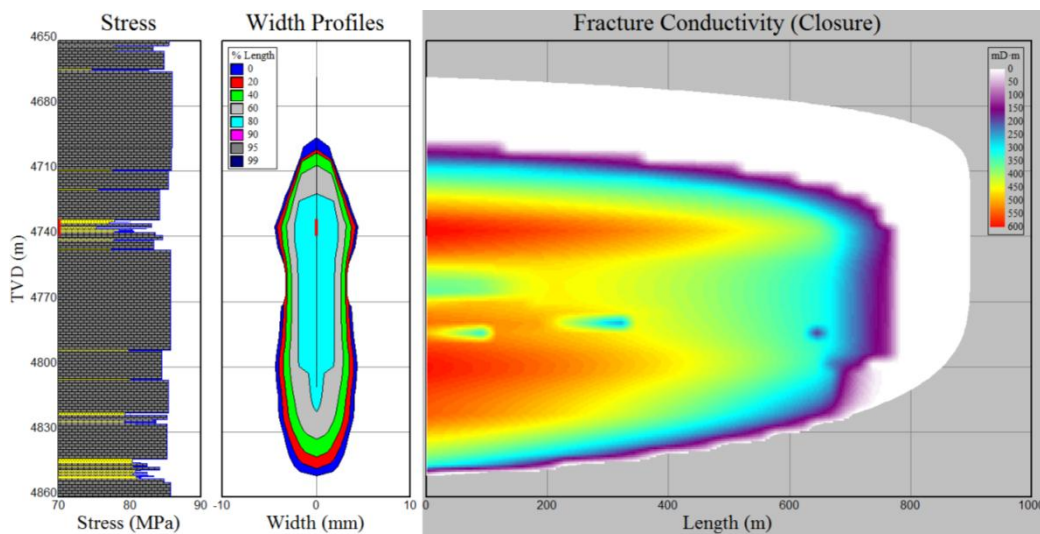
Figure 6.5   Stress profile and fracture dimensions of the first model scenario of LTG-01. Bluish spots are artefacts in the model.

Scenario 2: constant viscosity fracturing fluid

In the second scenario a different kind of injection fluid was used. A fluid with a constant viscosity keeps the proppant from settling in the later stages of injection. These kinds of fluids are very scarce in the MFrac database and in general as they are not used very often in conventional fracturing of oil and gas wells. This is because constant viscosity fluids are more difficult to clean up after the treatment.

The selected fluid is not ideal because the overall viscosity value is too low. However, it gives an idea of the possibilities of a constant-viscosity fluid. It results in a fully propped fracture after the treatment. A total of 1700 m³ was injected with increasing proppant mass from 700 to 2,200 tons kg. The proppant type is similar to the first scenario. Results of the simulation are shown in table 6.2. Visualization of the fracture design is shown in figure 6.6.

Table 6.2   Scenario 2 results fracture simulation of LTG-01

Ton prop (kg)	l (m)	w (mm)	h (m)	k (mD)
700	700	0.97	256	75,785
1,200	802	1.52	260	75,003
1,700	781	2.46	276	73,526
2,200	765	3.62	309	71,595
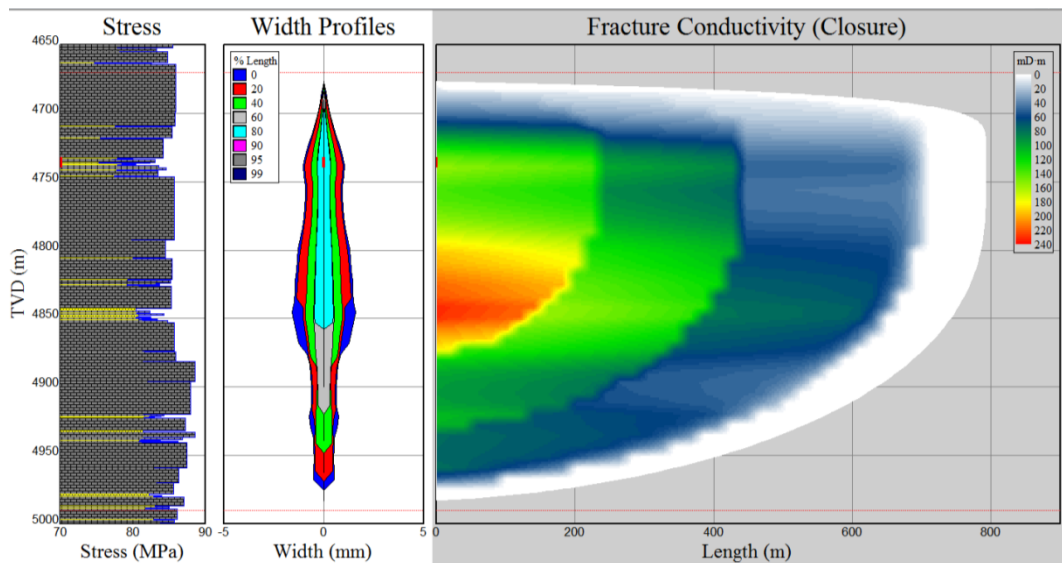
Figure 6.6   Stress profile and fracture dimensions of the second model scenario of LTG-01.

Comparison of both scenarios

The fracture permeability in the two scenarios is fairly constant. During both simulations the same proppant is used, only the concentration changes. In both scenario's, increasing the proppant mass results in larger height and width of the fracture. The length is not necessarily a function of proppant mass because it is mainly dependent on the volume of injected fluid and the leakoff (therefore reservoir permeability).

Overall it can be concluded that created fracture dimensions are likely to be high enough for sufficient flow rates and heat exchange between host rock and fracture fluid. The resulting dimensions and permeability will be incorporated into a reservoir model in the next chapter to show if this is the case.

The viscosity of the fracturing fluid has a major effect on fracture dimensions. The viscosity of the fluid in scenario 1 is a factor 10 higher. This has a positive effect on the width of the fracture. However, the fact that the viscosity decreases with time has a negative effect on the propped height and length. The viscosity of the fluid in the second scenario is relatively low. Therefore the width is less. However, the constant viscosity over time causes the fracture to be well-propped.

Lower viscosity fluids are generally more easily produced from the fracture and host rock after the fracturing treatment is finished. This cleaning of the fracture is required to prevent a decrease in permeability.

In deep geothermal projects like this one, high temperatures and pressure are encountered. These have a large effect on the fracturing fluid. A lot of research is ongoing to engineer fracturing fluids that have a desired viscosity vs time behavior. Contact with fracturing service companies is required to investigate whether these fluids are available at this moment. This can be incorporated into a future study.

6.3.2 Sensitivity analysis

The results of the sensitivity analysis are hard to interpret. There is not a direction relation between a change in a single input variable and the resulting output. This can be attributed to the complexity of the model. Single input parameters affect multiple output parameters (multiple fracture dimensions). This causes the sensitivity analysis results to deviate from the expected (qualitative) results shown in figure 6.2.

The relation between a change in input and the total fracture volume is more similar to literature findings. The change in fracture volume related to a change in input parameter is shown in figure 6.7
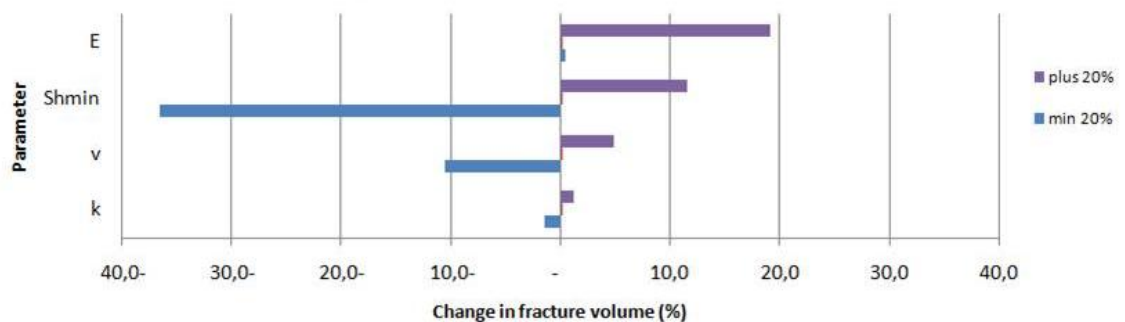
Figure 6.7   Effect of varying rock parameters on fracture volume.

We will not go into detail on why a certain parameter behaves like it does because it is outside the scope of this project at this point. The most important conclusions are presented here. To put the following results in perspective, the increase or decrease from the base scenario is 20% for every parameter.

- For the propped length, the maximum change resulting from a change in input is only about 10%. Considering the change in input varies up to 30%, this is a fairly minor effect. Young's modulus and the permeability, when increased tenfold, have the largest influence on the output.
- The maximum variation in propped height is about 30%; this is a significant amount. Young's modulus and the minimum horizontal stress are the largest contributors to this change. The effect of a factor 10 increase in permeability is only about 11%.
- The propped width changes with a maximum of about 13% after a change in input. Again, Young's modulus and the minimum horizontal stress have the largest effect.
- The fracture permeability is hardly affected by a change in one of the input parameters. It is mainly controlled by the proppant size and concentration. These have been kept constant throughout the sensitivity study.

Overall it can be concluded that the impact of a change in input parameter on the fracture dimensions is fairly limited. Only the propped height shows a significant variation in output value. But it has to be kept in mind that this is after a variation in input of 20%. These numbers are large and are expected not to occur in the simulated well, because the uncertainty in the input data is low.

The two parameters that have the largest impact on the output are Young's modulus and the minimum horizontal stress. The effect of the permeability is limited in most cases.

This could be caused by the extremely low value. The model could be more sensitive to permeability when it reaches a higher value.

6.4   Waterfracs

Waterfracs are a relatively novel method of stimulating a reservoir. The method is especially effective in ultra-low-permeability reservoirs. These reservoirs have limited leakoff of fracturing fluid from the fracture to the formation. This implies that a very large fracture can be created with a small volume of fluid.

To keep the fracture open, shear failure is required to establish some kind of misalignment of the fracture faces. Proppant is used only in very small concentrations, mostly to establish some permeability in the near-wellbore region. Because proppants are not used, the viscosity of the fluid can be kept low. Reducing proppant concentration and using water-based fracturing fluids is very cost effective.

The potential of shear failure increases with the presence of natural fractures (Moeck et al, 2009). However, quantifying this shear component is beyond the scope of this study. Also, the accuracy of current available data is not sufficient to perform calculations resulting in the shear stress. This was also noted in paragraph 5.3.

Fracturing treatments, whether in a naturally fractured reservoir or in a solid formation, are accompanied by seismicity. Whether or not this is potentially hazardous depends on a lot of factors. Seismicity can be kept below levels noticed by human beings if the right precautions are taken. Monitoring seismicity is always performed before, during and after a fracturing treatment.
Some treatments induce a higher risk than others. A waterfrac treatment is generally considered to be of a somewhat higher risk than a conventional (propped) fracturing treatment.

Future studies should focus more on the origin and effects of induced seismicity. These subjects can be attributed in a literature research.

6.5   Summary

In the previous chapters it was shown that the primary permeability of the Zeeland Formation is insufficient for conventional geothermal activities. Additionally, fault zones are hard to locate and therefore to exploit. As a backup scenario this study has focused on hydraulic fracturing to improve the reservoir properties of the Zeeland Formation.

MFrac software is used to simulate the initiation and propagation of a fracture. Data needed for this model is not available at the project location. Therefore, well LTG-01 was simulated to give an indication of the effects of a stimulation treatment in the Zeeland Formation. The most important input parameters are Poisson's ratio, Young's modulus, matrix permeability and the minimum horizontal stress.

Two scenarios were eventually modelled: a scenario with a decreasing viscosity fracturing fluid and one with a constant viscosity fracturing fluid. Four simulations with increasing proppant concentration are run for each scenario yielding eight runs in total.

Each run has resulted in a fracture with different dimensions (length, width and height) and permeability. In the following chapter these output values are put into a reservoir model to show which one of the designed fractures can facilitate the desired flow rate. Also, the effect of injecting cold water on the temperature of the produced fluid is investigated.

The pressure and temperature of the Zeeland Formation is expected to increase from LTG-01 to Hoogeveen. The lithology of the Zeeland Formation below Hoogeveen might also differ from that in the LTG-01 well. The mechanical rock properties -elastic moduli- can also change with lithology. A sensitivity analysis is performed to see the effect on the output.

Young's modulus and the minimum horizontal stress are the most sensitive parameters in the modelling. Accurately determining these parameters is key for a definitive fracture design in the future of this project.

Design parameters such as volume of injected fluid and proppant can be changed and this makes it possible to design a fracture with preferred dimensions for the required flow rate.

The concept of waterfracs is addressed very briefly. This kind of fracturing operation does not require a proppant to keep the fracture open and is therefore significantly cheaper. However, there is more uncertainty in resulting fracture permeability and the risk of induced seismicity is higher. Waterfracs show great potential but this concept should be studied into more detail in a following study.

7 Reservoir modelling

7.1 Overview of the simulations

Results from the fracture modelling resulted in two possible scenarios for LTG-01. Each of which consists of four different variants. Their properties -geometry and transport parameters- are listed in tables 6.1 and 6.2 respectively. With this information, eight reservoir models were constructed. Flow and heat transport modelling is carried out to assess the reservoir performance for each scenario and respective variants over a period of 30 years.

7.1.1 Model setup and reservoir parameters

The reservoir simulations are based on the system schematically shown in Figure 7.1. It is assumed that the fractures created will extend symmetrically from the producer to the injector. The fracture length determines the well spacing. In addition, it is assumed that the fractures do not interact thermally and therefore can be treated separately. Given the symmetry of the system only the area circled by the green dotted line is simulated.
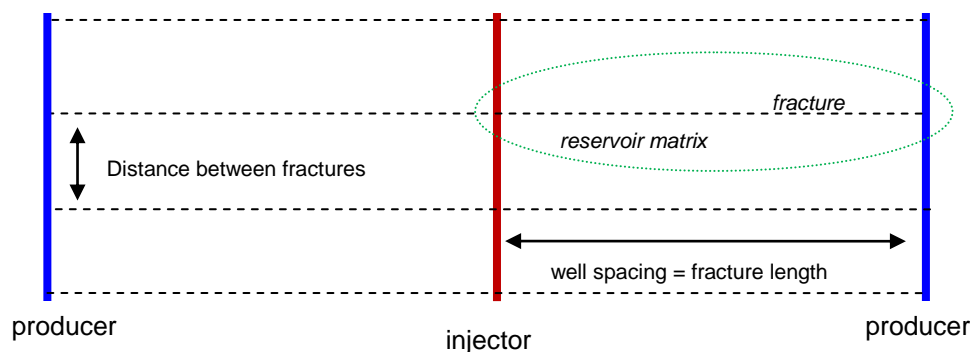
Figure 7.1 Schematic representation of the reservoir system. The green doted area corresponds to the modelled area.

The reservoir matrix is of very low permeability. However, the fractures create the necessary permeability for flow to take place between the wells. The fracture is represented in the models as a zone of high permeability grid blocks in the reservoir matrix. These grid-blocks extend from the edge of the injector to the edge of the producer. In addition, given the technique proposed to create the fractures (i.e. proppant injection) a degree of porosity is retained inside the fracture. The permeability and porosity of the fracture are assumed to be uniform along the fracture in the horizontal and vertical (when used) directions. The matrix and fracture characteristics are listed in Table 7.1

Table 1. Transport parameters

Parameter	Units	Reservoir matrix	Fracture
Permeability	[m^2]	10^{-15}	Varies (see table 7.3)
Porosity	[%]	0.01	0.3
Thermal conductivity	[W/m.k]	2,8	2,8

7.1.2 Numerical codes

The thermal simulations are carried out with the computer programme HSTWin-3D, a code specially developed for heat and solute transport in porous media. The code takes into account the dependency of the fluid properties such as viscosity and density on the temperature and concentration changes (Kipp, 1986). For the pressure calculations the computer programme MLU was employed.

7.1.3 Preliminary calculations

Preliminary calculations were carried out in order to investigate:
- the space needed between fractures to assume they are thermally independent.
- the importance of three dimensional effects (buoyancy flow inside the fracture) compared to two-dimensional. Grid convergence is also tested.
- the total number of fractures per scenario

Space between fractures
The spacing between fractures depends on the area of influence of the cold front created in the injection well. Because in the calculations it is assumed that each fracture is thermally independent, it is important to determine the optimum spacing required. Preliminary runs (not shown here) estimate that a distance of > 150 m between fracture fulfils this requirement. The general model characteristics are listed in Table 7.2. These parameters are obtained from information given in previous chapters.

Table 7.2   General model characteristics

Parameter	Units	Value
Initial reservoir pressure	[bar]	700 (hydrostatic)
Initial reservoir temperature	[°C]	257 (results of 1D temperature model –see Chapter 3)
Total flow rate	[kg/s]	110
Injection temperature	[°C]	70
Salinity level	[g/l]	110
Distance between fractures	[m]	150
Well spacing	[m]	Varies (see table 7.3)
Boundary conditions		Const P applied to right and left side of model
Thermal boundary conditions		Heat exchange with upper and lower layers

2-Dimensional vs 3-Dimensional modelling
Given the high permeability of the fractures (also in relation to the matrix permeability) and the large temperature difference between the initial reservoir value and the injection temperature, buoyancy driven flow (free-convection) may play a role.

Depending on the degree of buoyancy, the temperature front will 'tilt' when flowing between wells. This means that the sweeping behaviour will not be uniformly distributed vertically (as shown in Figure 7.2). Depending on the overall effects, an earlier (or later) thermal breakthrough may occur. It can be observed that buoyancy effects take place but will not be significant. This is also observed in Figure 7.3. It was therefore concluded that the reservoir and fracture system could be correctly modelled as a 2-dimensional system.
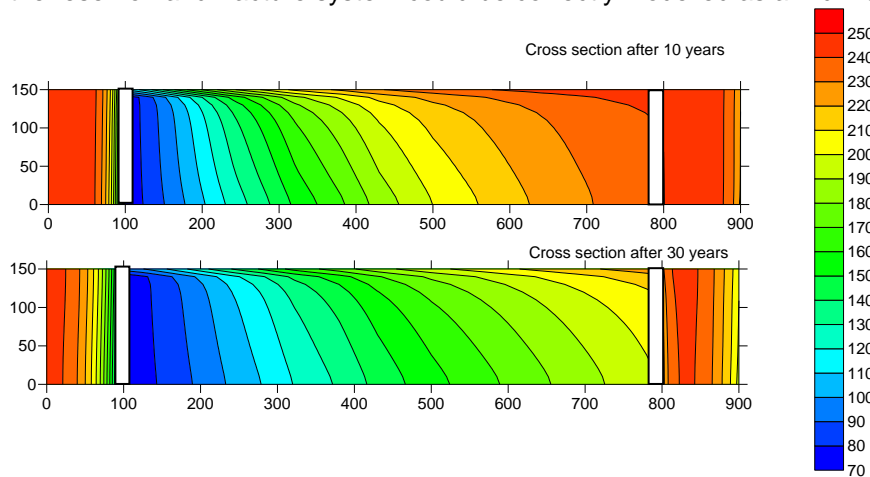
Figure 7.2 Temperature profiles after 10 and after 30 years. Preliminary runs assumed a fracture permeability of 70 Darcy.
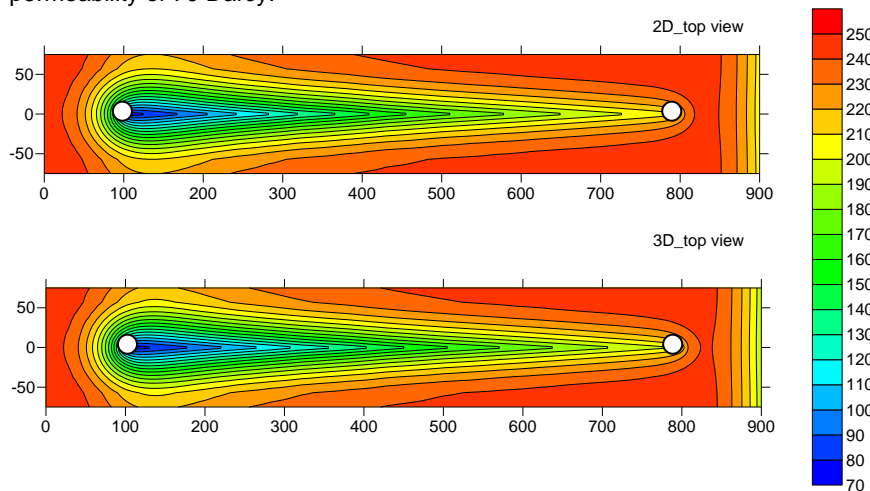
Figure 7.3 Comparison of temperature contours after 30 years of operation for a 2D and a 3D system. Top view.

Total number of fractures
By increasing the number of fractures, the desired flow rate can always be achieved. However, due to costs and technical constrains, the goal is to keep the horizontal wellbore section as short as possible. The number of fractures that can be created over this section depends on the spacing between fractures.

Analytical calculations were first performed to estimate the number of fractures needed to ensure that the temperature drop in the producer would only drop a few degrees after 30 years. The optimum value found is given in table 7.3 along with other general dimensions for each scenario. The numerical simulations will then confirm if the analytically-estimated total number of fractures is appropriate or should be modified.

Table 7.3   Specifications of each modelling scenario

Runs	well spacing (m)	fracture width (mm)	fracture height (m)	permeability (D)	first estimate of total number of fractures (analytical model)
Scenario 1a	769	3.5	107	69.4	35
Scenario 1b	853	3.8	129	69.6	30
Scenario 1c	750	5.2	143	69.1	25
Scenario 1d	552	8.1	77	68.8	60
Scenario 2a	700	0.97	256	75.7	20
Scenario 2b	802	1.52	260	75.0	15
Scenario 2c	781	2.46	276	73.5	15
Scenario 2d	765	3.62	309	71.6	15

7.2   Results of numerical simulations

The goal is for the dimensions of the engineered fracture to provide enough surface area:
- for the fluid to be sufficiently heated by the host rock on its path from injection to production well
- to facilitate the desired flow rate of 110 kg/s.

Simulations results showed that Scenario 2d had the better thermal performance with the minimum number of fractures and therefore only the results of this scenario are further discussed here. In addition, based on this scenario the resulting pressure changes are calculated.

Pressure calculations
The production and injection of water in the fractures generates certain pressure changes. The amplitude of the changes are dependent on the fracture transmissivity and injection/production rate. To calculate these pressure changes a MLU model was setup. Only one fracture, with a proportional rate (1/20 of the total rate), was modeled. With MLU it is not possible to take the transmissivity change due to temperature changes into account. To solve this problem a model with one transmissivity was made (based on the initial temperature) and the injection rate was scaled to compensate for the lower viscosity due to the lower temperature. In Figure 7.4 the calculated pressure distribution within the fracture is shown.
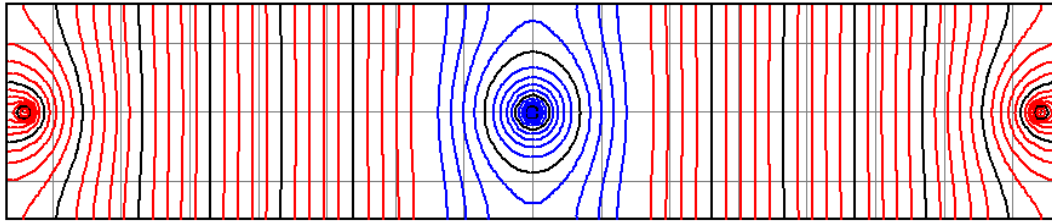
Figure 7.4   Pressure changes, pseudo stationary situation (blue: pressure decrease, red: pressure increase).

Pseudo-stationary conditions are achieved relatively fast in the producer whilst in the injector this occurs at a later time. A pressure difference between the injection and production well in the reservoir of around 150 bar was calculated with this model. To get the total pressure change within the systems this pressure change should be added by the pressure change within the production and injection well.

The pressure change within the production and injection well depends on several factors. The most important are the temperature of the water, the diameter and the length of the tubing and the flow. Based on the preliminary well design presented in this report the total pressure change within the production and injection well is calculated to be around 110 bar. This brings the total pressure loss of the systems on 260 bar.

Thermal calculations
Numerical simulations showed that the total number of fractures should be increased to 20 to maintain the temperature drop at the producer to only few degrees. This is shown in Figures 7.5 and 7.6.
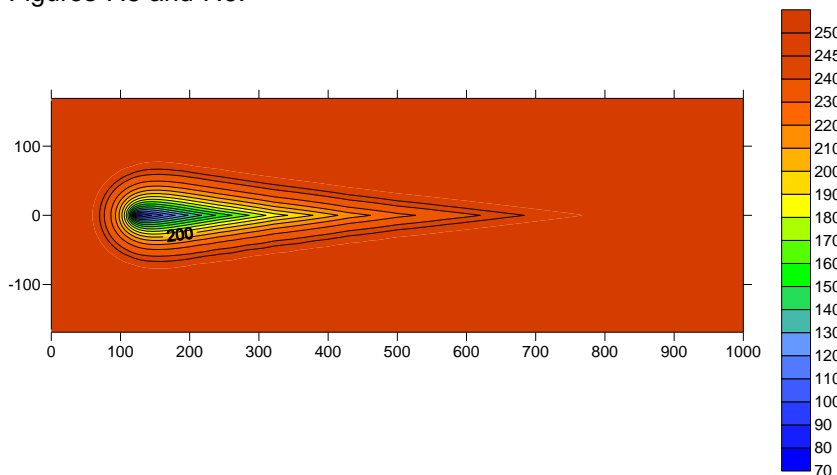
Figure 7.5   Isotherms after 30 years for scenario 2d assuming 20 fractures.

It can be seen that although the majority of the flow between the wells is expected to take place inside the fracture, the thermal effects actually extend outside the boundaries of the fracture. Outside the fracture heat conduction into and out the fracture and reservoir matrix are controlled by the temperature gradient the develops. The extent of the heat transfer area will be the largest where the temperature difference is the largest. This occurs close to and around the injection well.

The resulting temperature decline in the producer in the course of 30 years is shown in Figure 7.6.
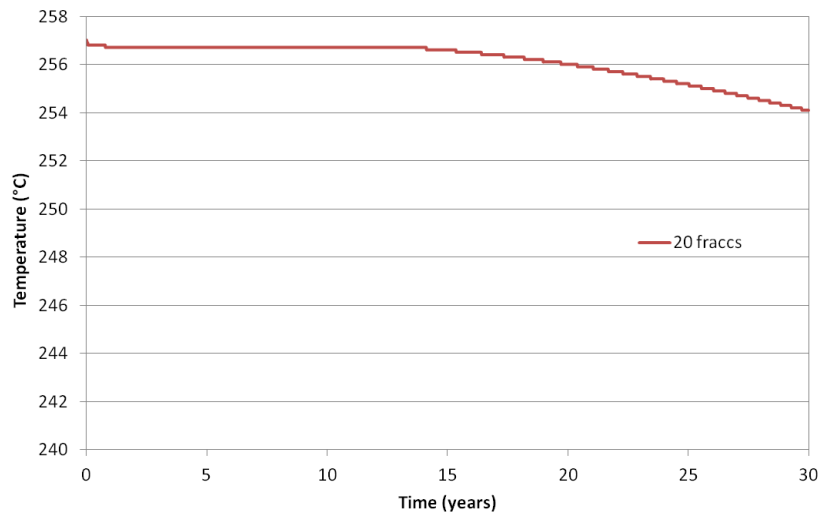
Figure 7.6   Temperature evolution at the producer assuming 15 and 20 fractures.

Previous figures also show that as the number of fractures decreases the total flow rate stay the same, flow rate per fracture increases and therefore the cool injected water reaches the production well quicker and therefore the temperature drop is larger. However, by increase the number of fractures to 20 a temperature decline of few degrees is achieve. Hence, assuming an average fracture spacing of 150 m and a number of 20 fractures, implies that a 3,000 m (horizontal) section has to be drilled and stimulated.

7.3   Summary

The performance of the eight different scenarios was tested with the aid of numerical simulations. Fracture permeability was added to the model by using high-permeability grid blocks. It was shown that for the conditions (reservoir setting and operational) 2D model setup represented accurately enough the system thermal behaviour.
Scenario 2d showed to have the best overall performance it terms of temperature drops, optimum number of fractures needed and dimensions. Assuming a total number of fracture of 20, with 150 m of minimum spacing between fractures, a horizontal section of 3.000 m has to be drilled and stimulated. These characteristics will be taken as the starting points in further chapters.

8 Well design

8.1 Introduction

A conceptual well design has been made by Well Engineering Partners for the location of Hoogeveen. The well design shows the layout of the production and injection wells. It also shows which casings (well protection tubes) are being used and the diameters of the ultimate liners placed in some sections of the wells. The length of the different tubes will depend on the lithology and structures of the subsurface and the ultimate purpose of the well.

The target for the wells is the Zeeland Formation. The top of the formation is estimated at 6,800 m below groundlevel. The thickness of the formation is estimated to be between 200 and 800 m.

It is very important for the project that a sufficient flow rate from the fractured reservoir is obtain. In the previous chapters it has been indicated that approximately 20 fractures should be created, with a minimum spacing of 150 m between the fractures. This implies drilling a horizontal section of some 3,000 m for optimal placement of the fractures.

Appendix 4 shows the current well design. This well design is based on current available knowledge of the geology below Hoogeveen. When more data becomes available in the course of this project, the well design will be adapted to reflect the latest knowledge.

8.2 Well layout

Appendix 4.1 shows a side view of the wells. The wells start to deviate at approximately one kilometre depth. The approach is to first drill 'vertically' -at a slight angle- to a depth of 7,000 m until the Zeeland Formation is encountered.

The presence of the fault at a depth of 7,000 m can only be proven when the well intersects this fault. In case the fault is not encountered, we have to rely on reservoir stimulation (fracturing the formation). This is described in more detail in chapter 6.

To ensure a large enough reservoir thickness, drilling is continued until the minimum thickness for a fracturing treatment is reached. With the current fracture design, this thickness is approximately 300 m. These steps are taken to reduce the uncertainty in the geology of the Zeeland Formation.

After confirmation of the potential of the Zeeland Formation, the wellhead will return to a shallower depth and start to drill horizontally. This is shown in the second figure of appendix 4.1. Because the Zeeland Formation is expected to dip towards the northeast, the "horizontal" well section is drilled at a slight angle, following the dip of the Zeeland formation. This is very beneficial for the drilling operation.

In the design of the subsurface fractured system, we assume to be needing two production wells and one injection well in between (as shown in chapter 7).

The layout of the production and injection well as shown in appendix 4.2 and 4.3 is very similar. The biggest difference is that the producer well will have a sidetrack. This sidetrack will run horizontally and parallel to the other horizontal sections of the producer and injection wells.

Because a flow rate of 110 kg/s is desirable, the flow conduit needs to be able to facilitate this flow rate. The smallest pipe diameter (outside) in the current design is 7 inch. This diameter is used over the majority of the horizontal section.

8.3   Cost estimate

An overview of the estimated costs for this drilling operation is provided in figure 8.1. The total amount of meters drilled is estimated to 24,000 m. This is for one injection well with a sidetrack and one production well. This figure also shows that most of the costs are spent on the materials. The choice of materials strongly depends on the composition of the geothermal fluid that is being produced. Because the latter is largely unknown, a more or less standard type of steel casing is used in these calculations.

Well Cost Hoogeveen (50/50 estimate)	
Scenario	1
Last liner	7"
Meters drilled injector + producer	24.212
Cost estimation	x 10^3 €
Site preparations	500
Operational cost	16.593
Additional services	10.932
Materials	21.548
Engineering and Supervision	1.940
Total (base case)	57.746
Project execution time (days)	469
Per Euro/m	2.385
Excluded:	
Insurances (7% of total costs)	4.042
Unforeseen (10% of total costs)	5.775
Fraccing per well (circa 5% of total costs)	2.887
Geological research	-

Figure 8.1   Cost overview of drilling operation for Hoogeveen.

The net cost is estimated on € 2.385 per meter. In the business case a price of € 3.250 is budgeted which includes insurances, unforeseen cost and possible cost overruns.

8.4 Conclusions

The application of two injection wells and one production well including horizontal sections is a fairly novel concept in the geothermal industry, although common in the oil and gas industry. The horizontal sections are required for proper placement of the hydraulic fractures.

The vertical section of the wells, drilled through the formations above the Zeeland formation are fairly straightforward and pose no significant troubles of hazards. In order to place the well in the most optimal way in the Zeeland formation, the uncertainty in the depth of the top of the Zeeland Formation has to be reduced. This may mean that the well is first drilled "vertical" through the Zeeland Formation to determine exactly where this is positioned and then deviated from a point higher in the well.

Drilling a well to a depth of 6,800 m is not yet done in the geothermal industry in the Netherlands, although it has been done often in the oil and gas industry. The large horizontal section needed for the hydraulic fracturing treatment is perhaps the most challenging part of the drilling process but with the experience from the oil and gas industry this drilling operation can be realized. Wells with horizontal displacements of more than 10 kilometers have been drilled very successfully in England and Germany.

The well design shown here is a conceptual design. Before actually drilling the wells, many other things need to be taken into consideration. Amongst which are safety measures, choice of drilling equipment i.e. rig, casing, mud etc., logging the wellbore, coring, logistics etc. These subjects are all attributed in the phase preceding the actual drilling phase.

9 Power plant

9.1 Introduction

This chapter analyses the technical and economical feasibility of the power plant. A conceptual design of the power plant is provided. This is a high level description of the most critical components of the power plant and the most important safety aspects and operation.

For the study on the power plant a well head temperature of 240 ⁰C and a flow rate of 120 kg/s were assumed. The outcome of the reservoir modeling is 110 kg/s, for the business case the capacity of the power plant has been correct linearly for the lower flow rate.

An overview using factsheets of each of the currently commercially available power plant types is provided as a first step in paragraph 9.2 The binary cycle or Organic Rankine Cycle (ORC) power plant is selected as the most suitable option, based on a quantitative and qualitative assessment in paragraph 9.3. Paragraph 9.4 contains the conceptual design of the power plant.

This chapter is a summary of a larger study[2] on the feasibility of the power plant that has been executed by KEMA.

9.2 Types of power plant

Geothermal power generation works according to the same thermodynamic principles as standard fossil fueled power plants: heat is converted into work and the work is converted into electricity by a generator. The main difference is that a geothermal power plant has no need for fuel or a boiler; instead the heat is extracted from the hot geothermal water (or brine). This report gives an overview of the different methods of converting this heat to electricity and a conceptual design of the most suitable power plant type.

9.2.1 Single flash (steam) cycle

The single flash steam cycle uses the brine directly in a steam turbine. This simple cycle is widely used, especially in the early stages of development of a geothermal field. The brine coming from the production well is often a water-steam mixture and by lowering the pressure the steam fraction can be increased (called flashing).

---

[2] Geothermal power production Hoogeveen, J.R. Smeets, KEMA, 23 January 2012.

This causes the temperature of the brine to drop, so this approach works most efficient for higher temperature wells (at least 180 °C).

The process flow sheet of a single flash cycle is shown in figure 9.1. The hot brine leaving the production well (PW) is often a two phase steam-water mixture or a compressed liquid, depending on the temperature and pressure of the geothermal reservoir. The liquid brine is (partly) flashed to steam when the pressure is reduced in the cyclone separator (CS) and the steam is separated from the liquid. The steam passes through a demister or moisture remover (MR) and the dry steam expands in a turbine to generate electricity. The low pressure steam leaving the turbine is condensed in a water cooled condenser (C) in this example. The cooling water is cooled using a cooling tower (CT). Finally the liquid brine from the flash vessel (CS), the remaining liquid from the cooling tower and possibly non-condensable gasses (after compression) are re-injected in the injection well (IW).
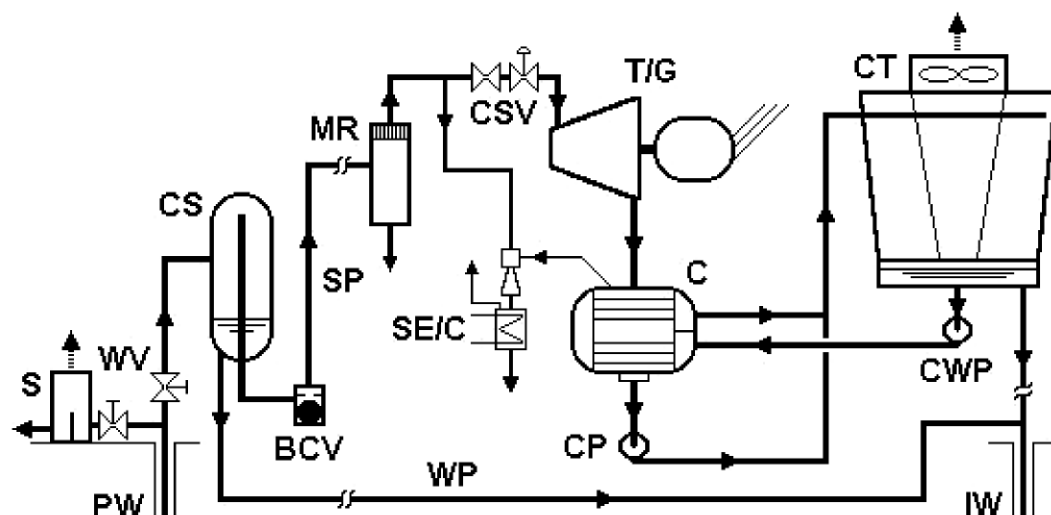
Figure 9.1   Simplified process schematic of a single flash power plant (DiPippo, 2008)

Nomenclature						
BCV	Ball check valve	CWP	Cooling water pump	SE/C	Steam ejector / condenser	
C	Condenser	IW	Injection well			
CP	Condensate pump	MR	Moisture remover	SP	Steam piping	
CS	Cyclone separator	PW	Production well	SR	Steam receiver	
CSV	Control & stop valves	S	Silencer	T/G	Turbine/generator	
CT	Cooling tower			WP	Water (brine) piping	
CW	Cooling water			WV	Wellhead valve	

Positive aspects:
1   Much operational experience: 159 units, 4015 MWe, sizes 0.3-110 MWe
2   Relatively simple cycle
3   Relatively low investment cost.

Negative aspects:
1 Moisture Remover and Cyclone Separator (flash vessel) have a high fouling risk and may require frequent maintenance
2 Acting safety measures might cause emissions to the environment
3 Relatively low efficiency.

9.2.2 Double flash (steam) cycle

The double flash cycle is an extension of the previously described single flash process. This technology is widely used throughout the world, often when additional plants are constructed on a well known geothermal field. The second flash results in a larger steam and overall power production, increasing the efficiency of the conversion process.

The hot brine leaving the cyclone separator (flash vessel) in the single flash plant still contains usable energy. The double flash cycle is developed to extract more of this remaining energy from the brine by adding an additional flash step. This second drop in pressure cause the temperature of the brine to drop further and a high starting temperature is required for this process to be efficient (at least 200 °C).

Figure 9.2 shows the simplified flow diagram of a double flash plant. The main difference with a single flash plant is that the hot brine after the first flash chamber (CS) is flashed again at a lower pressure (F) to produce more steam. This steam has a lower temperature and pressure and is fed to the turbine (T/G) at a lower pressure stage. Separate high and low pressure turbines are also possible.

Figure 9.1   Simplified process schematic of a double flash power plant (DiPippo, 2008)
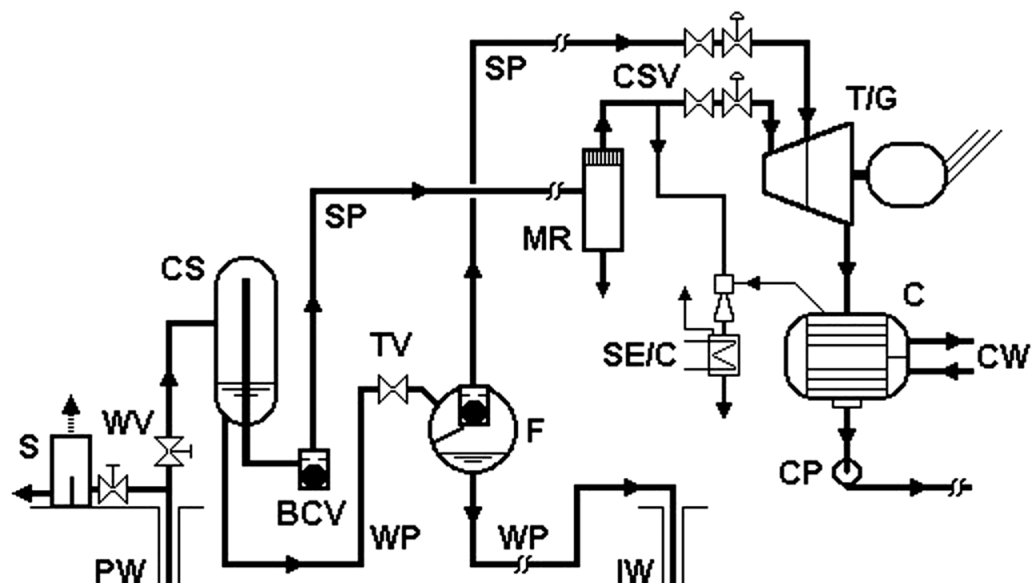
Nomenclature					
BCV	Ball check valve	F	Flash vessel	SP	Steam piping
C	Condenser	IW	Injection well	SR	Steam receiver
CP	Condensate pump	MR	Moisture remover	T/G	Turbine/generator
CS	Cyclone separator	PW	Production well	TV	Throttle valve
CSV	Control & stop valves	S	Silencer	WP	Water (brine) piping
CW	Cooling water	SE/C	Steam ejector / condenser	WV	Wellhead valve

Positive aspects:
1   Much operational experience: 69 units, 2192 MWe (in 2007), sizes 1-110 MWe
2   Higher efficiency compared to the single flash cycle
3   Still relatively low investment cost.

Negative aspects:
1   Moisture Remover and Cyclone Separator (flash vessel) have a high fouling risk and may require frequent maintenance
2   Second flash increases the risk of silica scaling even more
3   Acting safety measures might cause emissions to the environment
4   More complicated cycle and control.

9.2.3   Binary cycle: Organic Rankine Cycle (ORC)

Not all geothermal sources have a temperature high enough to create steam by flashing. The Organic Rankine Cycle (ORC) is developed to produce electricity from heat sources as low as 120 °C. In a normal steam cycle, or Rankine cycle, water is used as the process fluid. In order to operate at a lower temperature a fluid is needed that can be vaporized at a lower temperature. Organic fluids are well suited for this application and the resulting thermodynamic cycle is therefore called an Organic Rankine Cycle. The heat from the brine is exchanged to the organic fluid in a heat exchanger, thus two separate cycles are created: one cycle containing the brine and one closed cycle containing the organic fluid. This indirect use of geothermal energy is called a binary cycle.

The simplest version of the binary cycle is schematically shown in figure 9.3. The heat from the geothermal brine is extracted with heat exchangers (PH and E) to the binary cycle. The cooled brine is re-injected in the injection well (IW). In the binary cycle an organic fluid, such as pentane or hexane or a refrigerant such as R134a or R245fa, is used as the process fluid. This fluid is evaporated in the heat exchanger (E). The vapor drives a turbine, which produces electricity. The expanded vapor is condensed in the condenser (C) and pressurized again with the condensate pump (CP) to complete the cycle.

The two separate cycles allow for a more simple design. Operation is often done remotely. The control and stop valves (CSV) are used together with the condensate pump (CP) to control the flow based on the temperature of the fluid leaving the evaporator (E).

Positive aspects:
1   Much operational experience: 162 units, 373 MWe (in 2007), sizes 0.1-45 MWe
2   Higher efficiency compared to the flash cycle, especially at low temperature or small scale
3   Low maintenance cost
4   Remote operation common
5   Reliable and high availability.

Negative aspects:
1   Higher investment cost compared to flash plants
2   Organic fluids may be flammable or toxic. Additional safety measures may be required.
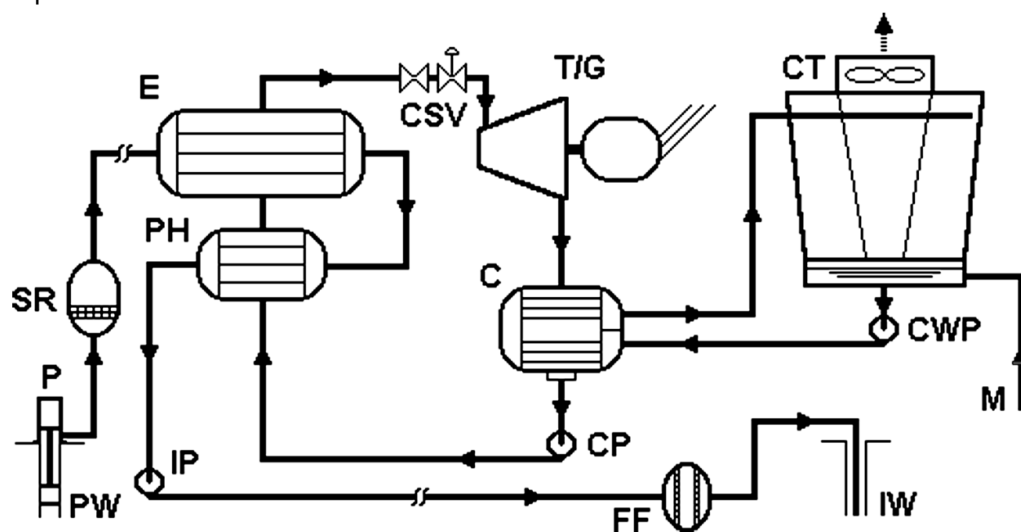
Figure 9.3   Simplified process schematic of a binary power plant (DiPippo, 2008)

Nomenclature					
C	Condenser	E	Evaporator	P	Pump
CP	Condensate pump	FF	Final filter	PH	Pre-heater
CSV	Control & stop valves	IW	Injection well	PW	Production well
CT	Cooling tower	IP	Injection pump	SR	Steam receiver
CWP	Cooling water pump	M	Make up water	T/G	Turbine/generator

9.2.4   Binary cycle: Kalina cycle

The Kalina cycle is a binary cycle like the ORC, but with an additional feature. It uses a solution of ammonia (NH3) in water as the process fluid. The concentration of ammonia is varied within the process cycle and this allows tuning of the fluid properties to the different requirements of different steps in the process. There are many different layouts of this cycle possible; in this factsheet the basic version is described.

The basic Kalina cycle is shown in figure 9.4. The geothermal brine is cooled in the heat exchanger (E) and injected in the injection well (IW). The heat is used to heat and partly vaporize the ammonia-water mixture and this mixture is then fed to a separator (S). The vapor in this separator is relatively ammonia rich as ammonia has a lower boiling point than water. The ammonia-rich vapor is expanded in the turbine (T) to drive a generator (G) while the liquid water with a low concentration of ammonia is cooled in a heat exchanger (PH). The low temperature fluid passes through an expansion valve (TV) to reduce its pressure to the turbine exit pressure and it is mixed with the low pressure vapor coming from the turbine. This mixture is cooled in a heat exchanger (RPH) and then condensed in the condenser (C).

The condensate pump pumps the liquid back to the required turbine inlet pressure and after passing through the preheating heat exchangers the fluid has completed the cycle.

The Kalina cycle is developed to increase the efficiency of low temperature electricity generation by better matching the fluid thermal properties with the different temperatures in the cycle. This technology is still in the development phase, there are only a few installations in operation at the moment. A 1.8 MWe installation has been built in 1999 at the Husavik power plant (Husavik, Iceland) and in 2007 a 3.3 MWe CHP plant in Unterhaching, Germany.
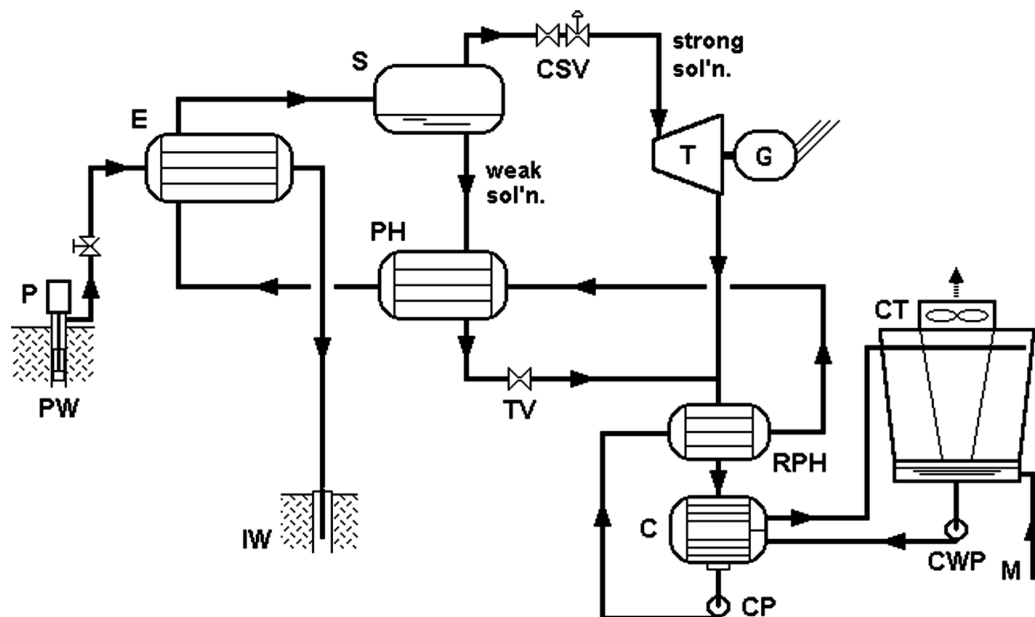

Figure 9.4   Simplified process schematic of a Kalina power plant (DiPippo, 2008)

Nomenclature					
C	Condenser	E	Evaporator	RPH	Recuperative preheat-er
CP	Condensate pump	IW	Injection well		
CSV	Control & stop valves	M	Makeup water	S	Separator
CT	Cooling tower	P	Pump	strong sol'n	Strong NH_3 solution
CW	Cooling water	PH	Preheater	T/G	Turbine/generator
CWP	Cooling water pump	PW	Production well	TV	Throttle valve
				weak sol'n	Weak NH_3 solution

Positive aspects:
1   Higher efficiency possible at low temperatures compared to ORC
2   Low maintenance cost
3   Remote operation possible
4   Reliability and availability could be high
5   The process fluid is inexpensive.

Negative aspects:
1   Little operational experience, not yet mature technology (1.8 and 3.3 MWe unit)
2   Slightly larger investment cost compared to ORC.

9.2.5   Combined cycle: single flash and ORC

The combined flash and ORC cycle is developed as an improvement of the single flash plant. Instead of flashing the low pressure brine again, as happens in a double flash plant, the heat from the remaining liquid brine is used in a bottoming ORC. This allows for a more efficient second cycle compared to the double flash plant.

The low temperature ORC can also be added in a later stage of the development of a geothermal field, for instance when several single flash plants are in operation and the available hot brine remaining is enough for an economical binary plant. This limits the initial investment cost and risk. The efficiency of this system depends on the temperature and the steam fraction of the brine at the production wellhead: the higher the steam frac-tion, the higher the conversion efficiency.

The combined cycle process in shown in figure 9.5. The hot brine from the production well (PW) is (partly) flashed to steam when the pressure is reduced in the cyclone sepa-rator (CS) and the steam is separated from the liquid. The dry steam expands through a steam turbine (ST) to generate electricity. The hot brine is cooled in heat exchangers (E and PH) and provides heat for the binary cycle and is injected together with the con-densed steam from the steam turbine into the injection well (IW). The organic fluid in the low temperature cycle (a-f) is evaporated in the brine heat exchangers (E and PH) and drives a binary turbine (BT). The low pressure vapor is condensed in the condenser (C) and pressurized with the condensate pump to complete the cycle.
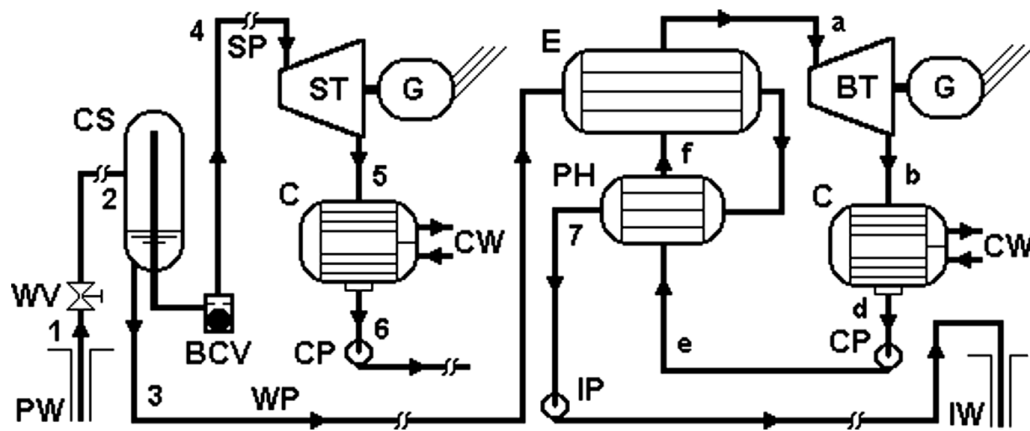
Figure 9.5   Simplified process schematic of a combined flash-ORC power plant (DiPippo, 2008)

Nomenclature					
BCV	Ball check valve	CS	Cyclone separator	PW	Production well
BT/G	Binary turbine / gen-erator	CSV	Control & stop valves	SP	Steam piping
		CW	Cooling water	ST/G	Steam turbine / gen-erator
C	Condenser	CWP	Cooling water pump		
CP	Condensate pump	IW	Injection well	WP	Water (brine) piping
		PH	Preheater	WV	Wellhead valve

Positive aspects:
1   Much operational experience: 46 units, 363 MWe (in 2007), sizes 1-110 MWe
2   Higher efficiency compared to flash plants
3   Investment in stages is possible: reduced risk.

Negative aspects:
1   High investment cost
2   Complicated system
3   Moisture Remover and Cyclone Separator (flash vessel) have a high fouling risk and may require frequent maintenance
4   Safety requirements for both high pressure steam and organic fluids.

9.2.6   Combined cycle: Cascade ORC

When a process spans a large temperature range, there is often not a single fluid with the best thermodynamic properties for this whole range. One way of solving this is the Kalina cycle by varying the composition of the process fluid, another possibility is by dividing the process in two steps and using two fluids. An organic fluid with a higher boiling point is used for the high temperature cycle and an organic fluid with a low boiling point is used for the bottoming cycle. By selecting the right organic fluids and optimizing the process parameters the efficiency can be increased compared to the standard ORC.

Figure 9.6 shows the schematic for a coupled high and low temperature ORC. The high temperature cycle (1-2-4-5-6) extracts the heat from the brine through heat exchangers (PH1 and E1) and the vapor is expanded through the turbine (HPT). The low pressure vapor is then condensed in the heat exchanger with the bottoming cycle (E2).

The low boiling point organic fluid in this second cycle (7-8-9-10-11) is evaporated and also expanded through a turbine (LPT). An induced draft air cooled condenser (ACC) is used in this example to condense the fluid and the condensate pump (CP2) pumps this fluid back to the process pressure.

Positive aspects:
1   High efficiency
2   Low maintenance cost
3   Reliability and availability could be high.

Negative aspects:
1   Little operational experience with this exact configuration
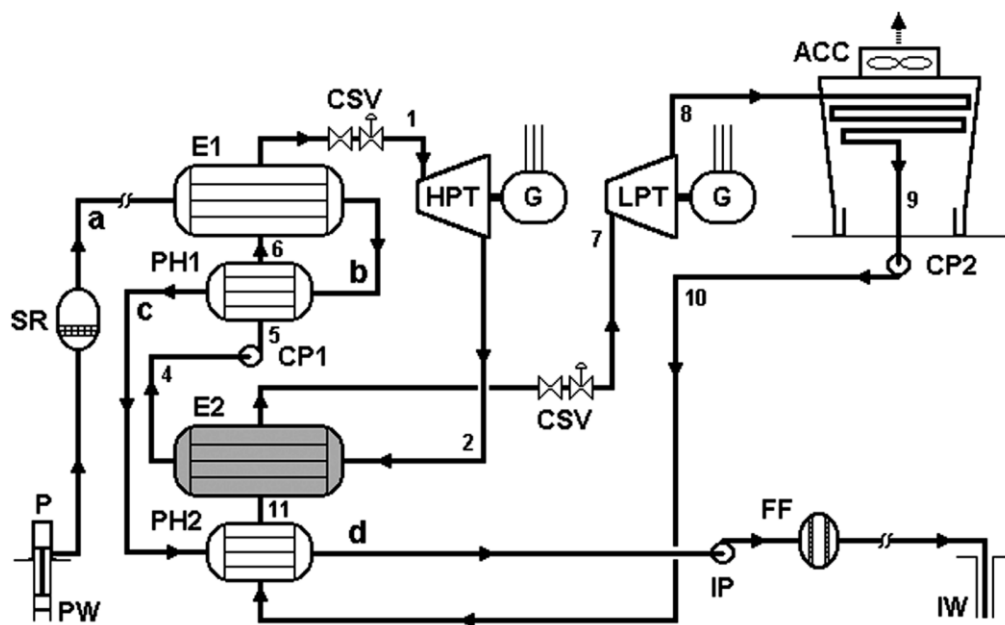2   More complicated cycle
3   High investment cost.

Figure 9.6   Simplified process schematic of a combined HP/LP ORC plant (DiPippo, 2008)

Nomenclature					
ACC	Air cooled condenser	E	Evaporator	LPT/G	Low pressure
CP	Condensate pump	FF	Final filter		turbine / generator
CSV	Control & stop valves	HPT/G	High pressure tur-	P	Pump
CW	Cooling water		bine / generator	PH	Preheater
CWP	Cooling water pump	IP	Injection pump	PW	Production well
		IW	Injection well	SR	Steam receiver

9.3   Power plant selection

This paragraph describes the selection of the geothermal power plant type that is most suitable for the process conditions expected near Hoogeveen. The definition of 'most suitable' is based on seven criteria that are discussed in this chapter. A summary of the results is shown in table 9.1.

The binary cycle ORC (organic Rankine cycle) is selected as the most suitable option, based on a comparison between six alternatives. The binary cycle combines a high availability with a high efficiency and has a modest investment cost and low operation and maintenance costs.

Table 9.1   Comparison of different geothermal power plant types.
Relative scores vary from -- (negative) to ++ (positive), X means not considered.

	flash		Binary cycle		Combined cycle	
	Single	Double	ORC	Kalina	Flash -ORC	Cascade ORC
1) Maturity of the technology	++	++	++	--	+	+
2) Yearly net power production [GWh]	65	80	127	X	97	138
3) Total investment cost [M€]	65	73	82	X	79	93
Specific investment cost [€/MW]	7.5	6.3	5.2	X	6.1	5.4
4) O&M cost [€/MWh]	5	9	2	X	6	3
5) Safety	+/-	+/-	+/-	+/-	+/-	+/-
6) Complexity	++	+/-	++	-	-	+/-
7) Environmental impact	-	-	+	+	-	+

Selection approach

The geothermal power plant selection process is divided in five steps to ensure all relevant options are thoroughly considered and an unbiased decision can be made on the most suitable type of power plant for this project.

The first step is creating a short list of power plant types to be considered. The six options are described in factsheets in paragraph 9.2. The second step is listing the criteria that will be used for evaluating each power plant type. The third step is a ranking in importance of the criteria, resulting in the list in Table 9.1.

Then each power plant type is judged using these criteria in step four. Some of the criteria are quantitative (power production, investment cost and O&M cost) and result in a numerical score, others are qualitative (maturity, safety, complexity and environmental impact) and have a relative score. The fifth and final step is discussing and weighting these scores to arrive at a choice for the most suitable power plant type.

Maturity of the technology

The energy conversion technology has to be mature enough in order to be considered a feasible option. There are a number of risks in developing a geothermal project and the power plant should not increase this risk without a good reason. The maturity of a technology is therefore a threshold or exclusion criterion; any option with a too low maturity is excluded.

For the six considered options there is only too little commercial operational experience with the Kalina cycle. There is also not so much experience throughout the world with the more advanced combined flash-binary cycle and the cascade ORC, but these are still commercially available from several suppliers. Based on the maturity criterion the Kalina cycle is excluded and not further investigated.

Yearly net power production

The amount of electricity that is produced each year by the geothermal power plant is the most important selection criterion. The higher the power production based on the same well conditions, the more renewable energy is produced. Table 9.2 provides an overview of the five remaining power plant options and their estimated yearly power production. The efficiency and net power are obtained from a simulation with the flow sheeting software Aspen Plus.

Table 9.2　　Comparison of yearly power production

| | Flash | | Binary cycle | Combined cycle | |
	Single	Double	ORC	Flash - ORC	Cascade ORC
Efficiency [%]	7.6	10.1	13.9	11.3	15.2
Net power [MW]	8.7	11.5	15.9	12.9	17.3
Availability [hour/a]	7500	7000	8000	7500	8000
Yearly power production [GWh]	65	80	127	97	138

Investment cost

The power plant in this project is only a part of the total investment. The investment costs of the geothermal power plant have to be considered along with the investment cost for the exploration phase, drilling of the wells and reservoir stimulation. The costs for the subsurface part of this geothermal project are assumed to be 50 M€, only for this comparison.

A difference in the real subsurface cost has only a small impact on the comparison of the (specific) total investment costs as all power plant types are affected by this difference. Table 9.3 gives an overview of the estimated investment costs for the power plant and the subsurface part of this geothermal project.

The results in Table 9.3 show the consideration between lower total investment cost and lower specific investment cost (lower cost per kW). The relatively low power production of the single and double flash plants result in high specific investment cost: 44% and 21% higher compared to the binary cycle. The combined cycle flash-binary option has a 17% higher specific investment cost. The difference between the specific investment cost for the binary cycle and combined ORC is very small and is within the range of uncertainty in this estimation.

Table 9.3   Overview of investment costs for different types of geothermal power plants

| | Flash | | Binary cycle | Combined cycle | |
	Single	Double	ORC	Flash - ORC	Cascade ORC
Power plant specific investment cost [€/kW]	1750	2000	2000	2250	2500
Net power rating [MW]	8.7	11.5	15.9	12.9	17.3
Power plant investment cost [M€]	15	23	32	29	43
Subsurface investment cost [M€]	50	50	50	50	50
Total investment cost [M€]	65	73	82	79	93
Specific total investment cost [M€/MW]	7.5	6.3	5.2	6.1	5.4

Operation & maintenance cost

The operation and maintenance (O&M) costs, or operating expenses (OPEX), are the second part of the economics of a geothermal power production. The O&M costs are often quoted as a percentage of the investment costs for power plants. The percentages are estimates for the surface facilities of the plant, based on literature and data from suppliers and account only for the power plant costs.

Table 9.4   Overview of operation and maintenance costs for different power plant types

| | Flash | | Binary cycle | Combined cycle | |
	Single	Double	ORC	Flash - ORC	Cascade ORC
Power plant O&M cost [% of investment]	2	3	1	2	1
Power plant investment cost [M€]	15	23	32	29	43
Yearly O&M cost [M€]	0.3	0.7	0.3	0.6	0.4
Yearly power production [GWh]	65	80	127	97	138
Specific O&M cost [€/MWh]	5	9	2	6	3

The maintenance costs for the flash plants are higher as the brine has to pass through a fine mesh to remove any liquid droplets remaining before entering the turbine. This mesh may clog quickly due to fouling. Silica precipitation is often encountered when flashing brine due to two reasons. First, the solubility reduces as a result of the drop in temperature and pressure when flashing. Secondly, the concentration increases as a part of the brine flashes and the silica is dissolved in less liquid after flashing.

The costs for ORC cycles are low because less supervision is required to operate such a plant and less scaling is expected because the pressure of the brine is kept high, reducing precipitation of solid particles.

Safety

All the power plant types will meet the safety requirements, but some technologies are inherently safer than others. This criterion evaluates the relative safety risks of different power plant types for the surroundings. The use of high pressure steam or vapor is always a risk. The direct use of steam in a steam cycle means that steam production cannot be stopped at once, as closing of the production well takes time. When the steam turbine suddenly stops, the steam that is continuously produced from the geothermal well has to be vented through a silencer and this may cause emissions.

The advantage of binary cycles is that their design is much more compact compared to a steam cycle. The complete separation of brine and thermal conversion process in binary cycles allows for a more controlled shut down and limits the risk of emissions during emergencies.

The safety of the ORC cycles can be improved by using a non-toxic and non-flammable refrigerant as the process fluid, for example R245fa, R245ca or R134a. Additional safety measures are required when more toxic or flammable fluids are used. At this moment the much better thermodynamic performance of hexane and pentane compared to R245ca or R245fa justifies their use. Therefore the safety score for the considered ORC cycles in table 9.1 are not increased compared to the flash cycles.

Complexity

The more complex an installation, the higher the chance of not meeting the rated output power and expected availability. The complexity is therefore also a measure for the expected reliability. The availability of a more complex power plant will be lower due to more planned and unplanned outages (respectively maintenance and repairs), as more components may fail.

For the combined flash-binary cycle there is an added project complexity as there is likely one supplier for the flash and steam turbine cycle and a different supplier for the binary cycle. This will require interface management to ensure a good integration of these separate parts. The single flash and binary cycle are the least complex power plant types; the combined flash-binary cycle is the most complex option.

Environmental impact

The environmental impact of the geothermal power plant should be minimal to create support for the project with the local public and to avoid discussions on the sustainability of the project.

The binary cycles have the advantage that the brine (together with all contaminants) is directly injected back into the reservoir after extracting the heat in a heat exchanger. The chances of emissions of brine or steam are therefore small. The loss of process fluid can be a risk for binary cycles, but this can be negated by using non-toxic organic fluids.

Flash plants need additional investments to separate dissolved gases and solids from the brine. The steam exiting the steam turbine has to be condensed and pressurized to be re-injected together with the separated gases.

The precipitated solids will have to be disposed of for flash plants, but this is a very small amount. Additional gas cleaning equipment will be required in flash plants to scrub the steam from the emergency steam vent in case of a malfunction.

Due to an increased chance of emissions, the rating for flash plants is lower than binary plants on the environmental criterion, but the difference is minimal.

Conclusions

The binary cycle, consisting of a single organic Rankine cycle, is the best option for Hoogeveen. This type of power plant has a good efficiency at the expected temperature and a high availability. Combined with a modest specific investment cost, this results in a power plant that is both economical and reliable.

The Hoogeveen geothermal power project combines a lot of challenging and innovative aspects, the power plant should not add to this complexity without very clear improvements in power production or costs.

The increase in power production from a power plant that consists of two cascaded organic Rankine cycles is relatively low at these temperatures. This small increase in expected production does not justify the higher investment cost and greater risk due to the more complex installation.

The single ORC design is also more flexible concerning the use of waste heat. Heat of any required temperature can be produced by increasing the turbine exit pressure. This reduces the amount of electricity generated, but this is more than compensated by the revenues and increase in efficiency resulting from the heat delivery.

9.4   Conceptual design binary power plant

This paragraph contains a conceptual design of the geothermal power plant near Hoogeveen. This is a high level description of the critical components of this system. Four components of the power plant are discussed in more detail in the next paragraphs: the ORC, the brine heat exchanger, the condenser cooling and the grid connection. Figure 9.7 shows the relation of these components in a schematic overview of the power plant.

The selection of these four components is based on the impact they can have on the power plant performance and the project costs or duration.
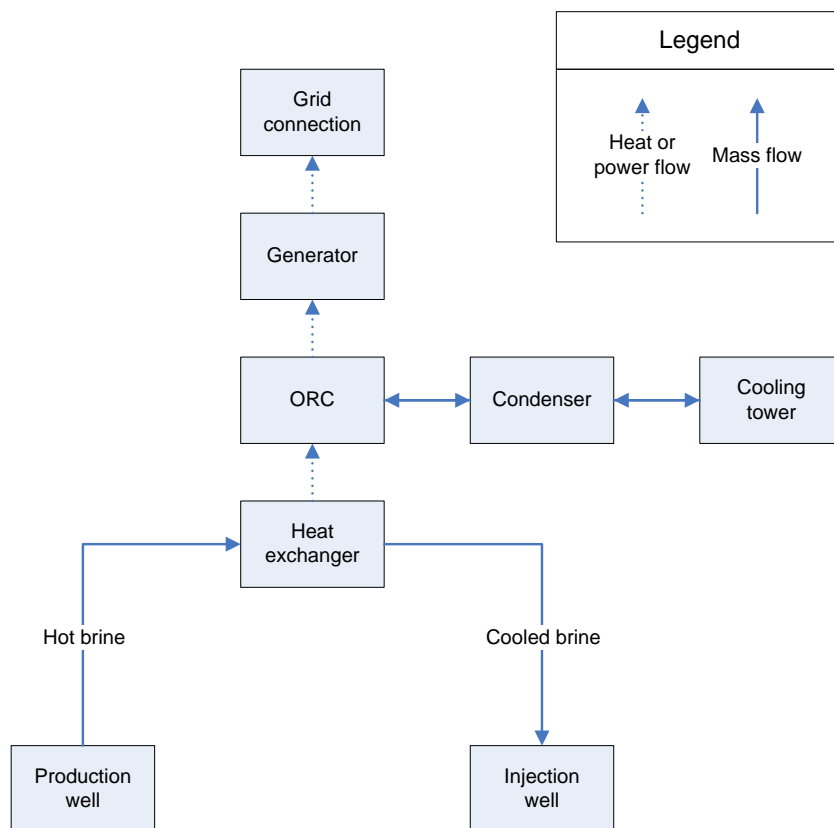
Figure 9.7   Schematic overview of the geothermal power plant

9.4.1   Energy conversion unit

Although the expected size of the installation is quite large for an ORC, there are suppliers that can deliver such an installation. A second option is to design a modular plant, consisting of 2 to 4 units of 10 or 5 MW each. A modular design comes with a higher total investment cost, but a reduced risk.

Should the flow rate of the geothermal well be significantly lower, then part of the investment costs can be saved by constructing less units. When a single ORC is designed, a much lower brine flow rate would require re-engineering, increased costs and possibly long delays. The modular option also increases the number of possible suppliers and more standard units can be used in that case.

Base case power production

The ORC with the highest expected power production is an ORC using hexane as the process fluid. The gross power production of this cycle is 18.4 MW_e. The parasitic load is 2.5 MW_e for the injection and condensate pumps and another estimated 1.8 MW_e for the condenser cooling water pumps and cooling tower fans. The net power production is 14.1 MW_e.

Lower initial brine temperature

Two worst case scenarios are modeled for a reduction of brine temperature. In the first scenario the temperature of the brine is not the expected 240 °C at the wellhead, but is instead only 210 °C. The flow rate is still 110 kg/s and the brine is still a compressed liquid. The heat supply from the production well is now 97 MJ/s, compared to 114 MJ/s in the base case.

The organic cycle is optimized for these conditions and the new gross power production is 15.5 MW$_e$. Because the temperature reduction is known from the start a smaller turbine with a different working fluid is chosen compared to the base case. Pentane is used instead of hexane for this lower temperature. The net power production is 11.0 MW$_e$.

Brine temperature decline

The second worst case scenario for a reduction in brine temperature is a gradual decline over the 30 year lifetime of the power plant of 1 °C per year. The same turbine and working fluid as for the base case are used. As the temperature of the brine decreases, the flow rate of the organic fluid in the cycle will also have to decrease. This reduces the inlet pressure of the turbine.

The isentropic efficiency decreases for normal steam turbines in partial as less vapor condenses in the final stage. The organic fluid never condenses in the turbine and operating in partial load has therefore a smaller impact on the turbine isentropic efficiency. This possible decrease in isentropic efficiency is not taken into account here. The process fluid flow rate is reduced from 150 kg/s to 125 kg/s and the resulting turbine inlet pressure is reduced from 20.0 bar to 16.8 bar.

The optimized process conditions result in a net power production of 10.0 MW$_e$.

Lower initial brine flow rate

There are also two worst case scenarios for the brine flow rate modeled. The first scenario is a lower brine flow rate of 90 kg/s. The other parameters are identical to the base case. This reduces the production well thermal power to 89 MJ/s. The process fluid flow is also reduced to 110 kg/s, resulting in a net power production of 10.8 MW$_e$.

Brine flow rate decline

The second worst case scenario for the brine flow is a decline of 1 kg/s per year of the flow rate. The approach is comparable to the temperature decline model. The same turbine and working fluid as for the base case are used. As the flow rate of the brine decreases, the flow rate of the organic fluid in the cycle will also have to decrease.

For a decline brine flow rate of 90 kg/s, the process fluid flow rate is reduced to 115 kg/s compared to 150 kg/s at the start. The turbine inlet pressure is reduced to 15.5 bar compared to 20 bar at the start. The optimized process conditions result in a net power production of 10.0 MW$_e$.

9.4.2 Brine heat exchanger

The brine heat exchanger is the part of equipment that is mostly influenced by the brine composition. The most likely type of heat exchanger to be used is a counter flow shell and tube type. The brine has a higher pressure and risk of fouling, scaling and corrosion and should therefore flow through the tubes. The organic fluid flows through the shell side.

The design of this heat exchanger is important as the efficiency of heat exchange directly influences the power production. The required heat exchanger area depends on the chosen construction material and amount of fouling that is permitted before the heat exchanger is cleaned. Vertical tubes should be used when there is a chance the brine will flash as horizontal tubes can be blocked by steam or gas bubbles. Using vertical tubes also helps with cleaning.

Depending on the brine conditions special materials might be required or arrangements to minimize downtime have to be considered. One example would be the use of two parallel heat exchangers to allow continuous operation while performing maintenance on one of the heat exchangers.

9.4.3 Condenser and cooling

There are three basic cooling options available for power plants: water cooling, wet cooling towers and air cooling. This paragraph gives a short description and comparison of the different cooling concepts. The most suitable option depends on the process and local conditions, aspects such as available cooling water and allowed visible impact of the installation.

Cooling is required as the process fluid in the thermodynamic cycle has to be condensed to complete the cycle and efficiently compress the fluid to the turbine intake pressure. The expected geothermal power plant will require about 80 MW of cooling power at 40-45 °C, this is a significant amount. The condenser and cooling design is a major part of a geothermal power plant and deserves attention in the detailed design of the power plant.

Water cooling
Water cooling is the most efficient form of cooling available and is used whenever a river or large quantities of water are available. Surface water is used to directly cool the condenser and returns at a slightly higher temperature. Often a temperature difference of 10 °C is used. Liquid water has very good heat transfer properties and this results in a small required heat exchanger area and a relatively low volume flow of water and associated pumping energy use (so called parasitic load). Investment costs are also the lowest for this option.

This form of cooling is restricted to locations with a large river or sea nearby. There are a small canal ("Hoogeveensche Vaart"), two surface water lakes from sand extraction near the A28 and several small streams, further research is required on the cooling capacity of the canal.

Natural convection cooling tower

Natural convection cooling towers are an efficient option when there is no large amount of surface water available for water cooling, but water is not scarce either. Cooling water is used to cool the condenser and the heated water is then sprayed into a large cooling tower.

This process requires a high cooling tower to create the natural draft; for a cooling demand of 80 MW, the height would still be around 60-80m. A white plume can form above the cooling tower when the additional moisture from the cooling tower saturates the air. An example of such a cooling tower is shown in figure 9.8 at the left. The footprint of this cooling tower is in the order of 2000 m^2 (50 meter diameter).

Figure 9.8   Natural convection (left) and fan assisted natural convection (right) cooling tower

Fan assisted natural convection cooling tower

The large height of cooling towers makes them stand out in the landscape. This height can be reduced to about 40 meters when fans are used to assist the natural convection effect at the base of the cooling tower. This is called a fan assisted natural convection cooling tower.

An example is shown in **Figure 9.8** at the right. The footprint of this cooling tower is also smaller, it is about 1000 m^2 (35 meter diameter). The fans require electricity, resulting in a lower net efficiency of the plant compared to a natural convection cooling tower. But the visual impact of the plant is somewhat reduced. There will still be a white plume visible when the additional moisture from the cooling tower saturates the ambient air.

Induced draft wet cooling tower

The induced draft cooling tower does not have the same shape as the natural convection cooling towers. It is most often designed as a cube shaped unit with a circular exhaust on top that houses the induced draft fan. Any number of these cells can be arranged in an array to create the required cooling power. An example of this is shown in figure 9,9 at the left.

Different kinds of packing can be used inside the cooling tower to increase the water-air contact area. These systems can be very compact in height (about 15 meters) and their footprint is about half compared to the natural convection cooling tower (1000 m^2). But they require more power for the fans and investment costs are higher.

It is possible to reduce the chance of vapor plumes from these cooling towers by installing a heat exchanger that reheats the water vapor saturated air before it leaves the top of the tower. These systems require again more power for the fans and investment costs are higher.

Figure 9.9   Induced draft (left) and forced draft (right) wet cooling tower example

Forced draft wet cooling tower
The forced draft cooling tower is similar to the induced draft version, except that high power fans push air in from the base of the cooling tower. These units are more often used for smaller scale applications such as air conditioning and refrigeration. The advantage of the side mounted fans is a reduction in noise and an even smaller tower height is possible. This comes at the expense of a higher parasitic load and is less of a benefit for installations at an industrial area. An example is shown in figure 9.9 at the right.

Induced draft air cooling
When there is no or little water available the last option available is to use air cooling. Convective cooling is used instead of using the evaporative heat of water. The cooling water stays in a closed loop and flows through a heat exchanger. Induced draft air cooling is similar to an induced draft wet cooling tower as fans mounted on the top of the tower are used to draw air through the unit.

An air cooled cell is larger compared to a wet cooling tower since a larger heat exchanger area is required as there is no direct contact between the air and cooling water. The visible impact is minimal as no water vapor plume is formed and the tower height is limited (about 15 meter), but the footprint is about three times larger than wet cooling towers (about 3000 m^2). As a result, investment costs are high. An example of a 20 MW$_e$ geothermal plant is shown in figure 9,10 at the left.

The efficiency of a power plant using air cooling is somewhat lower compared to water or wet cooling towers as the convective heat transfer requires a larger temperature difference between the cooling water and ambient air. This kind of cooling system is also more dependent on the current ambient temperature, making the control somewhat more complicated.

Figure 9.10   Induced draft (left) and forced draft (right) air cooling examples

Forced draft air cooling
Forced draft air cooling is similar to the induced draft version, except that the fan is mounted at the base of the cooling tower and the air is pushed through. Just as with the forced draft wet cooling towers, these units are more often used for smaller scale applications where there are stringent requirements for noise and space. This comes at the expense of an even higher parasitic load and is mainly used in the build environment. An example is shown in figure 9.10 at the right.

Water requirements for wet cooling towers
Wet cooling towers require additional cooling water (makeup water) as cooling water is lost due to three kids of losses: evaporative, blowdown and splash losses. The first two are the main sources of cooling water losses.

The *evaporative losses* are a result of the fact that wet cooling towers all rely for a large part (90-95%) on cooling by evaporating part of the cooling water. The heat required for this evaporation is removed from the remaining water. In this process a portion of the cooling water is lost as it leaves the cooling tower as water vapor.

The *blowdown losses* depend on the acceptable mineral concentration in the cooling water and the concentration in fresh makeup cooling water. As only water is evaporated in the cooling tower, the concentration of minerals would keep increasing when no water is rejected from the cooling loop (blowdown).

There are two sources of *splash losses*. The first source of splash losses is cooling water that is lost through the demister that separates water droplets from the outgoing airflow at the top of the tower.

The total makeup water requirements for a wet cooling tower are estimated at 200 m^3/hr or 1.7 million m^3/year. Half of this water can be returned to the surroundings as liquid water, the other half is lost as water vapor. These water losses can be important when salinization of the soil is a concern.

Comparison of different cooling options

This paragraph has given an overview of the different cooling options that are available for a geothermal power plant. Table 9.6 combines the results and is based on discussions with experts within KEMA, data available online (a.o. GEA, 2011) and design guidelines (Bauthier, 1993). For parameters that have two values, the induced and forced draft wet cooling towers, the top value is for the standard version and the bottom value for a tower with plume abatement measures installed.

Table 9.6   Overview and comparison of different cooling options

	Water cooling	Wet cooling tower				Air cooling	
	Water cooling	Natural convection	Fan assisted natural convection	Induced draft	Forced draft	Induced draft	Forced draft
Water usage [m^3/hr]	7200	200	200	200	200	0	0
Parasitic load [% gross power]	2	3.5	10	10 / 15	12.5 / 17.5	20	22.5
Investment cost [% power plant cost]	5	20	15	10 / 20	10 / 20	25	25
Maintenance	+	+	+/-	+/- / -	+/- / -	+	+
Visibility	++	--	-	+/- / +	+/- / +	+	+
Required area [1000m^2]	0.2	2	1	1	1	3	3
Noise	++	++	+	-	+/-	-	+/-
Environmental impact	-	+	+	+	+	++	++

The induced draft wet cooling tower, with no additional plume abatement equipment installed, is considered to be the best option for the geothermal power plant at Hoogeveen. This option is a balance between a low investment cost, parasitic load and visual impact. Plume abatement technology is the best option when visibility is a major issue.

9.4.4   Grid connection

The grid connection of a power plant can add significant costs and duration to the project. This is especially true when a large distance has to be covered to the nearest substation.

The cost of a connection will have to be paid for by the project developer and consist of a fixed amount for:
-   Breaking the network of the relevant network operator (the cut)
-   The facilities to secure the network (security)
-   For the cable between the network and the installation (connection)
-   And a periodic fee to cover the costs for maintaining the connection.

For all connections <10MVA the connection fee is regulated (NMA, Tariefbesluiten Rendo and Tariefbesluiten Enexis). The costs for a connection smaller than 10MVA, Rendo (including MS metering): 359.730 EUR + 242 EUR/meter and Enexis: 249.789 EUR + 137 EUR/meter. For all connections larger than 10 MVA the costs are based on the pre-calculated project costs, or *voorcalculatorische projectkosten* (NMA, 2009). For the 15 MW_e connection that is needed it is very hard to give even a broad estimation.

The connection costs depend heavily on several aspects:
What is the closest 25 or 50kV substation nearby (or 10kV in area were there is no 25 or 50kV)
-   If there is capacity in the substation to connect the installation
-   The type of soil
-   The number and type of crossings (road/river/etc)
-   The excavation work (is there space for a trench large enough for the cable)
-   Number of cables needed (for 10kV you probably need more than 1 cable).

The fixed or single connection costs may vary between 0.5 and 3 million EUR. The annual costs are small, but still can run between 5000 and 20.000 EUR/ year. For the base case scenario a location near an available substation is assumed. But a relatively remote location can result in an investment cost increase up to 10%.

The Dutch regulation requires that if the production-installation is seen as "sustainable" (or is smaller than 10MVA), the connection must be realized within 18 weeks. With the exception that it cannot reasonably be expected from the grid operator.

Other important aspects concerning the grid connection are:
In the legislation there are additional requirements for production units connected to the grid (NMA, Netcode Elektriciteit, 2011): voltage control, power factor, the available capacity of reactive power on the location, limitation of short circuit power, etc.
Congestion management (dispatch-restrictions because of congestion in the grid) is an issue in some parts of The Netherlands.

Because of all these grid connection-issues it is important to start discussions with the regional grid operator in a very early stage of the project (even before a final location has been found). Grid operators are willing and have the obligation to provide all necessary information to guarantee an efficient access (connection) to the grid (ELI, 2011).

9.5 Safety aspects

Safety aspects are important to consider in some detail to judge the feasibility of this type of power plant. In this paragraph operation and safety aspects concerning the power plant are discussed.

9.5.1 Emergency stops during power generation

The brine will be flowing from the production well with a flow rate of 120 kg/s (0.15 m3/s). This flow cannot be stopped instantaneous by closing of the wellhead without risk of damaging the wellhead and piping. The resulting water hammer pulse from closing the wellhead have been calculated. When the wellhead valve is closed in 1 second, the increase in pressure is 80 bar. This comes on top of the static pressure of the well. This shockwave most probably will damage the wellhead and piping. A wellhead valve closing time of 30 seconds or more is proposed, resulting in a maximum increase in static pressure of 2.7 bar.

Should the ORC turbine suddenly stop, it will be bypassed and the organic process fluid will instead pass through a throttle valve before going to the condenser, continuing the normal cycle. This ensures stable operation while either the production wellhead valve closes and the brine flow is stopped, or the turbine restarts and normal operation resumes. The separation of the brine and ORC cycle enables a relative simple and robust control strategy.

When a major failure occurs in one of the components in the brine cycle, such as the brine treatment, heat exchanger or injection pump, the brine flow to this component may have to be stopped instantaneous. This is achieved by switching the wellhead valves to force the brine directly from the production wellhead into the injection wellhead. This provides the required time to safely close the production wellhead valve and completely stop the brine flow.

9.5.2 Leakage of organic fluid

First it should be stated that the chances of organic fluid leakage are very small. The most likely organic fluids used in the ORC are at this moment hexane or pentane because of the good fit of its thermodynamic properties to the expected brine parameters. The flammability of the organic fluid is a major risk.

The explosion limits are 1.4 - 8.3% for pentane and 1.2 - 7.7% for hexane and their density is larger than air. A combination of early detection and ventilation has to be used to reduce the risks of leakages and ignition. Emergency valves should close off the turbine and drum when a leak occurs in the ORC cycle to limit the amount of pentane.

The most effective way to extinguish gas fires is by removing the fuel supply. In the case of an ORC this means stopping the pentane flow with automated valves when a pressure drop, a too high pentane concentration in the air or a fire is detected. Should the leaked pentane ignite, only the pentane present in the piping from the condensate pump to the safety valve just before the turbine will combust.

The total amount of pentane that may combust can now be estimated. With a flow rate of 150 kg/s and an estimated speed of 15 m/s this results in about 10 kg of organic fluid per meter piping. For an estimated piping length of 20 meter this means 200 kg of pentane or hexane. This is a considerable amount, but represents not an insurmountable risk.

The main safety measure is an airtight containment of the ORC installation, separated with a fireproof wall from the process control room. Sufficient ventilation has to prevent the buildup of the organic vapor near the floor. CO2 fire extinguishers can be used to extinguish the flames and limit damage to the installation. The detailed fire prevention and extinguishing installation design has to be coordinated with the local fire department and this safety issue is an important part of the environmental permit (MER).

Hexane and pentane are harmful fluids as they can cause irritation through inhalation, ingestion or skin absorption. This is a minor safety issue and effective ventilation is the main method to limit this risk for personnel.

9.5.3 Leakage of brine and dissolved gases.

The closed loop design of the geothermal wells results in a small chance of brine leakage. The main risk of brine leakage is the emission of gases that could be dissolved in the brine (CH4, CO2, H2S). Early detection is an important aspect of a safety system. Properly operating safety systems are in place at existing geothermal projects like the aardwarmte den Haag (ADH) plant. At ADH, a high amount of dissolved CH4 exists. This has led to extensive safety measures, also because the plant is in the middle of an urban area.

9.6 Operations

This chapter describes the operation of the geothermal power plant. The two main parts are the power production process control and expected issues with handling the brine and the available solutions.

9.6.1 Geothermal power production process description

Three different cycles are distinguished in the geothermal power plant: the brine cycle, the power production cycle and the emergency operation cycle. Figure 9.11 shows the most important components and processes in this power plant in a simplified schematic and is used to describe these three cycles.

Geothermal brine cycle
The brine flows from the production well, through the wellhead valve, to the brine treatment. Here non-condensable gases and solids are separated from the brine, depending on the encountered brine composition. Then the brine goes through the main heat exchanger and provides heat for the ORC process. The cooled brine is finally re-injected in the injection well by a high pressure injection pump.

Power production cycle

The ORC unit converts the geothermal heat to power. The heat from the brine is used to vaporize the organic fluid and this vapor drives a turbine connected to a generator. The vapor is condensed in the condenser that is cooled by an induced draft wet cooling tower. The produced electricity is exported to the electricity grid.

Emergency operation cycle

During normal operation the brine follows the loop 1-2-3-4-5-6. In case of a major failure with one of the components in the brine cycle, such as the brine treatment, heat exchanger or injection pump, the production wellhead valve switches to emergency operation. In this setting the brine is forced directly to the injection wellhead valve and back into the reservoir. The brine follows the loop 1-Emergency-6. During emergency operation the ORC turbine is bypassed as well and the power production process comes to a controlled stop as the production wellhead valve is closed.
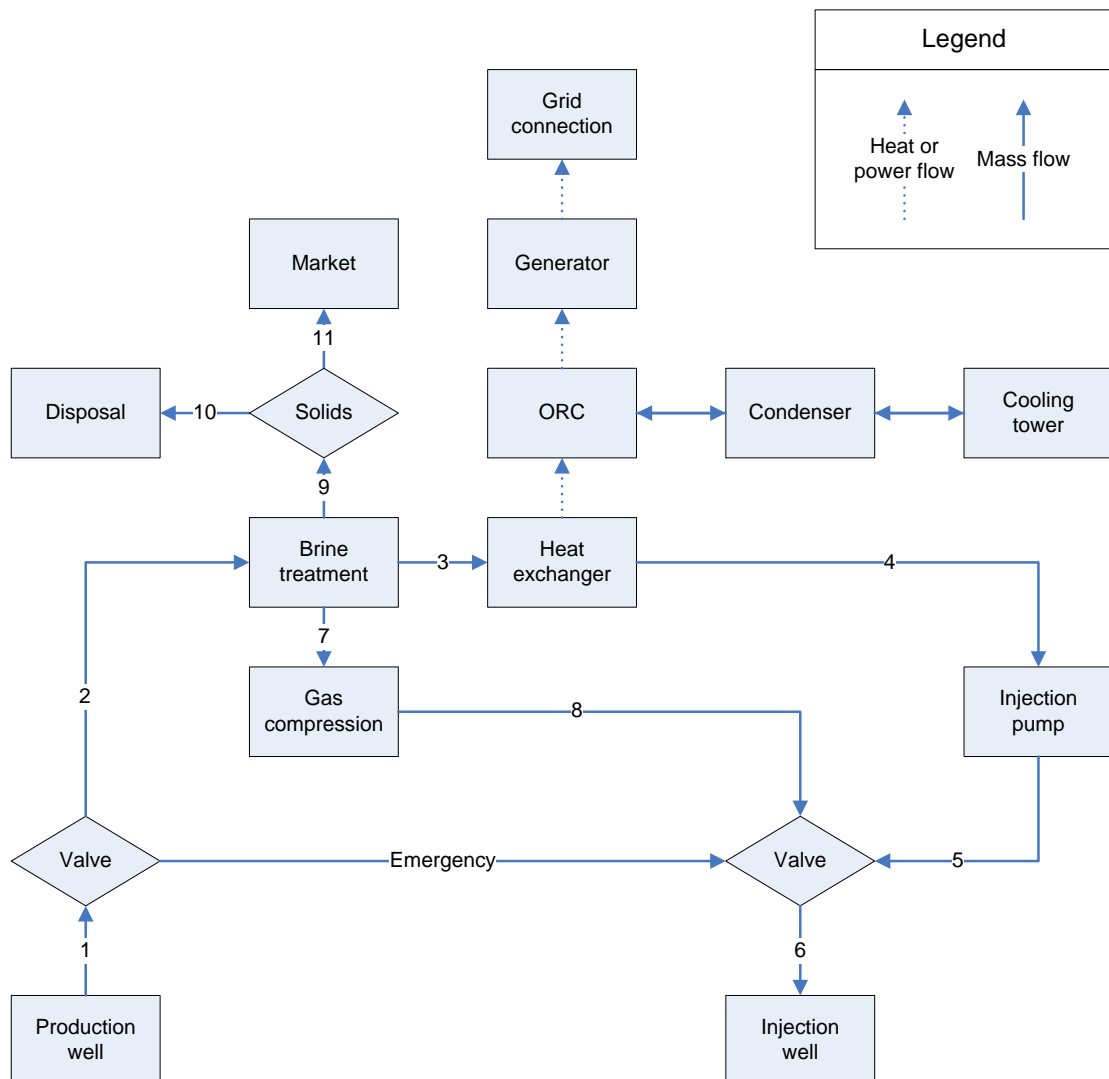
Figure 9.11 Schematic overview of the geothermal power plant processes

9.6.2   Brine treatment

The exact composition of the brine coming from the geothermal reservoir is unknown at this moment, however, some general remarks considering scaling & corrosion can be made.

Dissolved solids: silica and calcite scaling

Given the high temperature, and the large temperature drop, scaling will likely be an issue. From volcanic high enthalpy geothermal projects, it is known that silica scaling is the most frequently occurring scaling problem. The most frequently used method to prevent silica scaling is reducing the temperature drop. However, other methods may be used: acidizing and addition of scale inhibitors. These issues have to be worked out further in later stages of the project. In general this should not be a show stopper, considering the amount of experience with scaling prevention in the world of high enthalpy.

Acidity and corrosion risk

A high acidity increases the risk of corrosion of the equipment that is in contact with the brine. The acidity can therefore have an impact on the availability of the installation and maintenance costs

The risk of corrosion can be reduced by dosing anti corrosion inhibitors. There is a large variety of corrosion inhibiters available such as azoles. These are compounds that reduce corrosion of mainly copper containing alloys by forming an insoluble film on the free metal surface. The use of such additives results in higher operational costs.

Continuous operation of the installation, with a minimum of downtime for maintenance, is a result of balancing the pH value and additives to keep both corrosion and scaling under control.

Dissolved gases

Dissolved non-condensable gases in the brine can have both an impact on safety and increase operational costs. Likely gases that are present in the brine are CO_2, H_2S and CH_4. Especially H_2S can be a safety concern.

The operational costs increase when there is a large amount of non-condensable gases present as these have to be separated before the brine can be re-injected with the injection pump at high pressure. Depending on the composition of the gases these can either pass through a gas cleaning system and emitted to the atmosphere or they can be compressed to 160 bar in a compressor and be re-injected together with the brine.

This separation and especially compression require energy and reduce the net power of the installation. The presence of H_2S can lead to the deposit of elemental sulfur and plugging of the piping. Special dispersive chemicals for organosilicon compounds can be dosed to prevent this.

Entrained solid particles

Entrained solid particles can cause erosion of the piping and especially the injection pump. Depending on the amount of solid particles it can be required to separate these at the wellhead.

This requires additional investment in equipment and possibly maintenance as filters have to be cleaned periodically. This is not expected to be a significant problem, but this depends on the conditions encountered.

9.7 Summary

This chapter analyses the technical and economical feasibility of the surface part of the geothermal project. The power plant is a significant part of the investment; it represents one third of the initial investment costs and the greater part of the operational costs.

The binary cycle, consisting of a single organic Rankine cycle, is the best option for Hoogeveen. This type of power plant has a good efficiency at the expected temperature and a high availability.

A net power production of about 14.1 MWe is possible. This would meet more than the electricity demand of all households in the municipality of Hoogeveen.

10 Business case

The objective of this chapter is to assess the financial attractiveness of a geothermal project at Hoogeveen.

In the first paragraphs, the scenarios that will be applied and the most important parameters are described. In the following paragraphs the cost of investment and the savings are presented. In the last few paragraphs the environmental and financial results are described as well as the summary.

10.1 Scenarios

A number of scenarios for the business case have been composed, based on:
- Reservoir fracture systems (3)
- Subsidies (5)
- Percentage residual heat delivery (5)

Only one flow rate (110 kg/s) and one temperature (250 ºC) will be applied.

Since the drilling cost are the major part of the total investments, different reservoir fracture systems have been evaluated. In the table below the total drilling length depending on the fracture system are displayed.

Table 10.1   Total drilling length depending on depth and fracture system

	7.000 m.
Natural fracture system	17.142
Water fracture system	19.142
Proppant fracture system	24.212

Secondly, some scenarios have been based on the amount of subsidy:
- 0,070 €/kWh – Current level 2012
- 0,110 €/kWh
- 0,150 €/kWh
- 0,200 €/kWh
- 0,300 €/kWh – Feed-in tariff in Germany

The subsidy level has been determined for 2012 on 0,070 €/kWh. However, to demonstrate the gap with for example Germany, also the German feed-in tariff and some subsidy levels in between have been calculated.

Finally a number of scenario's have been based on the percentage of residual heat being delivered to a district heating network or industry:

- 0% no residual heat delivery
- 25%
- 50%
- 75%
- 100% all residual heat will be delivered: 10 MW$_{th}$

10.2 Important parameters

The most important parameter for the total investment are the drilling costs. The total drilling length have been discussed in the previous paragraph, the cost per meter are displayed in table 10.2.

Drilling cost depend on depth, mainly due to longer so-called tripping times at larger depths. The assumed drilling costs are being considered as conservative and have been validated by Well Engineering Partners (WEP).

Table 10.2   Major investment parameters

Investment parameters	Value
Drilling depth	7.000 meter
Drilling cost	3.250 €/meter
Power station	2,0 M€/MW

Table 10.3   OPEX parameters

OPEX Parameters	Value
M&O cost	2,00%
Insurance cost	0,50%

Table 10.4   Operational parameters

Operation parameters	Value
Load factor	90%
Operating hours	7.884

The OPEX data are based on experience with a number of previous geothermal projects.

All price related parameters are shown in table 10.5. The SDE subsidies for heat and electricity are based on the SDE+ for 2012 and will be further discussed in the next paragraph.

Table 10.5   Price parameters

Price parameters	Value
Electricity price - market	0,055 €/kWh
SDE subsidy electricity	0,039 €/kWh
Heat price	5,00 €/GJ
SDE subsidy heat	18,90 €/GJ
CO2 price	20 €/ton
SDE hours per year	4.667
General price index (inflation)	1,5%
Price index energy (additional)	1,5%

Table 10.6   Financial parameters

WACC	8,0%
Economic life	30 years

Most probable the real WACC for such a project will be higher, however, the WACC of 8% will be applied for the cost price calculations.

10.3 Subsidies

The subsidies are based on the Dutch SDE+ 2012 ("Subsidie Duurzame Energie") regulation on renewable energy. For geothermal energy, heat and combined heat and power (CHP or "WKK") are eligible for subsidy.

Combined heat and power (CHP)

To qualify for the subsidy on CHP, at least 5% of the produced energy must be electricity[3]. In the Hoogeveen scenario the focus will be on electricity with a far larger share of produced energy.

For CHP, the basic amount is 18,90 €/GJ, both for heat and for power. For heat a reference cost price is commonly 8,10 €/GJ assumed. The subsidy for the heat part will be the difference, being 10,80 €/GJ. The subsidy will be provided for 4.667 hours per year.

For the electricity part, 18,90 €/GJ expressed in kWh is 0,068 €/kWh. The reference cost price is also 8,10 €/GJ which is 0,029 € per kWh. The subsidy for the electricity part will be 0,039 €/kWh.

10.4 Investments

The total investment per scenario will vary due to variations in (1) drilling length and (2) hydraulic stimulation.

---

[3] Verbal statement by Paul Lako, senior researcher and specialist on SDE at ECN.

Table 10.7   Total investments for a natural fracture system

Investment	Unit	Natural	Water	Propped
Research and seismic survey	M euro	2,0	2,0	2,0
Other preperation cost	M euro	3,0	3,0	3,0
Two wells	M euro	55,7	62,2	78,7
Stimulation	M euro	1,0	4,0	8,0
Power plant	M euro	33,6	33,6	33,6
TOTAL	M euro	95,4	104,9	125,3

Investment parameters for drilling have been discusses in the previous paragraph.

For a natural fracturing system the cost for hydraulic stimulation are assumed to be relatively limited. For a water/shear fracturing system the cost are assumed to be 4,0 million euro. Water fracturing has substantial lower cost compared to proppant fracturing, since no proppants and no additives are required. For proppant fracturing investment cost have been estimated on 8,0 million euro.
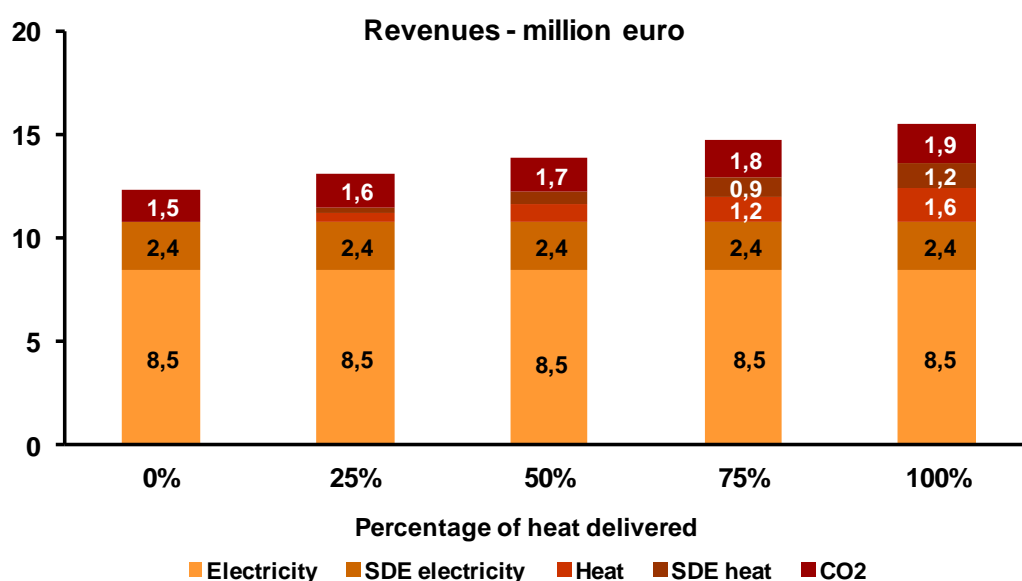
10.5 Revenues

Figure 10.1   Revenues for different percentages of residual heat delivery

On the income side of the equation, revenues come from 5 sources:
1.   Electricity revenues
2.   SDE electricity
3.   Heat revenues
4.   SDE heat
5. CO_2 credits

The total system has been focused on and optimized for power production (> 12 MW_e) and the potential heat capacity is relatively small (~10 MW_{th}). The relative capacities are reflected in the revenues as the revenues from power is in all scenario's the largest part.

It is assumed that for the amount of avoided CO_2 credits can be sold for a price of 20 €/ton. In that case, a structure with a company with CO2 obligations has to be researched and implemented.

10.6 Financial results

The financial results are the outcome of a model in which all above mentioned parameters and scenarios have been entered.

Cost price

The cost price for electricity varies between 0,08 and 0,11 €/kWh and depends strongly on the type of subsurface reservoir. For a natural fractured reservoir, no additional investments have to be made for horizontal wells, sidetracks and hydraulic stimulation. Although a natural fracture system has a low cost price, the probability of having the right sub surface conditions in Hoogeveen is low.
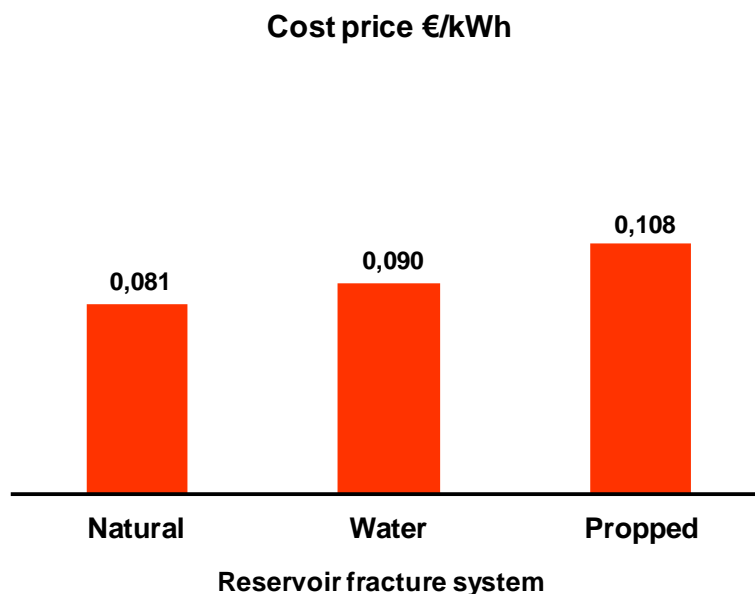
Cost price €/kWh

Figure 10.2   Cost price of electricity depending on type of reservoir

For a Water/shear fractured reservoir more investments for horizontal wells and hydraulic stimulation are required. A water/shear fractured reservoir is considered as the most promising option in Hoogeveen. Most financial scenarios in this chapter are based on this system.

The last system, a propped fracture system is the most expensive option. For a propped system also a sidetrack is required and the cost of proppants ('sand') will increase the investments for hydraulic stimulation.

Financial results – without heat delivery

The internal rate of return (IRR) for the base case –water/shear fracturing system– is about 7%. The simple payout time (SPOT = payback time) will be approximately 13 years.

Obviously for a natural fracture reservoir the business case is positive: about 8% IRR and a payback period of 11 years.

Internal rate of return (IRR)

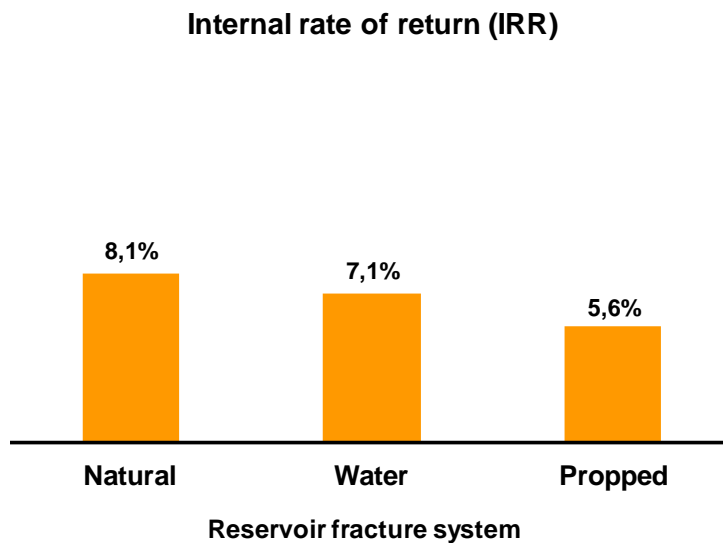Figure 10.3   IRR for different reservoir systems without heat delivery

The most certain and most expensive option –a propped reservoir– has the worst business case: a IRR of about 5 to 6% and payback period of 17 years. The positive aspect is that even in case other options are not providing a good performance, this option functions as a fall back option and the return is still positive.

Simple payout time (SPOT)

Natural: 11,3
Water: 13,0
Propped: 16,6

Reservoir fracture system
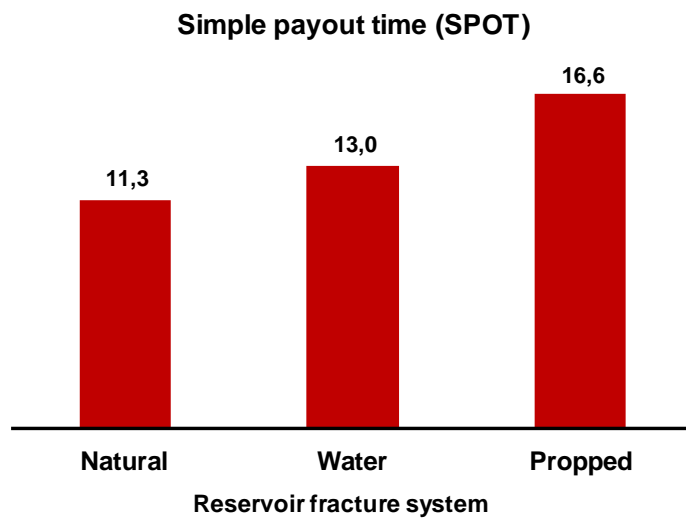
Figure 10.4   SPOT (in years) for different reservoir systems without heat delivery

Financial results – With heat delivery

The business case can be improved by delivering heat. Next to the electricity production, also residual heat can be delivered. The total thermal capacity is 10 MW$_{th}$.

Internal rate of return (IRR)

0%: 7,1%
25%: 7,7%
50%: 8,3%
75%: 8,8%
100%: 9,4%

Percentage of heat delivered

Figure 10.5   IRR for different percentages of heat delivery

In case 100% of the residual heat will be delivered, the IRR improves from about 7% to 9% and the SPOT decreases from 13 to 9 years.

Simple payout time (SPOT)
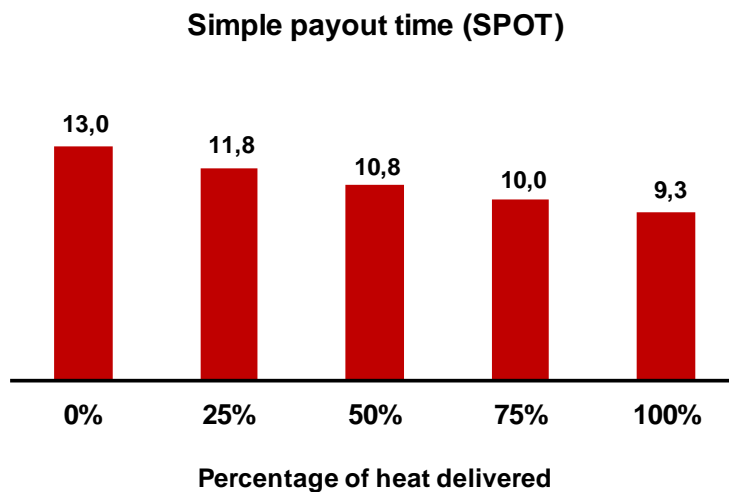
Figure 10.6   SPOT (in years) for different percentages of heat delivery

10.7 Sensitivity analysis

All technologies to be applied are separately considered as proven technology. However, the project is novel both in concept as well as in the drilling of a deep, horizontal section. As a consequence, intrinsic uncertainties are 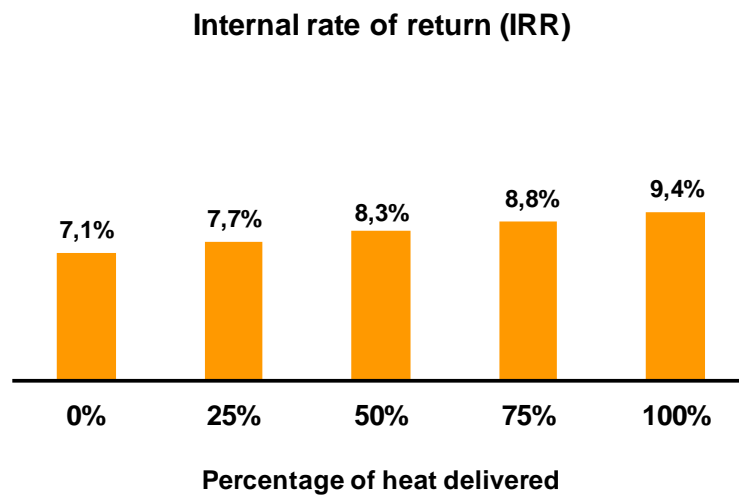large with their effects on economic parameters. Therefore a sensitivity analysis has been executed. For the base case residual heat delivery is assumed.
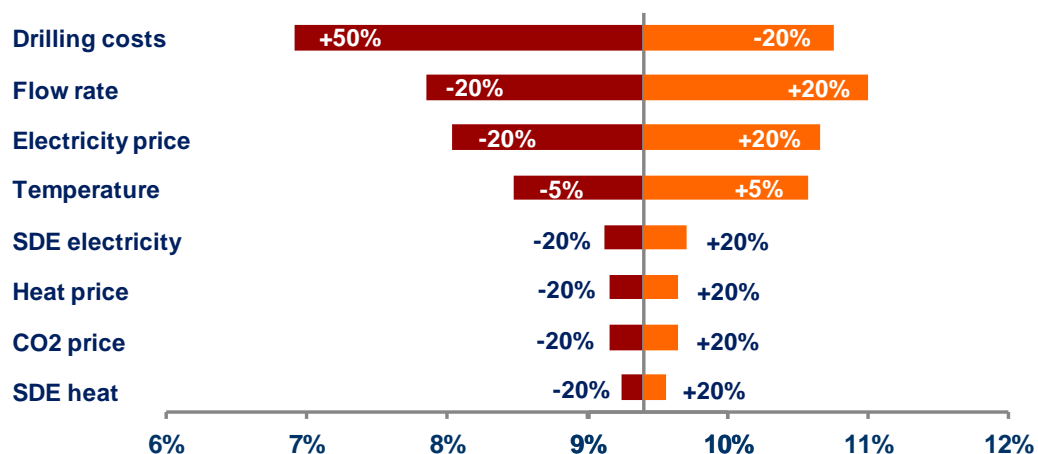
Figure 10.7   Tornado diagram with influence of main parameters on the IRR

A sensitivity analysis has been performed and the results have been displayed in a tornado diagram. Most major parameters have been varied with +/- 20%, except the temperature and drilling cost. A variation in temperature of +/- 20% would results in extreme values, therefore a variation of +/-5% have been applied. For drilling cost, an increase of 50% is assumed to be possible and therefore applied for the sensitivity analysis.

The drilling cost, flow rate and electricity price are important parameters influencing the business case significantly. If the drilling cost increase with 50%, the IRR will drop to over 7%, which is still a reasonable project return.

10.8 CO_2 reduction

For the CO2 calculations a gas fired STEG unit has been used as a reference. The main parameters for the calculations are displayed in the table below.

Table 10.8   CO2 parameters

CO2 parameters	Value
CO2 from gas	1,78 kg/m3 gas
m3 gas needed for 1 GJ	31,6 m3 gas/GJ
Conversion gas-to-power	52%

The CO_2 reduction depends on the amount of produced electricity and delivered heat. The produced electricity will avoid an equivalent of over 77.000 ton of CO_2. By also delivering heat, the amount of avoided CO_2 can be increased to over 100.000 ton.
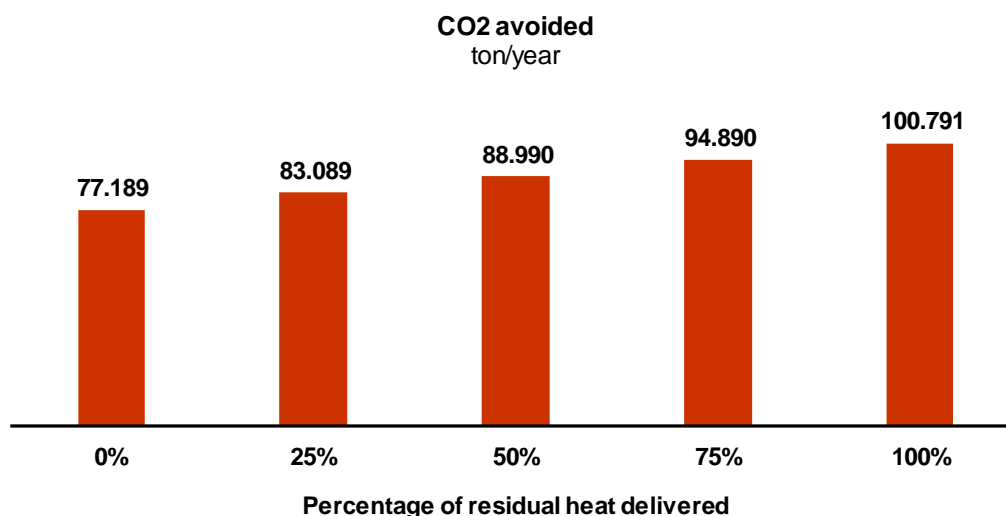
Figure 10.8 CO_2 reduction for residual heat delivery.

10.9 Summary

In this business case scenarios for (1) different fracture reservoirs, (2) different subsidy levels and (3) percentage of residual heat delivered have been analysed.

The base case scenario is based on a water fractured reservoir system with SDE and without residual heat delivery. The Internal Rate of Return (IRR) for the base case is about 7% and the simple payout time (SPOT) is 13 years. The cost price of electricity is about 0,09 €/kWh.

The business case becomes better with increasing residual heat delivery. In case all residual heat is delivered, the IRR will be over 9% and the SPOT will be 9 years.

In a worst case scenario the water fractured reservoir will not generate enough flow rate and a propped fractured reservoir has to be implemented. The investment for a propped fractures reservoir is higher, the cost price will be about 0,11 €/kWh. The IRR for the worst case is nearly 6% and the SPOT is 17 years.

A sensitivity analysis demonstrates that the drilling cost is the most important parameter. An increase of 50% of the drilling cost will result in an IRR of 7%, which is still a reasonable positive project return.

In the base case scenario the CO_2 reduction is over 77.000 ton per year. The CO_2 reduction increases with residual heat delivery up to over 100.000 ton per year.

11 Plan for public acceptance

11.1 Introduction

In order to obtain support and acceptance from main stakeholders and public groups, a plan has been drafted to communicate with these groups.

The first step is to identify all relevant stakeholders and groups. The second step is to draft a communication plan which includes communication channels and deliverables to reach the stakeholders. The final part of this chapter provides a high level description of the communication deliverables.

11.2 Stakeholders

For the project three main categories of stakeholders have been identified:
- Inhabitants
- Governmental bodies
- Environmental interest groups

The group of inhabitants that is relevant to the project is assumed to live in the city of Hoogeveen and the South-East corner of Drenthe. A main characteristic is the diverse nature of the group in terms of knowledge, interests, age, education and so on. The size of the group is estimated on 100.000 persons.

Table 11.1   Overview of relevant stakeholders

Stakeholder	Geographical reach	Size of target group
Municipal governance	Municipality	~ 10 persons
Provincial governance	Province	~ 10 persons
State governance	Country	~ 20 persons
Local inhabitants	Municipality / Province	~ 100.000 persons
Local environmental interest groups	Municipality / Province	~ 50 persons
National environmental interest groups	Country	~ 50 persons

The governmental bodies are the municipality, province and state institutions. A main characteristic is the professional nature of the group with a focus on sustainability themes and legal compliance. The number of relevant persons is estimated on approximately 40 persons in total.

The environmental interest groups may be organized locally or nationally. The main characteristic of the group is a focus on environment and sustainability, with a tendency to be very critical. The number of relevant persons is estimated on approximately 100 persons in total.

11.3 Communication plan

The main objective of the communication plan is to obtain public support and acceptance from the several groups of stakeholders.

In table 11.2 a communication plan is presented. In the plan a match has been made between the communication deliverables and the target stakeholders groups to ensure that all target groups are being served properly.

Table 11.2   Communication deliverables and target stakeholders

Deliverable	Target stakeholder group	Frequency
1-to-1 meeting	Leaders of local environmental groups	1 or 2 each
Meeting and presentation Environment and sustainability (in detail)	Local and National environmental interest groups	Few
Meeting and presentation Sustainability and legal compliance	Governmental bodies	Few
Meeting and presentation Environment and sustainability (easy to understand)	Local Inhabitants	Few
Press releases	All	Few per year
Newspaper interviews	All	Few per year
Website	All	Once with updates

The communication deliverables can be categorized into three main groups:
- Personal 1-to-1 communication for important key influencers
- Meetings with presentations for groups with a limited number of participants. This communication tool will be tailored depending on the group of participants
- Mass media tools, targeting all groups at all levels and the larger population.

11.4 Messages and content of main deliverables

In general, all communication deliverables should contain three types of messages:
- General advantages of the geothermal project, such as climate impact (CO_2 reduction), stable and independent energy supply;
- Advantages for the local inhabitants, 'what's in it for me'
- Addressing disadvantages and potential objections. Main issues are the use of chemical additives in the hydraulic fracturing operations and the risk of larger-than-usual micro seismicity.

General advantages of the geothermal project

An important part of the communication messages is to emphasize the advantages, importance and sense of urgency.

Climate impact
According to an analysis of Müncher Rückversicherungen, the number of climate related catastrophes have been tripled since 1950. In general it is assumed that CO2 is contributing for a large part to climate change and weather related catastrophes.

The geothermal project at Hoogeveen will reduce CO2 emissions with 77.000 to 100.000 tonnes per year.

Scarce energy resources
The global energy demand is expected to increase with 100% in 2050. At the same time, the production of a number of energy sources is expected to decline over time. An example is oil: in a large number of countries the oil production is declining. As a result, the oil price is now more than a year over $100 per barrel.

Heat from the earth is abundantly available, enough to provide the global energy demand for about 1000 years.

Independent energy supply
Locally produced energy will avoid dependency on other countries and fluctuating prices due to market circumstances and political interests.

Landscape impact
Many energy sources have major impact on the landscape. An equivalent of capacity of wind energy will result in about 10 to 15 large wind turbines with a height of over 100 meters.

An equivalent capacity of solar cells will cover a large part of the municipality of Hoogeveen. The same applies to bio-mass: large pieces of land are required to feed the bio mass power stations.

The geothermal power station can be located in an industrial area for which about 1 hectare of land is required.

Advantages for the local population

Local emissions
With the geothermal power plant local emissions will be reduced significantly, allowing the local community to contribute to the CO_2 emissions targets.

Local district heating
Assuming a local district heating system will be implemented, inhabitants will have stable energy prices and renewable heating for their homes.

Share ownership (optional)
For the project local funding may be considered, mainly to create a sense of ownership amongst the local community members.

Addressing issues

Micro-seismicity
During realization and operation micro seismicity will occur. Under normal circumstances, the level of seismicity is below human perception.

To ensure that the level of seismicity will not reach a critical level that can be felt, the following measures will be taken:
- Before the realization phase starts, research will be executed to predict the levels of natural and gas-production induced seismicity. If necessary, the subsurface design will be adjusted.
- A measurement system will be implemented to detect micro seismic events. Such implementation will be executed in collaboration with the Seismology department of KNMI.
- A hotline will be implemented where anybody can report seismic incidents.
- Just in case, in the unlikely case an event occurs that causes damage, procedures will be followed along guidelines to reimburse damages.

Use of chemicals

The prime intention is not to use chemicals at all and to make use of water fracturing.

In case the application of water fracturing is not possible, the following procedure will be executed. Research will be executed to explore possible alternatives for additives that are not harmful. In case such additives do exist and are reasonably affordable, such an additive will be applied.

When no alternative can be found, additives for hydraulic fracturing purposes that have been allowed by national and European legislation will be applied.

12 Action plan

12.1 Project phases

For the total project seven phases have been defined to realize a geothermal installation. An overview of the phases is provided in table 12.1. This study concerns phase 2, the next steps in the action plan focus on phase 3.

After each phase a go / no go decision needs to be taken. With each progressing phase the risks and uncertainties are being diminished. At the same time the costs are increasing with each phase. The cost of the exploration phase (phase 4) consists mainly of the execution of a geophysical study.

Table 12.1   Project phases with an indication of costs.

Phase	Description	Cost range
1	Feasibility – First assessment	15 - 25 k€
2	Feasibility – Potential	50 - 100 k€
3	Feasibility – Flow rate risk	200 - 300 k€
4	Feasibility – Other risks	300 - 500 k€
	- Pre FID -	
5	Exploration	3,0 - 5,0 M€
6	Realization preparation	500 - 800 k€
	- Final Investment Decision (FID) -	
7	Realization	90 - 120 M€

The cost estimate concerns content / technical cost. General project development costs such as for permits, communication, insurances etc. is not included in the estimate.

At the end of phase 3 a 'Pre Final Investment Decision' has been defined. At this point in time all feasibility studies have been completed and insight on the overall feasibility should be available. Further, a decision for major investments has to be taken.

At the Final Investment Decision (FID) at the end of phase 5, the total cost for feasibility and preparation is estimated to be 3 to 5 million euro.

12.2 Recommendations

Geology

To reduce the uncertainty in interpretation of the depth and thickness of the Zeeland Formation, new seismic lines need to be shot. This is a costly solution and is recommended to be executed at phase 5 (table 12.1).

Tensile (propped) fracturing

Fracturing fluids are usually not designed for the high temperatures and pressures that are encountered at 7 km depth. For this project, a suitable fracturing fluid needs to be found or developed. The fluid should be stable and have enough viscosity at high temperatures of up to 250 ºC. These kind of fluids are not available in the software database so they could not be included in the fracture design modelling. Contact with fracturing service companies or research institutes is desired to find a suitable fluid.

Proppant sand is subject to high pressures at depths of 7 km. For these depths, usually ceramic proppants are used because they are harder. It is possible that the cheaper sand proppant may experience some crushing after the fracture closes. This could reduce the fracture permeability. To what extend this could affect flow rates in the fracture requires further literature studying.

Both the fracture fluids and properties of proppant sand will be partly studied in phase 3 (Flow rate risks) and in phase 6 (preparation).

Shear (water) fracturing

The potential of waterfracs is very high. In many EGS projects worldwide waterfracs have been applied. To be able to apply this kind of treatment, the reservoir needs to meet certain requirements. An inventory of these requirements, the limitations, risks and advantages needs to be set up. This requires extensive literature studying.

Lab tests could give an indication of fracture permeability if shear failure occurs and the two fracture planes misalign. Information from literature on this subject is relatively scarce. Moreover, the effects of shear failure differ per lithology. However, the waterfrac treatment is cheaper in that it uses less expensive fracturing fluids and low to zero proppant masses.

A literature study is required to assess the mechanisms and risks of induced seismicity. Fracturing treatments are always accompanied by some degree of induced seismicity. How and when this is triggered and to which extend this can be controlled requires literature study and looking at other sites.

Shear fracturing will be a substantial part of the next phase 3 on the flow rate risk.

Modelling

The rock properties of UHM-02 need to be determined from the logs of the well. They need to be compared to LTG-01 to see to what extend the properties of the Zeeland Formation vary spatially. A fracture design study can also be carried out on the UHM-02 well.

In our modelling studies, the reservoir is assumed to be isotropic. This concerns all rock parameters. Also, a natural fracture network is assumed to be non-existing. This is a common assumption in the industry in which the model software is used. However, from well logs and core interpretations the presence of naturally occurring fractures is quite certain. To which extend the secondary permeability of these fractures can be utilized for an EGS system requires further studying. Detailed studying of cores and image logs could yield a database of fracture dimensions, density and permeability. This could be implemented into a fractured network model to model fluid flow, heat flow and reservoir stimulation in a fractured system.

Also, to which extend these natural fractures affect reservoir stimulation processes needs further literature studying. Possibly model software is available to model hydraulic fracturing in a naturally fractured reservoir.

Further well analysis and the impact of natural fractures on hydraulic fracturing will be researched in the next phase.

12.3 Action plan

The next items will be part the of the next phase 3 on flow rate risk:
A. Decision tree and integral risk model
B. Basic information
C. Modeling shear (water) fracturing system
D. Modeling tensile (propped) fracturing system

A. Decision tree and integral risk model

Decision tree
In the decision tree, the various options (shear/water, tensile/propped) are processes for the creation of the subsurface heat exchanger. Also the possibility of implementing more (or less) fractures is included in the decision tree.

Integrated risk model
The decision tree is converted into a statistical model and the models (part C and D) are integrated. The statistical distributions of input parameters are entered in the model and with a Monte Carlo function, the statistical distribution of the output (flow rate, productivity) will be determined.

B. Basic information

Additional petrophysical analysis
A petrophysical analysis will be carried out on a number of additional wells to gain a better understanding of the characteristics of the formation. Among other things the porosity and permeability of the Zeeland Formation will be determined. The information will be translated to the properties of the Carboniferous Limestone Group at the location of Hoogeveen.

Of importance is investigating the difference in potential between limestone and dolomite. Karstification is another subject that requires further studying. Karst sequences in the limestone can be attractive if they are thick enough, because of their increased permeability.

Laboratory tests - mechanical rock properties
Through testing and analysis of existing cores, data is collected on rock properties. Of interest are the porosity, permeability and mechanical properties of the Zeeland Formation. Lab tests may also show the brittleness of ductility of the limestone and dolomite. These are of importance for modeling reservoir stimulation.

Laboratory tests - Fracture properties
Analysis of existing cores will provide information on natural fracture properties. This information is important for more accurate modeling of flow through fractured systems. Analysis should include distinguishing between natural and induced fractures, checking core recovery factor, checking stylolite presence, quantifying natural fracture dimensions and density

Stress analysis - breakout analysis
The subsurface stress field is of importance to determine whether or not to the fractures are 'open' as well as the direction of the fractures. On the basis of boreholes in the vicinity of Hoogeveen as well as regional data, the direction and magnitude of the stress field will be determined.

Slip and dilation tendencies
The slip and dilation tendencies are indicators of the degree to which the fractures are 'open' position for the flow of liquid. Slip and dilation tendencies are determined on the basis of stress magnitude and stress directions.

C and D. Modeling shear (water) and tensile (propped) fractured systems

Model for shear (water) fractured system
A model is established to determine the output (flow rate, productivity) of a water / shear fracture system. Important factors are the shear stress, the quantity of injected water and the fracture surface properties of the rock.

Model tensile (propped) fractured system
A model is established to determine the output (flow rate, productivity) of a tensile/propped fracturing system. Important factors are Young's modulus, Poisson ratio, the stress situation and permeability. Further the proppant and fluid quantities play a major role.

Probability distribution profiles input parameters
For all input parameters of the above three models statistical distributions are determined. Already available data, the basic data from part 1B or literature data will be applied. In extreme cases, conservative assumptions are made.

References

Cercone, K.R., Deming and D., Pollack, H.N. (1996). Insulating effect of coals and black shales in the Appalachian Basin, Western Pennsylvania. Org. Geochem, Vol. 24, No. 2, p. 243-249.

Cloetingh, S., van Wees, J.D., Ziegler, P.A., Lenkey, L., Beekman, F., Tesauro, M., För- ster, A., Norden, B., Kaban, M., Hardebol, N., Bonté, D., Genter, A., Guillou-Frottier, L., Ter Voorde, M., Sokoutis, D., Willingshofer, E., Cornu, T. and Worum, G. (2010). Litho- sphere tectonics and thermo-mechanical properties: An integrated modelling approach for Enhanced Geothermal Systems exploration in Europe. Earth Science Reviews, Vol. 102, I. 3-4, p. 159-206.

de Jager, J. (2007). Geology of the Netherlands Edited by Th.E. Wong, D.A.J. Batjes & J. de Jager Royal Netherlands Academy of Arts and Sciences, 2007, p. 5–26.

Doornenbal, J.C. and Stevenson, A.G. (2010). Petroleum Geological Atlas of the South- ern Permian Basin Area. EAGE Publications b.v., p. 354.

Dunham, R. J. (1962). Classification of carbonate rocks according to depositional texture. In: Ham, W. E. (ed.), Classification of carbonate rocks: American Association of Petro- leum Geologists Memoir, p. 108-121.

Frikken, H.W. (1999). Reservoir-geologische aspecten van productiviteit en connectiviteit van gasvelden in Nederland. Proefschift TU Delft.

Geluk, M.C., Dusar, M., de Vos, W. (2007). Geology of the Netherlands, Edited by Th.E. Wong, D.A.J. Batjes & J. de Jager, Royal Netherlands Academy of Arts and Sciences, p. 27–42

Heidbach, O., Tingay, M., Barth, A., Reinecker, J., Kurfeß, D., and Müller, B. (2008). "The 2008 release of the World Stress Map", www.world-stress-map.org.

Hsu, K.J. (1966). Origin of dolomite in sedimentary sequences: A critical analysis. Minera- lium Deposita, Vol. 2, p. 133-138.

IFWEP (2011). Diepe geothermie 2050; een visie voor 20% duurzame energie voor Ne- derland. pp. 87.

Kipp, K.L. (1986). HST3D; A Computer Code for Simulation of Heat and Solute Transport in Three-Dimensional-Ground-Water Flow Systems, " United States Geological Survey, Water Resources.

Kombrink, H. (2008). The Carboniferous of the Netherlands and surrounding areas; a basin analysis. Geologica Ultraiectina No. 294. pp. 184.

Moeck, I., Schandelmeier, H., Holl, H.G. (2009). "The stress regime in a Rotliegend reservoir of the Northeast German Basin." International Journal of Earth Sciences, Vol. 98, p. 1643-1654.

Morris, A., Ferrill, D.A., Henderson, D.B. (1996). "Slip-tendency analysis and fault reactivation." Geology 24, p. 275-278.

Nederlands Instituut voor Toegepaste Geowetenschappen TNO (2004). Toelichting bij kaartblad IX Harderwijk-Nijmegen, Utrecht, p. 122

Paproth, E., Dreessen, R., Thorez, J. (1986). Famennian Paleogeography and Event Stratigraphy of Northwestern Europe. Belgian Geological Survey, p. 175-186.

Rafavich, F.K., Kendall, C.H.S.C., Todd, T.P. (1984). The relationship between acoustic properties and the petrographic character of carbonate rocks. Geophysics, Vol. 49, p. 1620-1636.

Unknown author, 1986. The Netherlands Onshore; GEVERIK-1 well study. www.nlog.nl

Van Hulten, F.F.N. and Poty, E. (2008). Geological factors controlling Early Carboniferous carbonate platform development in the Netherlands. Geological Journal, Vol. 43, p. 175-196.

Wolburg, J. (1963). Das Unterkarbon- und Devonprofil der Bohrung Munsterland-1. Fortschritte Geologie Rheinland und Westfalen 11, p. 517–538.

Wright, V.P. (1992). A revised classification of limestones. Sedimentary Geology, Vol. 76, p. 177-185.

Ziegler, P.A. and Dezes, P. (2005). Crustal evolution of Western and Central Europe. European Lithosphere Dynamic Edited by D.C. Gee and R.A. Stephenson: Memoir of the Geological Society, London.

Zoback, M.D. (2008). Reservoir Geomechanics. Cambridge University Press, New York, pp. 449

Appendix 1 Carbonate characterization

1.1 Types of limestone

First, it is convenient to define the term 'matrix'. Matrix refers to material of silt and clay grade, meaning that they are less than 64 um in diameter. The matrix is also referred to as mud. Grains are material larger than 2 mm. This includes fossil material.

- A calcimudstone is defined as a lithified material composed of over 90%, in volume, of silt and clay-grade calcite. It is different from a mudstone that is composed of silicate silt and clay-grade material. The size of the components is the same (silt and clay-grade), but the composition is different (calcite vs. silicate). Calcimudstones are deposited under low-energy conditions.

- Wackestones are also matrix-supported, meaning the matrix material is always connected. They include a higher content of grains than the calcimudstone.

- Packstones are grain-supported, but have intergranular spaces filled by matrix material.

- Grainstones are grain-supported, matrix-free limestones and generally represent deposition in settings where mud-grade matrix would have been removed, i.e. high-energy environments.

- Cementstones are reef limestones composed of fibrous cement, in which grains or biogenic material does not constitute a framework. Cements are replaced or recrystallized original limestone features.

- *Kieselkalk* is a German classification for a diagenetic quartz-rich limestone.

- *Schiefer* is a German classification for shale. Shale is a clastic rock composed of mud-size materials. It is different from a mudstone in that it is flaky, a mudstone is not.

Claystones (or *tonstein* as they are called in Germany) are not limestones but they are mentioned here to note the difference. Claystones are clastic sediments with grain sizes of less than 2 um, consisting primarily of clay minerals as kaolinite, illite, smectite. Other materials that could be present include quartz and carbonates. It is different from a mudstone in that the majority of the materials is clay-sized, whereas the mudstone has a higher silt-grade (without calcite material).

1.2 Depositional environment

The depositional environment of carbonates during the Early Carboniferous in the Netherlands can be visualized by figure 1. On the platforms, reef-like limestones can be found. These can be categorized as grainstones and wackestones. They indicate a high-energy environment. Moving away from the platform the depositional environment becomes less energenic and here wackestones and packestones are likely to be found. The basin is characterized by calcimudstone, indicating low flow velocities and settling of carbonate shells.
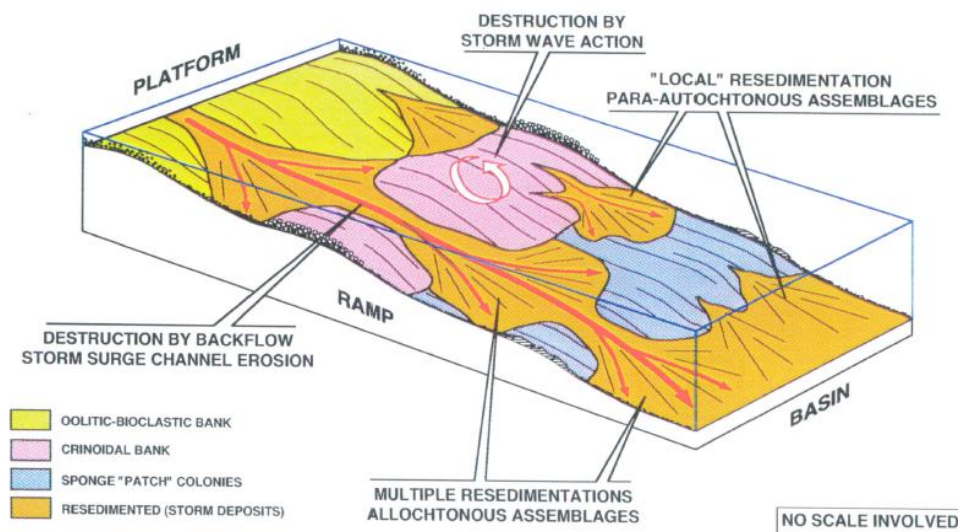

Figure 1   Stratigraphic record of a carbonate ramp (Elf Aquitaine, 1986).

1.3 Carbonate alteration processes

Karstification

Karstification is the process of dissolution of carbonates by some fluid. This can also occur in deep formations as the Zeeland Formation.

According to literature the matrix porosity of the Zeeland Formation is usually only a few percent. The secondary dolomites of the Beveland Member show increased porosity (Geluk et al, 2007). The petrophysical analysis in the next chapter will give a more detailed indication of the porosity of the Zeeland Formation.

The process of karstification is important as it creates a reservoir. A limestone that is primarily tight and nonporous can become very porous after karstification. A limestone sequence in the Heibaart Dome in the north of Belgium is now a very permeable reservoir in which gas is currently stored, after a 5 million year period of karstification.

The lowering sea level at the end of the Early Carboniferous gave rise to an important karstification event at the top of the Zeeland Formation. There are indications of karstification in the deep Dutch wells. These consist of fluid losses and an increased caliper size (borehole geometry measurement tool). However they occur just above the Zeeland Formation.

This can still indicate a karstified sequence right below the depth of the mud losses, i.e. in the top of the Zeeland Formation. An increased caliper size, however, is closely related to the specific depth at which it occurs.

Analysis of caliper data, borehole breakouts and fluid losses is required to assess the potential of karstified sequences in the Zeeland Formation.

Dolomitization
Dolomites originate when carbonate minerals form a solid solution. Magnesium and other ions can freely substitute in the crystal structure of the minerals. A carbonate rock can range from pure calcite to pure dolomite.

Dolomites can be either primary or secondary, though it is believed that most dolomites are of secondary origin. There is evidence that the forming of dolomite can occur through pressure solution at greater depths. This does not necessarily require water, but large pressure. However, dolomites are also formed near the earth's surface. Therefore, it is possible that magnesium could have been supplied by surface waters. The distributions of this kind of dolomite would be related to the chemistry of surface waters. Hsu (1966) reasons that shelf deposits were often exposed during times of regression. Hydrodynamic heads were set up to induce the motion of subsurface waters through the exposed shelf sediments. Dolomitization could be related to this water movement. He concludes that major dolomite deposits are closely associated with shallow epicontinental shelves or oceanic banks.

The occurrence of the thick dolomitic limestone beds in the northern wells could be explained by a period of regression after the deposition of Tournaisian limestone. This would coincide with a period of sea-level fall in the south of Belgium, where Tournaisian and Early Visean dolomitized shallow-marine limestones have been found. Van Hulten and Poty (2008) note that dolomitization has not been observed in deep water facies.

In all of the four wells, dolomite or dolomitic limestone is found. The wells also have in common that the dolomite is found in the bottom of the Zeeland Formation. Thicknesses are varying from tens to hundreds of meters. A petrophysical and geomechanical analysis of log data is required to assess the potential of dolomite as being different from that of limestone. Though it is generally believed that the limestones encountered in the deep wells are very hard and will not show large differences in lithology and rock properties compared to the underlying dolomites.

1.4   Fossils

Fossils that are found in the cores of the deep wells of the Zeeland Formation from the four wells are:

- Foraminifers are marine organisms, usually with a calcareous shell.
- Radiolaria are marine organisms that possess a siliceous shell and are found in all seas of the world.
- Bryozoans are found both in fresh and salt water. Their skeleton is calcareous.
- Brachiopods are found solely in salt water.

- Gastropods are adapted to marine, freshwater and terrestrial life. They have a carbonate shell.
- Trilobites were essentially marine.
- Crinoids are exclusively marine.
- Conodonts are marine fishes.
- Peloids are fecal pellets that collect in lagoons and shallow intertidal zones.
- Ooids are carbonate sedimentary grains, most commonly found in shallow tropical seas.

Appendix 2 Lithostratigraphy deep wells

2.1   Lithostratigraphic descriptions

Münsterland-1 (5,438 m- 5,507 m MD)

Uppermost 20 meters consist of dark-grey to black claystone with presence of pyrite. No sand is present. Cracks are filled with calcareous deposits. The next 10 meters are the same as the upper 20 meters, but there are also pieces of limestone. Limestone is *kieselig*, referring to mixing of some quartz grains.

In the next 10 meters the content of limestone increases but the claystone remains the abundant material (65%). Layering of limestone, claystone and *kieselkalk* and occasional tuff. The limestone is dark-grey and dolomitic. The claystone is black, dolomitic, contains pyrite but no sand. The limestone and *kieselkalk* break conchoidal. Open fractures have not been found. Fractures that have been found are filled with calcite.

In the next 20 meters dolomitic limestone becomes the abundant material. *Kieselkalk* only as separated splinters. The last 10 m section is dated as Lower-Tournaisian by Wolburg (1963).

LTG-01 (4,305 m - 5,076 m TVD)

Uppermost 100 m white-grey limestone. Limestone is soft to firm. Traces of calcite and pyrite. Limestone mostly calcimudstone.

Next 100 m calcimudstone with minor laminations of claystone (max. 3 m thick). Calcimudstone is grey to dark grey and harder than uppermost 100 m. Traces of pyrite and calcite. Loose quartz grains found (very fine) within 10 m interval.

Next 300 m mostly calcimudstone as above. Few claystone layers (max. 2 m thick) in upper 30 m. Also parts of grainstone but not as abundant as calcimudstone.

Next 200 m as above. With traces of dolomite.

Bottom 80 m white to light-grey, soft to firm calcimudstone/packstone with intercalations of dolomite.

No visible porosity in any of the sections.

In the interval between 4,725 to 4,900 m tabulate coral have been observed. In the bottom 100 m no fossils are noticed, whereas in the rest of the column large amounts of fossils were encountered.

if

UHM-02 (4,670 m - 5,332 m TVD)

The top 30 m of the Zeeland Formation is characterized by massive white recrystallized cementstone.

In the next 10 m the limestone is less massive. Increasing content of wackestone/packstone.

In the next 10 m the content of packstone increases to 20%. Rest is still cementstone.

The next 40 m is characterized by packstone and calcimudstone. The content of calcimudstone increases towards the bottom of this section.

In this entire 80 m section (which is described in great detail) presence of gas is abundant. The limestone is always white. Fossils (pelloids/ooids and occasional crinoids) occur in the entire section.

The remaining part of the Zeeland Formation (350 m) is not described in great detail. The composite well log describes the total section as limestone without any further remarks. Core samples of the section were taken only every ~40 m. Samples comprise a mixture of grainstones and packstones. Visible porosity is zero is the entire Zeeland Formation.

The transition from the Zeeland Formation to the Beveland Member is defined at 5,118 m by NLOG.
The entire Beveland Member section (220 m) is defined as dolomitic limestone, according to the composite well log. Core samples show that indeed there is an increase in dolomitic material, but there are also samples that contain grainstones like above. Some samples in the dolomite section show intercrystal porosity but in most samples porosity is zero due to compaction or calcite filling. This section fits the description in the Geology of the Netherlands Atlas of the Beveland Member (Geluk et al, 2007).

WSK-01 (4,270 m – 4,457 m TVD)

The following interpretation is based solely on the lithostratigraphic description in one of the well logs. This log was not very detailed so there is some uncertainty in the classification.

Uppermost 30 m intercalations of limestone, siltstone and claystone. Traces of pyrite. Classification of limestone according to Dunham has not been made.

Next 90 m consists mainly of limestone, with thick claystone beds and siltstone intercalations.

The next 30 m consists mostly of claystone with limestone beds. Some shale beds are found in the upper part. The portion of claystone increases towards the bottom of the section.

The bottom 40 m consists of intercalations of limestone, claystone and siltstone.

One core sample is documented. The percentage of soluble carbonates was less than 10%. The sample is characterized by a darker color than the cores from LTG-01 and UHM-02. The core consists definately of massive limestone but with a high content of organic matter or shale input.

The core deposits from the depth of 4,433-4,441 m are correlated with the *Ostracodenkalk* in the Ruhr area in Germany and the *Hastiere Formatie* in Belgium, based on palynologic research. This facies forms the base of the Lower Carboniferous (Stratigraphische Einführung, unknown author). It is a limestone facies.

2.2   Lithostratigraphic columns

Münsterland-1

LTG-01

Luttelgeest-01

Legend:
- Fine sandstone
- Sand and clay
- Claystone
- Chalkstone
- Marl
- Coal rich claystone
- Limestone with dolomite

Age [Ma]	Group	Dominant lithology	TVD [m]

Groups (top to bottom):
- Upper North Sea Group
- Middle North Sea Group
- Lower North Sea Group
- Ommelanden Formation
- Rijnland Group
- Upper Rotliegend Group
- Caumer Subgroup
- Geul Subgroep
- Carboniferous Limestone Group
- Banjaard Group

Ages: 65.5, 299, 318.1, 359.2

TVD depths: 0, 500, 1000, 1500, 2000, 2500, 3000, 3500, 4000, 4500, 5000

Group legend:
- Upper North Sea Group
- Middle North Sea Group
- Lower North Sea Group
- Chalk Group
- Rijnland Group
- Upper Rotliegend Group
- Limburg Group
- Carboniferous Limestone Group
- Banjaard Group

if

UHM-02

Uithuizermeeden-02

Legend:
- Fine sandstone
- Sand and clay
- Claystone
- Chalkstone
- Marl
- Evaporite
- Coal rich claystone
- Limestone with dolomite

| Age [Ma] | Group | Dominant lithology | TVD [m] |

Groups (from top):
- Upper North Sea Group
- Middle North Sea Group
- Lower North Sea Group
- Chalk Group — 65.5
- Rijnland Group — 145.5
- Lower Germanic Trias Group — 251
- Zechstein Group
- Upper Rotliegend Group — 270.6
- Caumer Subgroup — 299
- Geul Subgroup
- Carboniferous Limestone Group — 318.1
- Banjaard Group — 359.2

TVD scale: 0, 500, 1000, 1500, 2000, 2500, 3000, 3500, 4000, 4500, 5000

Bottom legend:
- Upper North Sea Group
- Middle North Sea Group
- Lower North Sea Group
- Chalk Group
- Rijnland Group
- Lower Germanic Trias Group
- Zechstein Group
- Upper Rotliegend Group
- Limburg Group
- Carboniferous Limestone Group
- Banjaard Group

if

WSK-01

Winterswijk-01

Legend:
- Fine sandstone
- Evaporite
- Limestone with dolomite
- Sand and clay
- Marl
- Claystone
- Coal rich claystone

Age [Ma]	Group	Dominant lithology	TVD [m]

Groups shown in column:
- Upper North Sea Group
- Middle North Sea Group
- Altena Group
- Upper Germanic Trias Group
- Lower Germanic Trias Group
- Zechstein Group
- Upper Rotliegend Group
- Caumer Subgroup
- Geul Subgroup
- Carboniferous Limestone Group
- Banjaard Group

Age markers: 199.6, 251, 299, 318.1, 359.2

TVD markers: 0, 500, 1000, 1500, 2000, 2500, 3000, 3500, 4000, 4500, 5000

Color legend:
- Upper North Sea Group
- Middle North Sea Group
- Altena Group
- Upper Germanic Trias Group
- Upper Germanic Trias Group
- Zechstein Group
- Upper Rotliegend Group
- Limburg Group
- Carboniferous Limestone Group
- Banjaard Group
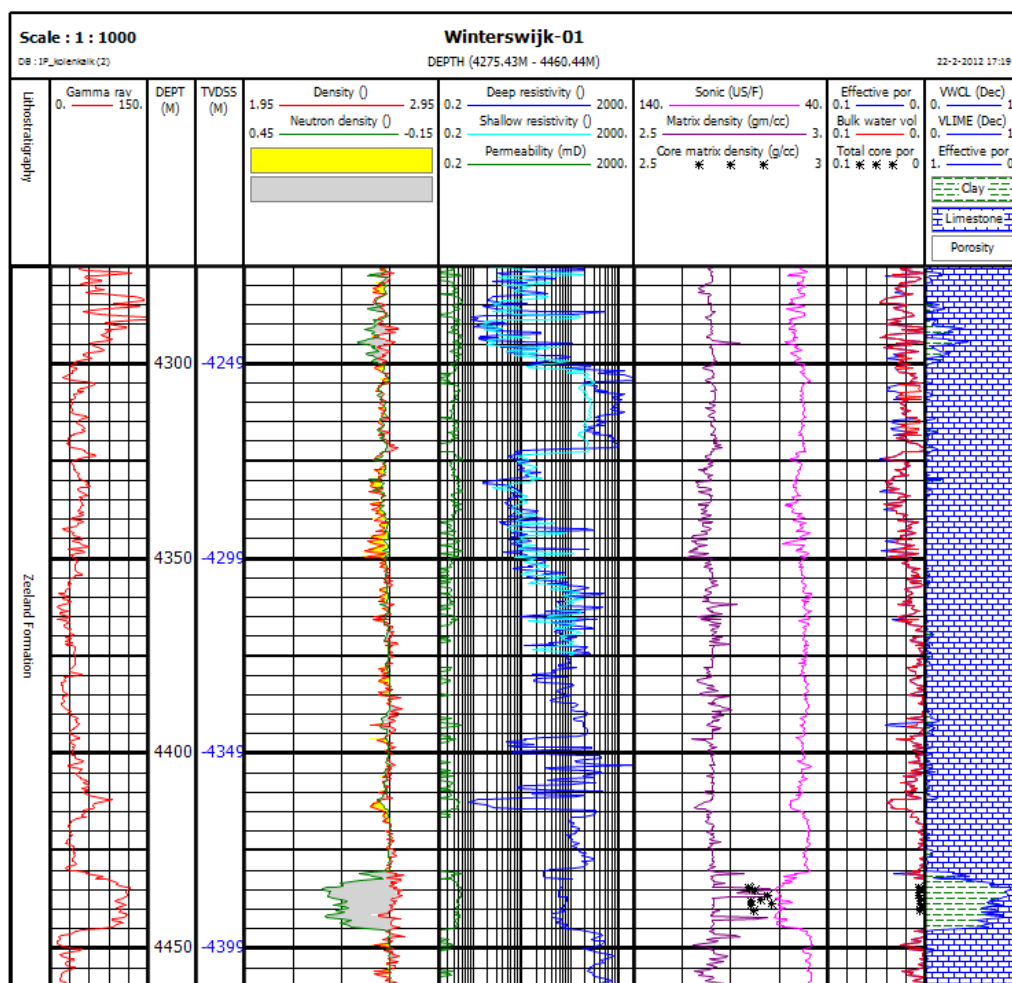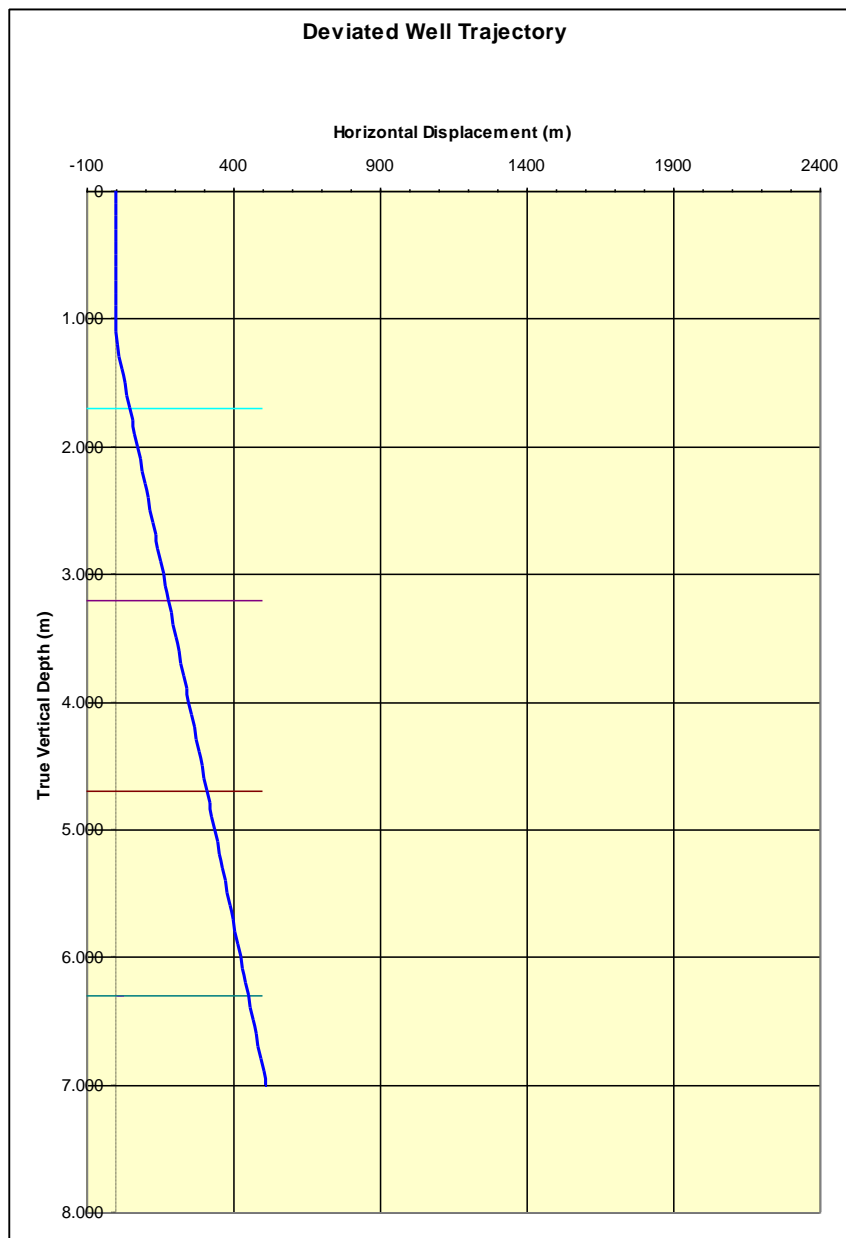
Appendix 3 Log plots

Appendix 4 Notional Well design

4.1   Side view of well layout
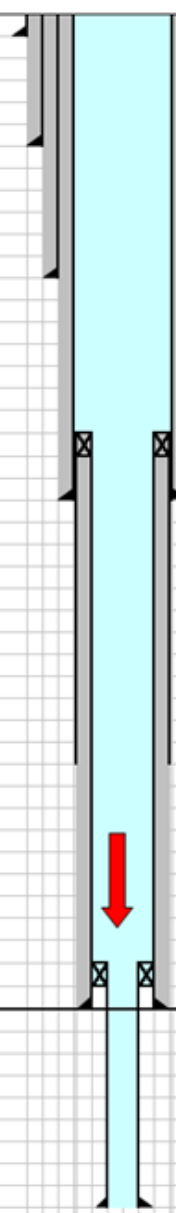

Deviated Well Trajectory

Deviated Well Trajectory

4.2 Well layout production well

Nr.	Item Description	Wellhead and Xmastree	Depth m tvd	Depth m ah	Hole ID in	Pipe OD in	Collar OD in	Pipe ID in Drift
1	28" x 1" X 52E conductor shoe							
2	24" 174 ppf K55 Big Omega							
3	18 5/8" 114 ppf K55 Big Omega casing							
	Linerhanger 13 3/8" x 9 5/8"							
4	13 3/8" 68 ppf L80 VAM-TOP casing							
5	11 3/4" 54 ppf, L80, Expandable liner							
	Linerhanger 9 5/8" x 7"			6200				
6	9 5/8" 47 ppf L80 VAM-TOP casing		6300	6300	12 1/4	9,625	10,386	8,599
		HORIZONTAAL						
7	7" 29 ppf L80 VAM TOP		6300	9300	8 1/2	7,000	7,644	6,059

4.3   Well layout injection well

Nr.	Item Description	Wellhead and Xmastree Hoogeveen	Depth	Depth	Hole ID	Pipe OD	Collar OD	Pipe ID
			m tvd	m ah	in	in	in	in Drift
1	28" x 1" X 52E conductor shoe		60	60	driven	28,000	welded	26,000
2	24" 174 ppf K55 Big Omega		600	600	26	24,000	25,000	22,437
3	18 5/8" 114 ppf K55 Big Omega casing		1700	1700	22	18,625	20,000	17,280
	Linerhanger 13 3/8" x 9 5/8"			3100				
4	13 3/8" 68 ppf L80 VAM-TOP casing		3200	3200	16	13,375	14,175	12,259
5	11 3/4" 54 ppf, L80, Expandable liner		4700	4700	12 1/4	12,250	12,250	11,250
	Linerhanger 9 5/8" x 7"			6200				
6	9 5/8" 47 ppf L80 VAM-TOP casing		6300	6300	12 1/4	9,625	10,386	8,599
					HORIZONTAAL			
7	7" 29 ppf L80 VAM TOP		6300	9300	8 1/2	7,000	7,644	6,059

if